

NAM

CPT in Thinly Layered Soils

Validation Tests and Analysis for Multi Thin Layer Correction

Deltares

D.A. de Lange

Date August 2018

Editors Jan van Elk & Dirk Doornhof

General Introduction

Cone penetration test provide crucial data for the preparation of the geological model of the shallow subsurface (Ref. 1 to 3) and therefore for the assessment of site response (Ref. 4) and liquefaction (Ref. 5). The CPT data are stored together with other data of the shallow subsurface and soils in a database (Ref. 6).

However, interpretation of CPT data is difficult for thin layered soils. The current reports investigated the interpretation of CPT in thin layers based on experimental laboratory CPT tests performed in artificially built up layered soil.

References

1. Geological schematisation of the shallow subsurface of Groningen (For site response to earthquakes for the Groningen gas field) – Part I, Deltares, Pauline Kruiver, Ger de Lange, Ane Wiersma, Piet Meijers, Mandy Korff, Jan Peeters, Jan Stafleu, Ronald Harting, Roula Dambrink, Freek Busschers, Jan Gunnink
2. Geological schematisation of the shallow subsurface of Groningen (For site response to earthquakes for the Groningen gas field) – Part II, Deltares, Pauline Kruiver, Ger de Lange, Ane Wiersma, Piet Meijers, Mandy Korff, Jan Peeters, Jan Stafleu, Ronald Harting, Roula Dambrink, Freek Busschers, Jan Gunnink
3. Geological schematisation of the shallow subsurface of Groningen (For site response to earthquakes for the Groningen gas field) – Part III, Deltares, Pauline Kruiver, Ger de Lange, Ane Wiersma, Piet Meijers, Mandy Korff, Jan Peeters, Jan Stafleu, Ronald Harting, Roula Dambrink, Freek Busschers, Jan Gunnink
4. Modifications of the Geological model for Site response at the Groningen field, Deltares, Pauline Kruiver, Ger de Lange, Ane Wiersma, Piet Meijers, Mandy Korff, Jan Peeters, Jan Stafleu, Ronald Harting, Roula Dambrink, Freek Busschers, Jan Gunnink
5. Liquefaction sensitivity of the shallow subsurface of Groningen, Deltares and TNO-GSN: Mandy Korff, Ger de Lange, Piet Meijers, Ane Wiersma, Fred Kloosterman, November 2016.
6. Background document NAM database of subsurface information, Version date of database - 29 March 2018, Deltares, Pauline Kruiver, Fred Kloosterman, Ger de Lange, Pieter Doornenbal , March 2018

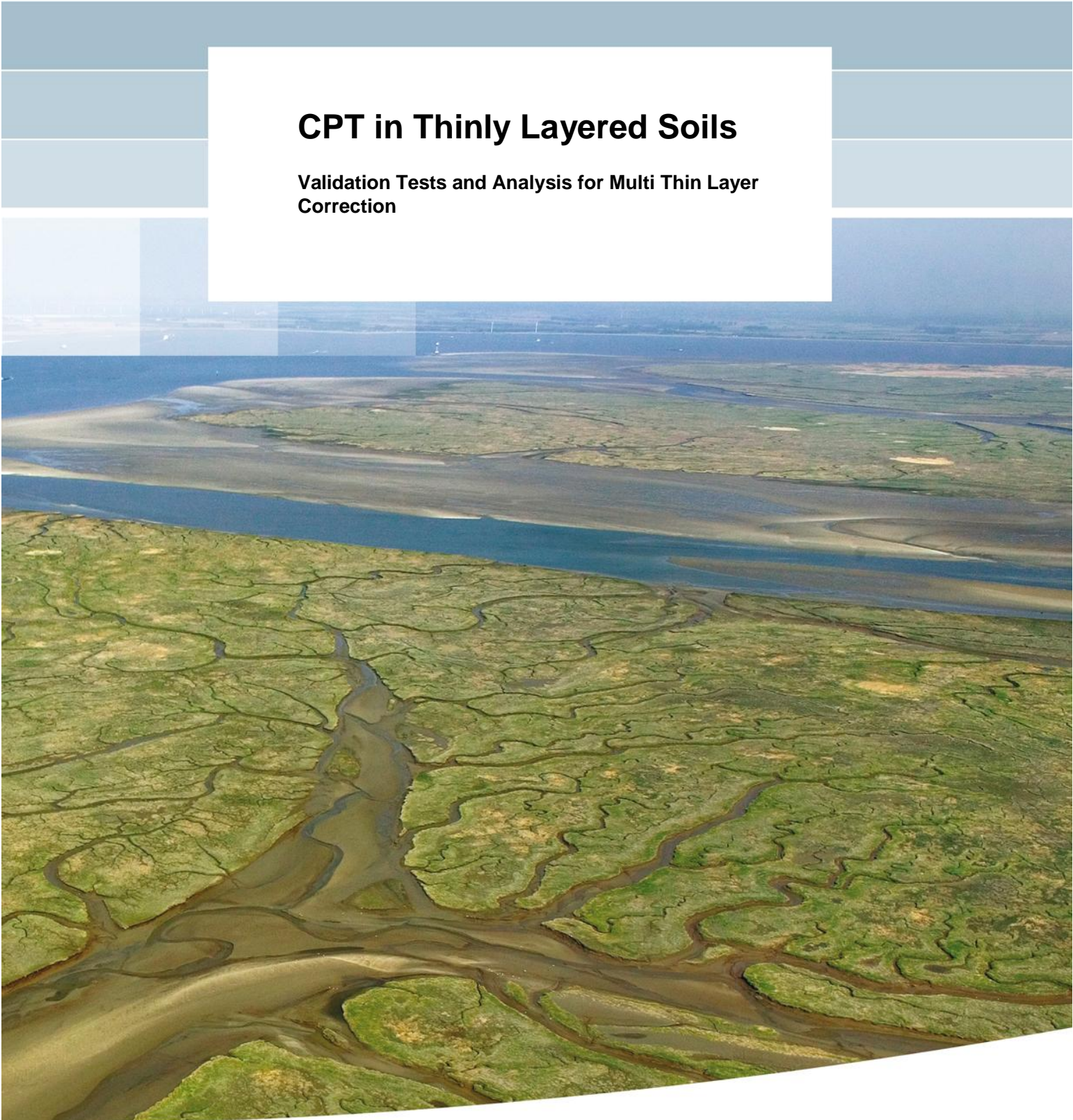


NAM

Title	CPT in Thinly Layered Soils Validation Tests and Analysis for Multi Thin Layer Correction		Date	August2018
			Initiator	NAM
Autor(s)	D.A. de Lange	Editors	Jan van Elk and Dirk Doornhof	
Organisation	Deltares	Organisation	NAM	
Place in the Study and Data Acquisition Plan	<p><u>Study Theme:</u> Shallow Geology and Soil Description</p> <p><u>Comment:</u> Cone penetration test provide crucial data for the preparation of the geological model of the shallow sub-surface (Ref. 1 to 3) and therefore for the assessment of site response (Ref. 4) and liquefaction (Ref. 5). The CPT data are stored together with other data of the shallow subsurface and soils in a database (Ref. 6). However, interpretation of CPT data is difficult for thin layered soils. The current reports investigated the interpretation of CPT in thin layers based on experimental laboratory CPT tests performed in artificially built up layered soil.</p>			
Directly linked research	<p>(1) Ground Motion Prediction (2) Liquefaction (3) Active Clays</p>			
Used data				
Associated organisation	NAM			
Assurance				

CPT in Thinly Layered Soils

**Validation Tests and Analysis for Multi Thin Layer
Correction**



CPT in Thinly Layered Soils

Validation Tests and Analysis for Multi Thin Layer Correction

Dirk de Lange

1209862-006

Title
CPT in Thinly Layered Soils

Client	Project	Attribute	Pages
Nederlandse Aardolie Maats chappij B.V., ASSEN	1209862-006	1209862-006-GEO-0007	55

Keywords
CPT, density, layered soil, liquefaction, clay, sand

Summary
To generate a broader base for thin layer correction for laminated soil deposits which contain multiple layers with thicknesses similar or smaller than the cone diameter calibration chamber tests are performed. Cone penetration tests are performed in artificially built up layered soil at vertical effective stress levels up to 100 kPa. The influence of stress level, soil density and layer thickness is investigated.

Several soil models have been created, having different layer configurations and/or densities. Based on the measured cone resistance profiles, distinction can be made between the effects of the layered part as a whole, relative to the surrounding soil, and the effects of the individual thin layers. Greater contrast in cone resistance of the thin stronger and weaker layers is found for higher sand density, higher stress level and larger layer thickness. The resistance measured in the thin clay layers is also affected by the sand density and the stress level, while the layer thickness (up to 4 cm for a 25 mm cone) seems to have a smaller influence.

Thin layer correction factors for laminated soil deposits have been derived which contain multiple layers with thicknesses similar or smaller than the cone diameter. Correction factors between 1.5 and 6 are found. The derived correction factors show clear dependency of layer thickness relative to the cone size, sand density and stress level. A good fit with the lower bound of an estimated range based on examination of field data of Youd et al. (2001) is found for layer thicknesses of 1.6 and 3.2 times the cone diameter, while the relation proposed by Moss et al. (2006) provides a good estimate of the correction factors derived for layer thicknesses of 0.56 and 0.8 times the cone diameter. Besides correction factors for sand layers, also correction factors are derived for clay layers.

The test results are simulated by existing analytical methods. The slightly adjusted method of Koppejan shows a good fit for the factors derived from the test results. The method can be used to derive correction factors for other H/d_{cone} ratios.

After analysing some CPT data from the field, a method for application in practice is proposed based on a statistical analysis of the test results.

Version	Date	Author	Initials	Review	Initials	Approval	Initials
01	Aug 2018	ir. D.A. de Lange		dr.ir. M. Korff		ing. A.T. Aantjes	
02	Oct 2018	ir. D.A. de Lange		dr.ir. M. Korff		ing. A.T. Aantjes	

Status
final

Contents

1	Introduction	1
1.1	Project background	1
1.2	Project objective	4
1.3	Approach, scope, limitations	4
1.4	Report structure	4
2	Test program, equipment and procedure	5
2.1	Test program	5
2.2	Test equipment	6
2.2.1	Test setup	6
2.2.2	Calibration chamber	7
2.2.3	CPT equipment	10
2.3	Test procedure	10
2.3.1	General Procedure	10
2.3.2	Applying stress levels and consolidation time	11
2.3.3	Cone penetration testing	11
2.3.4	Boundary effects and penetration disturbance	12
2.3.5	Local density measurements	13
3	Soil model	14
3.1	Configurations	14
3.2	Material characteristics	14
3.2.1	Baskarp sand	14
3.2.2	Vingerling clay	15
3.3	Preparation method	18
3.4	Preparation accuracy	19
3.5	Post-test local density measurements	20
4	Test results	21
4.1	Data processing	21
4.2	General remarks on the tests	21
4.3	Example – 36 mm cone tests	22
4.4	General observations layered soil models	24
5	Multiple thin layer correction	27
5.1	Introduction	27
5.2	Reference tests	28
5.3	Reliability results layered soil models	30
5.4	Effect of multiple layers	32
5.5	Derived thin layer correction factors	33
5.6	Additional information from the cone resistance profile	38
6	Numerical simulation	41
6.1	Analytical methods	41
6.1.1	Joer et al. (1996)	41
6.1.2	Method of Koppejan	41
6.2	Simulation of test results	42

7 Discussion	50
8 Proposed correction method	52
9 Conclusions	53
10References	54

Appendices

A Test results	A-1
A.1 Soil model 1	A-2
A.2 Soil model 2	A-4
A.3 Soil model 3	A-6
A.4 Soil model 4	A-8
A.5 Soil model 5	A-10
A.6 Soil model 6	A-12
A.7 Soil model 7	A-14
A.8 Soil model 8	A-16
A.9 Soil model 9	A-18
A.10 Soil model 10	A-20
B Additional measurements	B-1
B.1 Post-test local density measurements	B-1
B.2 Stress and volume measurements	B-12
B.3 Volume change of soil model after cone penetration testing	B-15
C Start-up phase	C-1
C.1 Test setup and procedure	C-1
C.1.1 Description setup	C-1
C.1.2 General Procedure	C-2
C.2 Soil models	C-3
C.2.1 Configurations	C-3
C.2.2 Model preparation	C-4
C.3 Test results	C-4
C.3.1 Soil model 1	C-4
C.3.2 Soil model 2	C-7
C.3.3 Soil model 3	C-9
C.3.4 Soil model 4	C-12
C.3.5 Soil model 5	C-14
C.4 Overview and discussion test results start-up phase	C-17

List of Symbols

BC	boundary condition
CPT	cone penetration test
d_c / d_{cone}	cone diameter
D_{eq}	equivalent diameter
d_{50}	grain diameter mass median
H	layer thickness
I_c	soil behaviour type index
I_D	density index
K_H	thin layer correction factor
K_0	coefficient of neutral lateral earth pressure
LL	liquid limit
N_k	empirical cone factor
n_{max}	maximum porosity
n_{min}	minimum porosity
p'	mean effective stress
PL	plastic limit
PI	plasticity index
q	deviator stress
$q_{b,max}$	pile bearing capacity
q_c	cone resistance
$q_{c;Lunne \& Christoffersen}$	cone resistance according the relation proposed by Lunne & Christoffersen (1983)
$q_{c;m}$	measured cone resistance
$q_{c;m;layer,max}$	the maximum value of the cone resistance measured in the stronger layer
$q_{c;m;layer,min}$	the minimum value of the cone resistance measured in the weaker layer
$q_{c;"true"}$	the cone resistance that would have been measured in this same soil if the measurement was not influenced by the overlying and underlying weaker soil
q_{cN}	cone resistance normalized for the stress level
S_u	undrained shear strength
U_b	pore water pressure measured at the bottom of the sample
w	water content
ε_z	vertical strain
σ_v	vertical stress
σ'_v	vertical effective stress

1 Introduction

1.1 Project background

Cone penetration test (CPT) measurements are used for many applications, for example foundation design, liquefaction analysis and soil stability calculations. CPT measurements are influenced by a certain volume of soil around the cone tip. The dimensions of this zone of influence depend on the cone size and the strength and stiffness characteristics of the soil. The cone resistance depends on the sequence and properties of all soils within the zone of influence.

Around a soil layer interface there is a zone where the measured resistance will be influenced by both the under- and overlying layer. This zone is called the transition zone. In other words, at a certain distance from the interface the underlying layer will be felt (sensing distance) and a certain penetration in the underlying layer is needed to get rid of the effect of the overlying layer (development distance), see Figure 1.1.

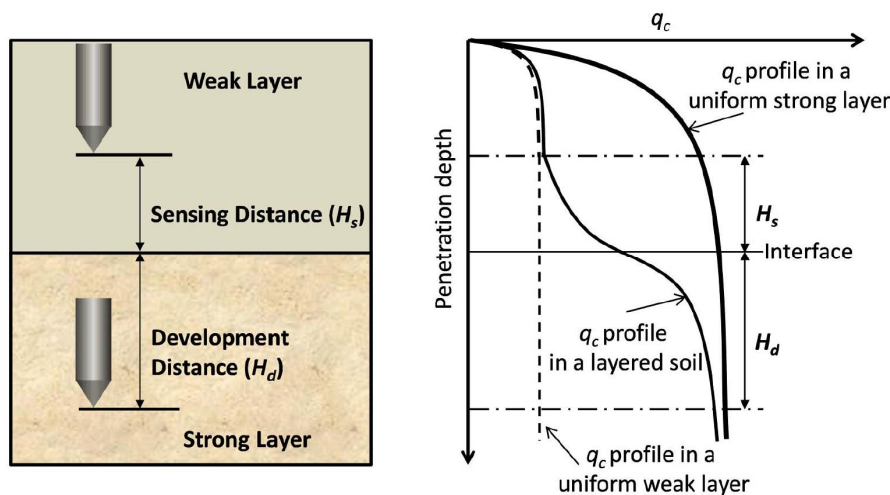


Figure 1.1 Sensing and development distance (after Tehrani et al. 2017)

When interbedded layers become thin relative to the cone size, the “true” resistance won’t be developed fully. Therefore, CPT measurements from thinly layered soil deposits may give unrepresentative values of the resistance of the individual layers. The “true” resistance is defined as the resistance that would have been measured in this same soil if the measurement was not influenced by the overlying and underlying soil.

An example is given in Figure 1.2. In 1995, CPTs were performed at Deltares in a layered soil model during centrifuge tests (acceleration level of 40g). The model consisted of 40 cm Spesswhite Kaolin clay on top of sand. A sand layer of 2 cm thickness was placed at the middle of the clay layer to shorten the consolidation time of the clay. The CPTs were performed with a model cone, having a diameter of 11.3 mm. In another model a CPT was performed in sand alone, having a similar density as the sand layers of the layered soil model. As can be seen, only a small part of the cone resistance is developed in the thin sand layer compared to the full soil model, while stress level and density of the thin sand layer are virtually the same as the full sand model.

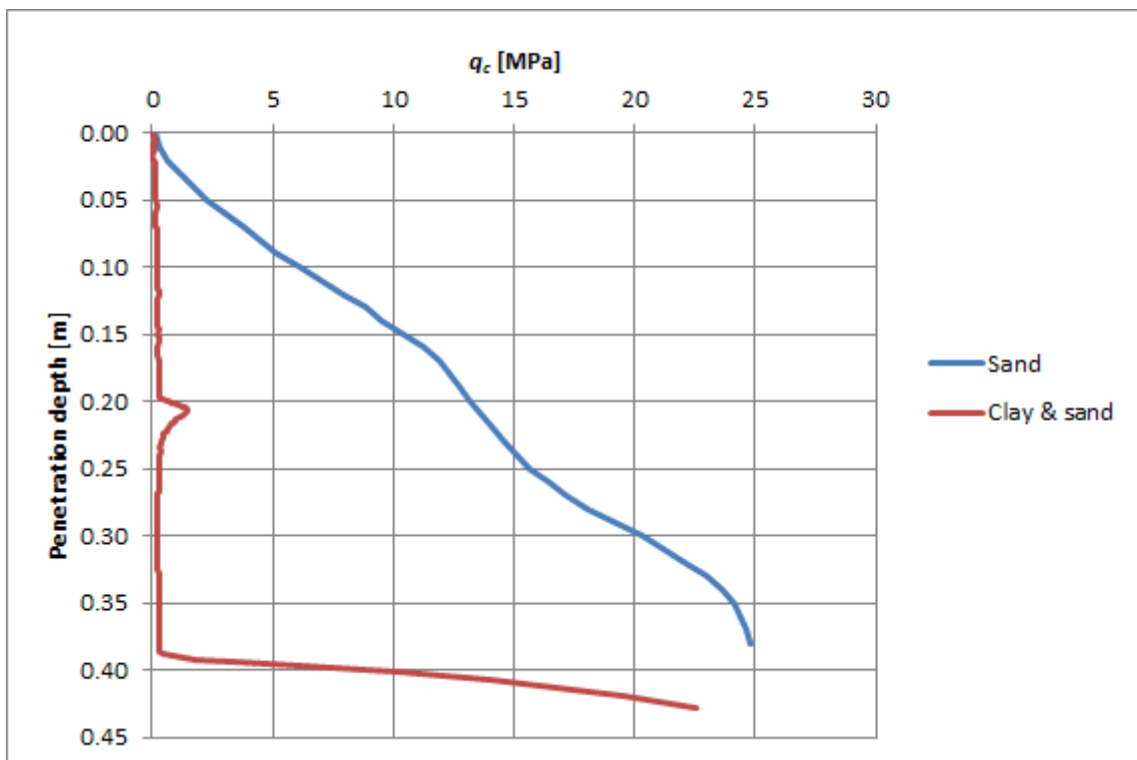


Figure 1.2 Cone resistance measured by a model cone ($d = 11.3$ mm) in a sand and a layered model (clay and sand) during centrifuge testing (acceleration level of 40g)

In engineering practice, a wide range of soil properties is estimated based on correlations with CPT data. However, these correlations are not applicable for thinly layered soil deposits, since the “true” resistance is not measured. For several applications an estimate of the “true” resistance of thin layers would be beneficial. A thin layer is defined as a layer which has not sufficient height to develop the “true” resistance. To have a realistic estimate of soil properties based on correlation with CPT data a correction on the CPT data is needed for thin layers.

For the estimation of the liquefaction potential of marine depositions of the Groningen area, called ‘tidal flats’ or ‘flaser beds’, also a correction on the CPT data is needed. These depositions can be characterized as fine sands with quasi regular sequences of small (10 - 20 cm width) and thin (3 - 15 mm thick) bands of clay and/or silt, see Figure 1.4. Without correcting the CPT data, the void ratio and therefore also the susceptibility to liquefaction will be overestimated, if the soil is classified as a sand.

Robertson and Fear (1995) derived an expression for the thin layer correction based on analytical linear elastic solutions (Vreugdenhil et al. 1994). Youd et al. (2001) recommends a range of correction factors based on ‘field data’, see Figure 1.3. Unfortunately no report or paper describing these field data is available. Other thin layer factors are given by Ahmadi and Robertson (2005), based on axisymmetric nonlinear analyses, and by Mo et al. (2017), based on cavity expansion based solutions. In the current available methods the thin layer factor is a function of both layer thickness and the ratio of stiffnesses or “true” cone resistances of the individual layers. However, the characteristics of the individual thin layers are unknown.



Figure 1.4 Example of flaser bed deposition

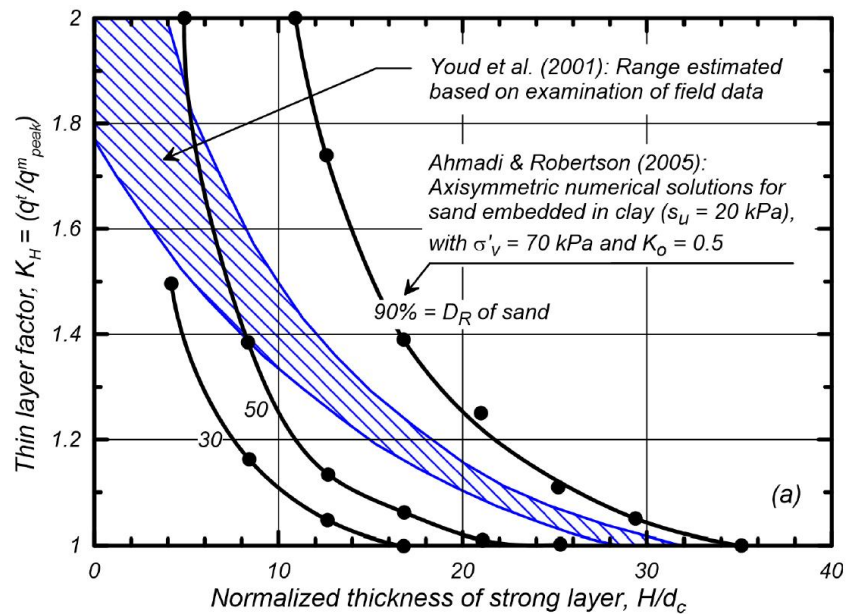


Figure 1.3 Thin layer factors inferred from field data (Youd et al. 2001) compared to axisymmetric numerical analyses by Ahmadi and Robertson (2005) after Boulanger and DeJong (2018).

Experimental data is available on CPT in layered soil. Van den Berg et al. (1996) and Mlynarek et al. (2012) performed tests in soil models, which consisted of sand and clay. Others performed tests in layered sand models. However, only two or three layer systems were considered, having soil layers of at least 10 cm thickness. Only Hird et al. 2003 performed miniature piezocone tests in soil models consisting of multiple thin sand/silt layers in clay. Although the cone resistance was measured, the influence of layering on the cone resistance was not a topic of interest in their investigation.

No experimental data was available on the effect of multiple thin layers on the cone resistance, where the layer thickness is similar or smaller than the cone diameter. Therefore Van der Linden (2016) performed some cone penetration tests on artificially built soils which contain multiple thin sand and clay layers (feasibility study). The tests were performed at low effective stress level. These tests were performed successfully and it appeared to be possible to simulate these tests by existing analytical models. However, a thin layer factor for multiple

thinly layered soil deposits would have to be validated for a range of relevant stress levels, layer thicknesses and soil strength/stiffness to be applied in practice.

1.2 Project objective

The research objective of this study is to generate a broader base for thin layer correction for laminated soil deposits which contain layers with thicknesses similar or smaller than the cone diameter by means of calibration chamber testing. Therefore the influence of stress level, void ratio and layer thickness relative to the cone size is investigated. A relevant range of stress levels, sand porosities and layer thickness is covered related to the top 10 m of tidal flats as is present in Groningen.

1.3 Approach, scope, limitations

To generate a broader base for thin layer correction for laminated soil deposits which contain layers with thicknesses similar or smaller than the cone diameter calibration chamber tests are performed. Cone penetration tests are performed in artificially built up layered soil. The tests are not primarily meant to simulate a real situation in the field, but to investigate the influence of some governing factors (stress level, void ratio and layer thickness relative to the cone size).

Several soil models have been created, having different layer configurations and/or porosities. The layered models contain thin layers of equal thickness; other configurations have not been investigated. Layer thicknesses of 20, 40 and 80 mm are applied (0.56, 0.8, 1.6 and 3.2 times the cone diameter). Artificial clay is used to model the weaker layers. Loose and medium dense sand layers are prepared to model the stronger layers. Besides layered models, also homogeneous sand models were prepared to measure the “true” sand cone resistance. All soil models are fully saturated.

Cone penetration tests are performed at vertical effective stress levels up to 100 kPa. In most soil models multiple tests are performed at different stress levels. Besides the 25 mm diameter cone, also the more common 36 mm cone is applied in some soil models.

The test results are used to derive thin layer correction factors for laminated soil deposits which contain layers with thicknesses similar or smaller than the cone diameter.

The outcome of the physical modelling tests has simulated by means of analytical methods. Simulations can be used to gain a better understanding and to derive thin layer correction factors for cases that aren't covered by the physical modelling test program.

1.4 Report structure

The structure of the report is as follows:

- Chapter 2 describes the test program, setup and procedure.
- Chapter 3 describes the soil model preparation the soil properties.
- Chapter 4 describes the test results (remarks and examples are given to better understand the measurements).
- Chapter 5 describes the derivation of thin layer correction factors from the test results.
- Chapter 6 presents the outcomes of the simulations by analytical methods.
- Chapter 7 discusses some aspects with respect to the test results and practice and
- Chapter 8 concludes with the conclusions of this study.

2 Test program, equipment and procedure

2.1 Test program

A physical modelling parametric study is defined to investigate the influence of stress level $\sigma'_{v,}$ void ratio and layer thickness H relative to the cone diameter d_{cone} on the measured cone resistance. This test program is given in Table 2.1. CPTs are performed in saturated layered soil deposits, which are artificially built up in a cylindrical container. In most soil models successive tests are performed at different stress levels, since the preparation of a soil model takes a lot of effort. Cone penetration tests are performed at vertical effective stress levels up to 100 kPa. The stress level is limited by the test setup.

Next to 25 mm diameter cones, also the more common 36 mm cone is applied in some soil models. Loose and medium dense sand layers/models are prepared. The density index I_D gives the relative position of the void ratio with respect to the minimum and maximum void ratio. The layered units of multiple thin clay and sand layers, each having an equal thickness H , were sandwiched between two thicker sand layers. Uniform loose and medium dense sand models are prepared in addition to the layered models to serve as a reference (indicated as "REF" in Table 2.1).

Besides tests in which the dependency on stress level, void ratio and layer thickness is investigated, also tests are included regarding:

- Effects of prior cone penetrations (soil model 5: three CPTs at the same stress level).
- The layer configuration (soil model 9: the layered part is sandwiched between two thicker clay layers instead of two thicker sand layers).

Soil model	d_{cone} [mm]	I_D [%]	H [mm]	H/d_{cone} [-]	No. of CPTs	$\sigma'_{v;CPT1}$ [kPa]	$\sigma'_{v;CPT2}$ [kPa]	$\sigma'_{v;CPT3}$ [kPa]
1	25	30	REF	-	3	25	50	100
2	25	30	40	1.60	3	25	50	100
3	25	30	20	0.80	3	25	50	100
4	25	60	40	1.60	3	25	50	100
5	25	60	REF	-	3	100	100	100
6	36	30	REF	-	1	50	-	-
7	36	30	20	0.56	1	50	-	-
8	25	60	20	0.80	3	25	50	100
9	25	30	20	0.80	3	25	50	100
10	25	30	20	0.80	3	10	20	30

Table 2.1 Test program

The test program is a continuation of earlier work (Van der Linden, 2016). However, a new test setup had to be created to apply higher stress levels. This tests setup has been developed and tested during the start-up phase. During this setup phase also some CPTs are performed in both layered and homogeneous soil models. More details about the test setup and the results of this start-up phase are given in Annex C.

From the start-up phase it is concluded that the test results are affected by:

- Side wall friction and arching effects, since the results indicated a non-uniform stress distribution over the height of the soil model.
- Effects from the rigid top plate: the uniform displacement condition leads to a non-uniform stress distribution under the plate and counteracts the soil deformations at surface level as result of the penetration process.
- Non-homogeneous distribution of the void ratio due to the preparation method and/or the above mentioned arching and/or the way of applying the vertical stress by hydraulic jacks and the rigid top plate.

Therefore some improvements are made for the final test program, which are described in Paragraph 2.2.

2.2 Test equipment

2.2.1 Test setup

The test setup consists of the following components:

- A bottom plate, acting as a base for the test setup, which is placed on a rubber mat in order to reduce vibrations transferred through the floor (loose models are susceptible to disturbance due to vibrations).
- A hydraulic jacking unit in order to push the cone into the soil model and a reaction frame for this hydraulic jacking unit.
- A calibration chamber which contain the soil model.

Figure 2.1 (left) gives an impression of the test setup (the hydraulic jacking unit is not present at the photographs).

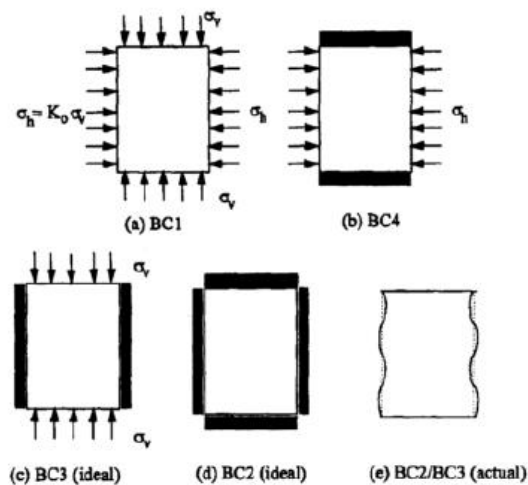


Figure 2.1 Impression of the test setup

The maximum penetration depth is limited by the stroke of the hydraulic jacking unit, which is equal to 1 m. Due to cone penetrometer positioning and the height of the attributes on top of the soil model, the maximum soil penetration is approximately 0.75 m.

2.2.2 Calibration chamber

Salgado et al. (1998) distinguish between calibration chambers based on the boundary conditions, see Figure 2.2. The boundary condition can be a constant stress or a no displacement condition. During the start-up phase the calibration chamber had only non-displacement boundaries. However, the results were not satisfying and therefore some improvements are made to have constant stress boundary conditions. A BC1 calibration chamber, with exception of the bottom boundary condition (no displacement), is created. No wall friction will be present when “constant stress” lateral boundary conditions are applied. Therefore also possible soil arching effects will be reduced. Further, a “constant stress” top boundary condition leads to a uniform stress distribution over the area of the soil model.



Type of Boundary Conditions	Lateral Boundary Conditions	Top and Bottom Boundary Conditions
BC1	Constant Stress	Constant Stress
BC2	No displacement	No displacement
BC3	No displacement	Constant Stress
BC4	Constant Stress	No displacement

Figure 2.2 Types of boundary conditions in a calibration chamber (after Salgado et al, 1998)

The calibration chamber consists of the following components:

- Cylindrical stackable steel cells with inner diameter of 0.9 m which contain the soil model, see Figure 2.1. Soil models with a total height of 0.96 m are prepared. Rubber O-rings act as a seal between the cell interfaces.
- The cell wall is lined with a flexible rubber membrane and the space in between can be filled with a film of water. A porous geotextile is placed in between the wall and the membrane in order to ensure that water can enter the space between the wall and the membrane. The membrane is placed over a height of 0.72 m by stacking it in between cells, see Figure 2.1 (right). After filling the space between the membrane and the container wall with water, the water pressure can be controlled and the soil model will be pressurized. In this way the soil model isn't in direct contact with the container wall. No side friction will occur, since water cannot mobilize shear stresses. A coefficient of lateral earth pressure $K_0 = 0.5$ is applied for all tests.
- A flexible water filled cushion on top of the soil model to control the vertical stress level. The cushion has four holes to be able to penetrate the soil model. Tubes are placed to fixate the holes. The cushion has a height of approximately 0.15 m. A vertical stress can be imposed by controlling the water pressure inside the cushion. This cushion is fabricated at Deltares by sealing porous foam with flexible silicone, see Figure 2.4 (left). The stress level that can be applied at the soil model is limited by the water cushion, since leakage takes place at high pressure levels.
- A circular steel plate on top of the cushion (also with four gaps) which is fixed to a steel ring on top of the cells. This plate acts as reaction frame for the water cushion, see Figure 2.4 (right).

- A total stress transducer at a depth of 0.72 m to measure the total vertical soil stress. The total stress transducer is manufactured by Kulite, and of the type IPT-10N-750-200A, with a range of 0 to 137.9 kPa. Typical accuracy is better than 5 kPa.
- A circular plate at the bottom of the cells. A circular filter plate is placed on top of this plate and a circular geo-textile in between in order to guarantee drainage over the whole area.
- A drainage tap connected to the circular bottom plate in order to allow for a controlled variation of the water level.

The applied lateral and vertical stress is measured using pressure transducers connected to the water supplies. Any change in volume of the soil model was monitored by measuring the volume change in the water supply of both the membrane and the cushion and any water dissipated through the bottom drain of the test setup. A schematization of the test setup is given in Figure 2.3.

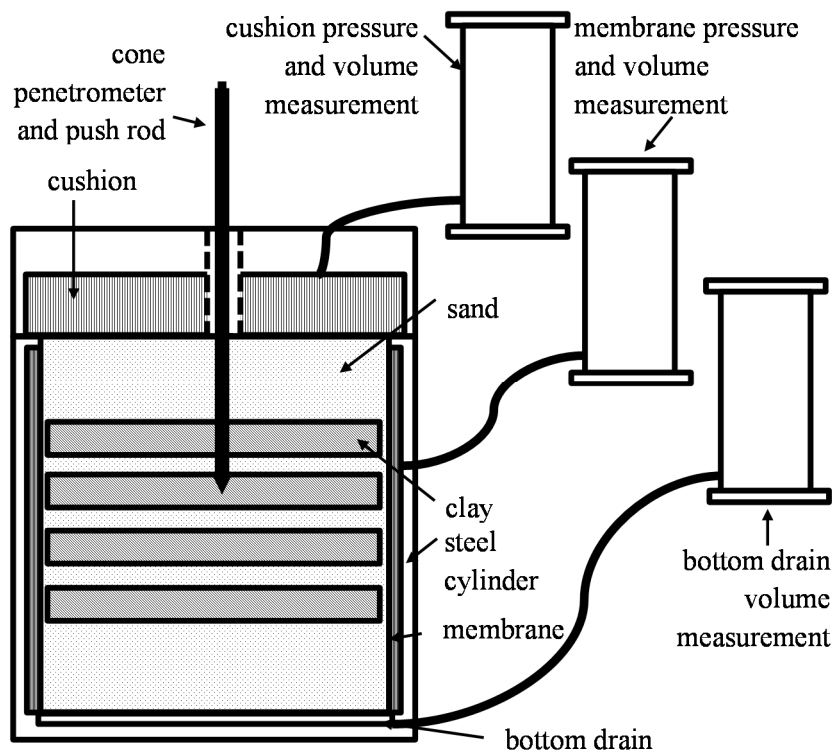


Figure 2.3 Schematized test setup

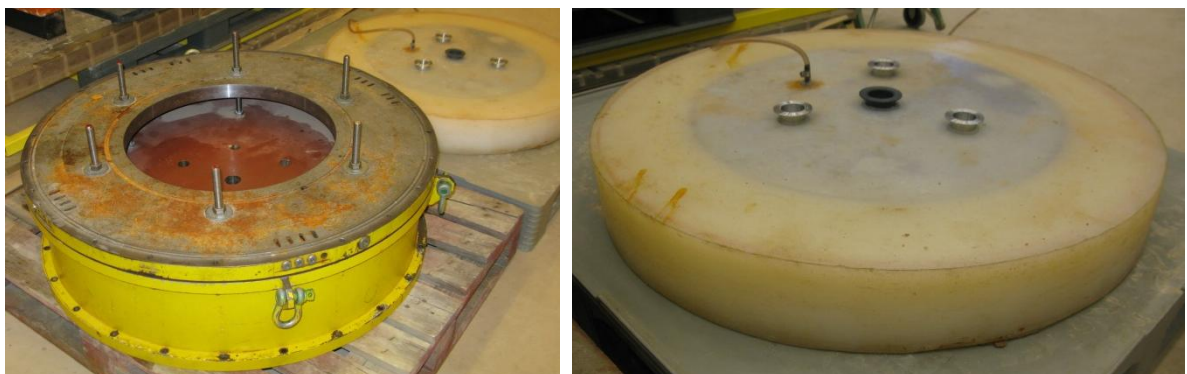


Figure 2.4 Water cushion (right) and reaction frame for the water cushion (left)

2.2.3 CPT equipment

Subtraction cone penetrometers are employed and are manufactured and calibrated by Fugro Engineers B.V. Three cone penetrometers with a diameter of 25 mm and one with a diameter of 36 mm are applied. Table 2.2 provides an overview.

Cone Penetrometer	25 mm	36 mm
Cone Face Area	500 mm ²	1,000 mm ²
Cone Diameter	25.3 mm	35.8 mm
Cone Net Area Ratio	0.50	0.45
Calibrated Range	0 to 15 kN	0 to 25 kN
Maximum Rating	0 to 150 kN	0 to 50 kN
Max. Sampling Frequency	4 Hz	4 Hz

Table 2.2 Cone Penetrometer Characteristics

The penetrometers are not equipped with pore pressure transducers. Based on earlier experience (Van der Linden, 2016) it was assessed that excess pore pressures during sounding are near hydrostatic, in which case the influence of excess pore pressure on the cone tip resistance due to geometry is less than one percent of the measured value.

The penetration depth of the cone penetrometer is measured using a depth encoder, type CAN-Encoder 7501. Typical accuracy is better than 1 mm.

The measurement uncertainty of the cone resistance has been estimated with the uncertainty provided in the calibration certificates. In the softer clay layers of about 500 kPa cone resistance the measurement uncertainty is about 35 kPa (or 7.0 % of the indicated value). In loose sand with a cone resistance of about 3.5 MPa, the measurement uncertainty is assessed to be about 45 kPa (or 1.3 % of the indicated value).

2.3 Test procedure

2.3.1 General Procedure

In general, the testing procedure is as follows:

- During model preparation the membrane for applying lateral pressure is held under vacuum. This prevents soil model disturbance due to unwanted membrane deformation or movement.
- After completion of the soil model preparation, the water-level is lowered to approximately 0.2 m below the soil surface level. This will result in a small negative pressure which provides additional soil strength due to capillary action while maintaining soil saturation and void ratio. This additional strength will limit any soil model disturbance due to placement of the cushion which is used for applying vertical stress on the soil model.
- Positioning of the cushion and the steel reaction ring using an overhead crane.
- Assembling the reaction frame and the hydraulic jacking unit onto the bottom plate.
- Increasing the vertical and horizontal stress level by incrementally increasing hydraulic pressure in the cushion and behind the membrane, respectively.
- Allowing for consolidation of the clay layers before cone penetration testing.
- Connecting the cone penetrometer and pushing the cone to the desired penetration depth using a hydraulic jacking unit.
- In case of multiple CPTs (when employing the 25 mm diameter cone penetrometer), the vertical and horizontal stress are increased to the desired stress level and a subsequent CPT is performed, leaving the previous cone(s) in place.

- After the final cone penetration test, the cone penetrometer is disconnected, the pressure of the cushion and the membrane is released and the steel reaction ring, the cushion, the jacking unit and the reaction frame are removed. The cones and rods remain in the soil body.
- During excavation of the soil model, soil samples are taken to determine the local porosity. This can't be done for the thin layers, since sufficient height (> 5 cm) is needed to take a sample. Also the height of the soil interfaces is measured during excavation. Additionally, photographs of the excavated soil model are taken to capture the displacement pattern around the cone and the rods.

2.3.2 Applying stress levels and consolidation time

The horizontal stress level is 50% of the vertical stress level (the K_0 -value is considered to be circa 0.5). In order to reach the desired stress levels, the stresses have to be increased very carefully and smoothly, since it is known that abrupt increases or movement may alter the void ratio. A rate of 1 kPa/min is applied.

The cone resistance in clay layers depends on the degree of consolidation. Therefore, when the soil model contains clay, full consolidation has to take place before cone penetration is performed. Table 2.3 presents the theoretical consolidation time for different layer thickness H for a consolidation degree of 90% (based on a c_v -value of $1.8 \cdot 10^{-8} \text{ m}^2/\text{s}$). These values are used as a guideline. Also the development of the volume changes over time is used to determine when a CPT can be performed.

H (m)	t (h)
0.02	1.3
0.04	5.2
0.08	20.9

Table 2.3 Time needed for a degree of consolidation $U=90\%$ for different layer thicknesses (t_{layer})

2.3.3 Cone penetration testing

CPTs with a 25 mm diameter cone penetrometer are performed at 300 mm distance from the cell wall. The mutual distance between the penetrations is 260 mm. CPTs with the 36 mm diameter cone are performed in the centre of the cell. See Figure 2.5.

For the 25 mm cone tests three penetrations are performed in the same soil model. Three cones are used, since the cones are left in place after reaching the desired penetration depth to minimize soil model disturbances and to make excavation and examination of the deformed layers possible. When CPTs are performed at different stress levels, the first CPT is performed at the lowest stress level and the last at the highest.

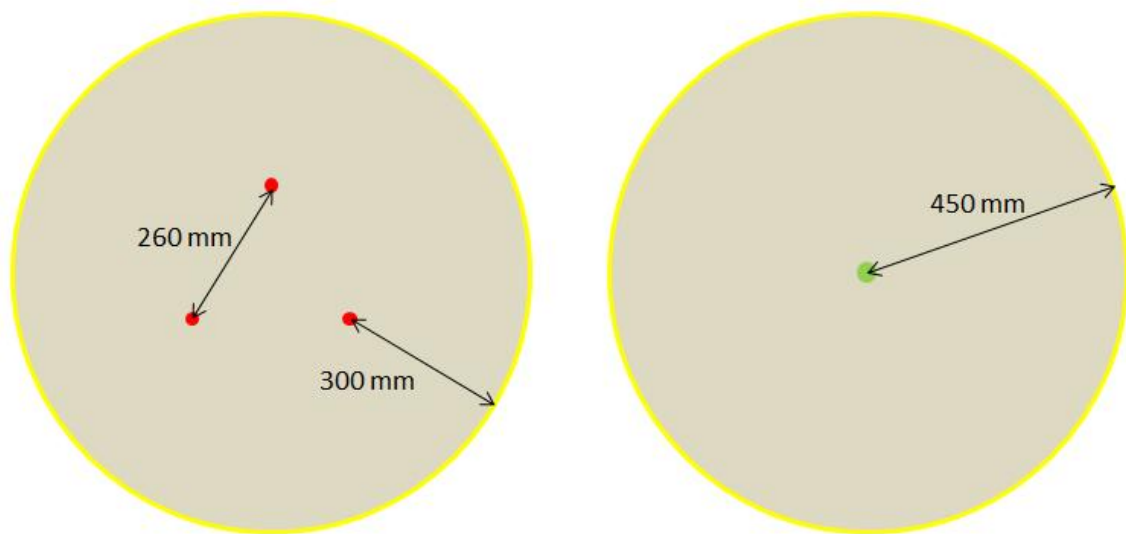


Figure 2.5 Top view with the locations of the cone penetration tests: (left) tests with a cone diameter of 25 mm and (right) tests with a cone diameter of 36 mm

A penetration rate of 4 mm/s is applied in order to obtain one sample every mm, as the maximum sampling frequency of the data acquisition unit is 4 Hz. This penetration rate is lower than requirements according to ISO 22476-1:2013 (which is 20 ± 5 mm per second). Possible rate effects in cohesionless soils are considered to be limited, as discussed in Van der Linden (2016).

2.3.4 Boundary effects and penetration disturbance

Regarding possible boundary effects and the influence zone around the penetrated cone and rod, it was considered to be feasible to perform three cone penetrations tests at one soil preparation when deploying the 25 mm cone penetrometers. This is an efficient way to utilize the soil models, optimizing time and budget. The minimal ratio between the cell diameter and the cone diameter is 25 and the minimal ratio between the distance to the cell wall and the cone diameter is 11. These ratios are considered to be sufficient for the applied void ratios in order to minimize the effects of the rigid lateral walls (Bolton et al. 1990). For the 25 mm cone penetrometers, the ratio between intermediate distance and the cone diameter is about 10. This was assessed to be sufficient to limit soil disturbance between subsequent tests. The rigid bottom boundary will affect the cone resistance near the bottom of the soil model. The boundary effect of the rigid bottom is mitigated by reserving one single steel cell ring (0.24 m) below the cone penetration.

Installation of cone penetrometers will change the void ratio primarily close to the penetration location. Change in bulk density index due to soil displacement by only the cones and rods is estimated (2D) as follows:

- From initially 30% to 30.4% due to the volume displacement of one cone (with rods) with a diameter of 25 mm (surface area of 50 mm^2).
- From initially 30% to 31.1% due to the volume displacement of three cones (with rods) with a diameter of 25 mm (surface area of 150 mm^2).

However, during penetration the surrounding soil will also be sheared, which may lead to further compaction.

2.3.5 Local density measurements

When feasible, samples were taken after cone penetration testing to determine the local density. These measurements are performed in order to check for any local variation. The test procedure and apparatus for these local density measurements are described in Van der Linden (2016). It should be noted that the measurements are performed in disturbed soil, since they are taken after cone penetration testing.

3 Soil model

3.1 Configurations

Cone penetration tests are performed in artificially built up layered soil. The tests are not primarily meant to simulate a real situation in the field, but to investigate the influence of some governing factors (stress level, void ratio and layer thickness relative to the cone size).

Several soil models have been created, having different layer configurations and/or porosities. The layered models contain thin layers of equal thickness. The layered units of multiple thin clay and sand layers were sandwiched between two thicker sand layers to minimize boundary effects. Layer thicknesses of 20, 40 and 80 mm are applied. Artificial clay is used to model the weaker layers. Loose and medium dense sand layers are prepared to model the stronger layers. Besides layered models, also homogeneous sand models were prepared to measure the “true” sand cone resistance. The soil models are fully saturated.

3.2 Material characteristics

Baskarp B 15 sand and Vingerling K147 clay have been used to create the soil models. Principle reasons for using these include extensive prior experience and known characteristics. Additionally, the Vingerling clay is easy to handle and the Baskarp sand has a low coefficient of uniformity (d_{60}/d_{10}), promoting model homogeneity.

3.2.1 Baskarp sand

Some characteristics of Baskarp B15 sand are given in Table 3.1. The minimum and maximum porosities are measured to determine the density index of the soil models. Figure 3.1 shows the grain size distribution for four different samples taken from the batch of Baskarp sand used for the soil models. The sand can be described as fine sand and has a small deviation in grain size.

Characteristic	Abbreviation and unit	Value
Mass-Median-Diameter	d_{50} [mm]	0.136
Coefficient of Uniformity	d_{60}/d_{10} [-]	1.4
Particle Density	ρ_{grains} [kg/m ³]	2650
Minimum Porosity	n_{min} [%]	35.6
Maximum Porosity	n_{max} [%]	47.1

Table 3.1 Characteristics of the applied Baskarp B15 sand

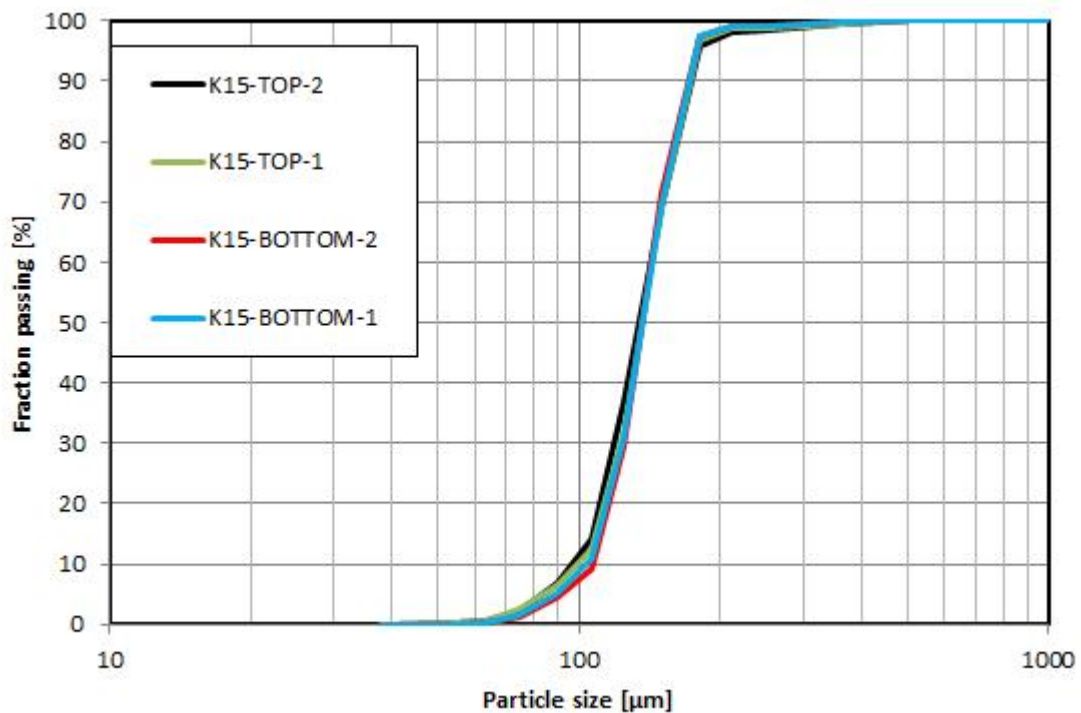


Figure 3.1 Grain size distribution of the Baskarp B15 sand used in the experiments

3.2.2 Vingerling clay

The Vingerling K147 clay is classified in terms of water content and Atterberg limits. These characteristics are given in Table 3.2.

Characteristic	Abbreviation and unit	Value
Water Content	W [%]	22.8 ± 0.3
Liquid Limit	LL [%]	32.3
Plastic Limit	PL [%]	15.8
Plasticity Index	PI [%]	16.5
Liquidity Index	LI [%]	46.7

Table 3.2 Characteristics of the applied Vingerling clay (K147)

A K_0 -CRS test is performed to determine the compressibility parameters. From the results the volume change of the soil models due to increasing the stress level can be derived. Figure 3.2 gives the stress-strain diagram obtained from this test. Since the clay is extruded in a vacuum press, the clay has a pre-consolidation stress. However, it is hard to estimate the pre-consolidation stress from this test, since no clear distinction between over-consolidated and normally consolidated behaviour can be made. Further, the permeability, the coefficient of consolidation and the K_0 can be derived from this test.

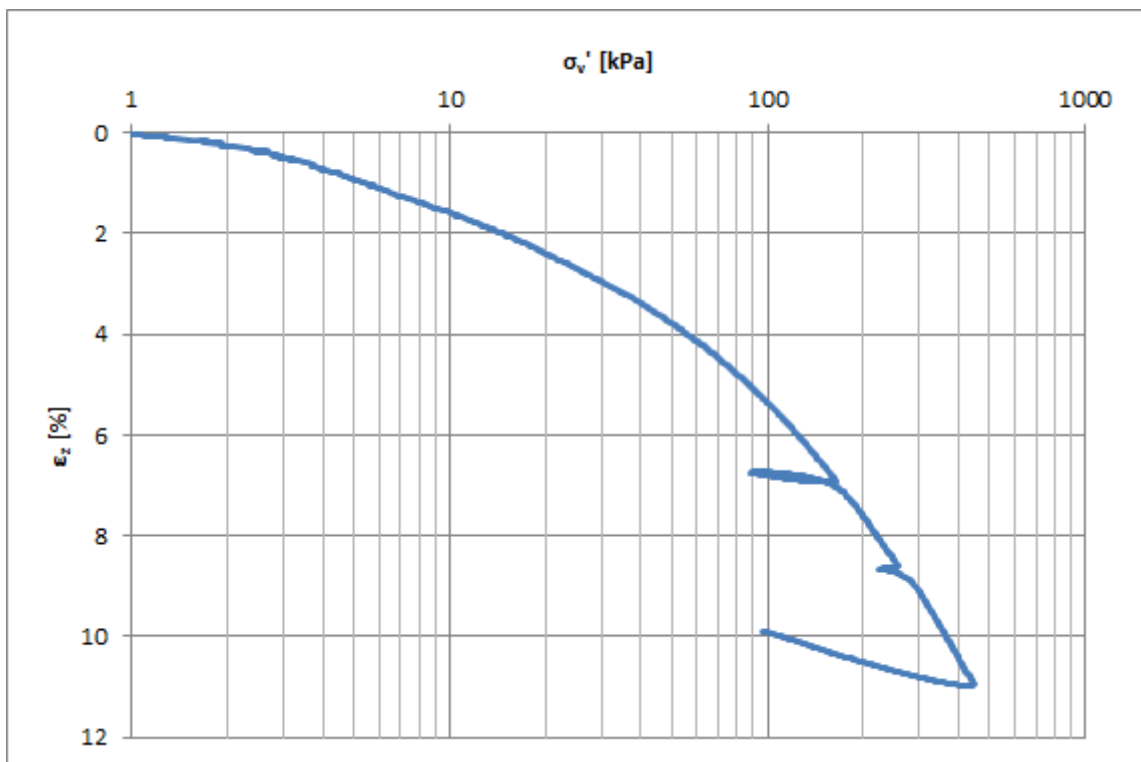


Figure 3.2 Stress-strain diagram as result of K_0 -CRS testing

Four single stage undrained anisotropic consolidated triaxial compression tests are performed to determine the undrained shear strength of the Vingerling K147 clay. A shear rate of 1%/h/hour is applied. The results are given in Table 3.3, Figure 3.3, Figure 3.4 and Figure 3.5. The undrained shear strength can be used to estimate the cone resistance in a pure clay profile. For vertical consolidation stress of 25 and 50 kPa negative excess pore water pressure are found at large strain (critical state), which means that these samples behaves over-consolidated.

$\sigma_{v;cons}$ [kPa]	$\sigma_{h;cons}$ [kPa]	S_u [kPa]
25	16.25	23.8
50	32.5	27.9
100	65	37.9
200	130	60.4

Table 3.3 Undrained shear strength for different consolidation stresses

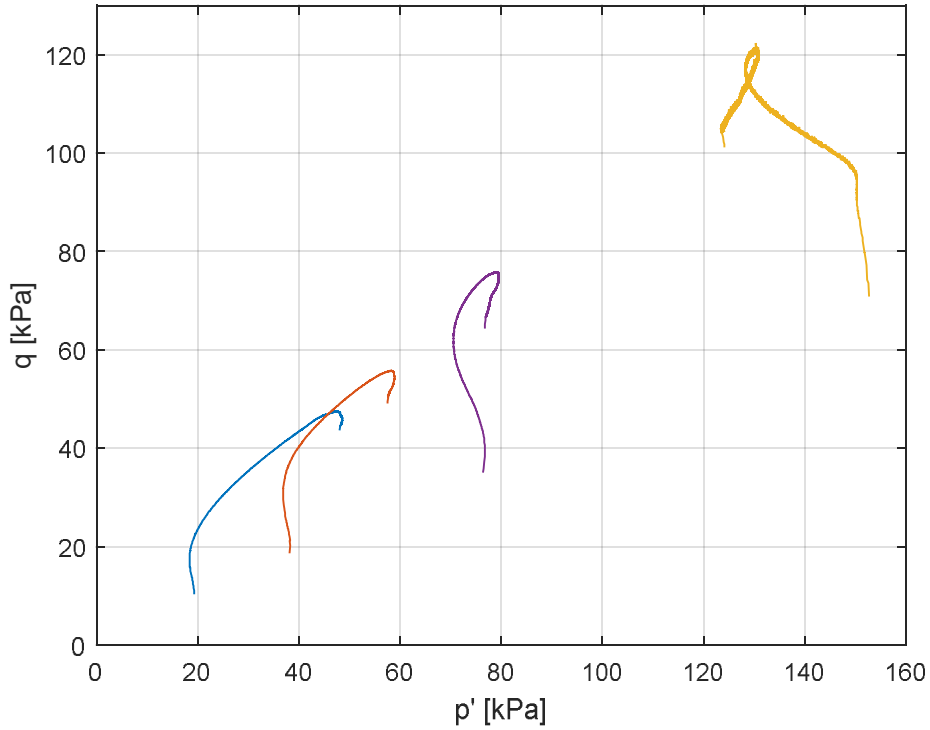


Figure 3.3 Stress paths shear phase

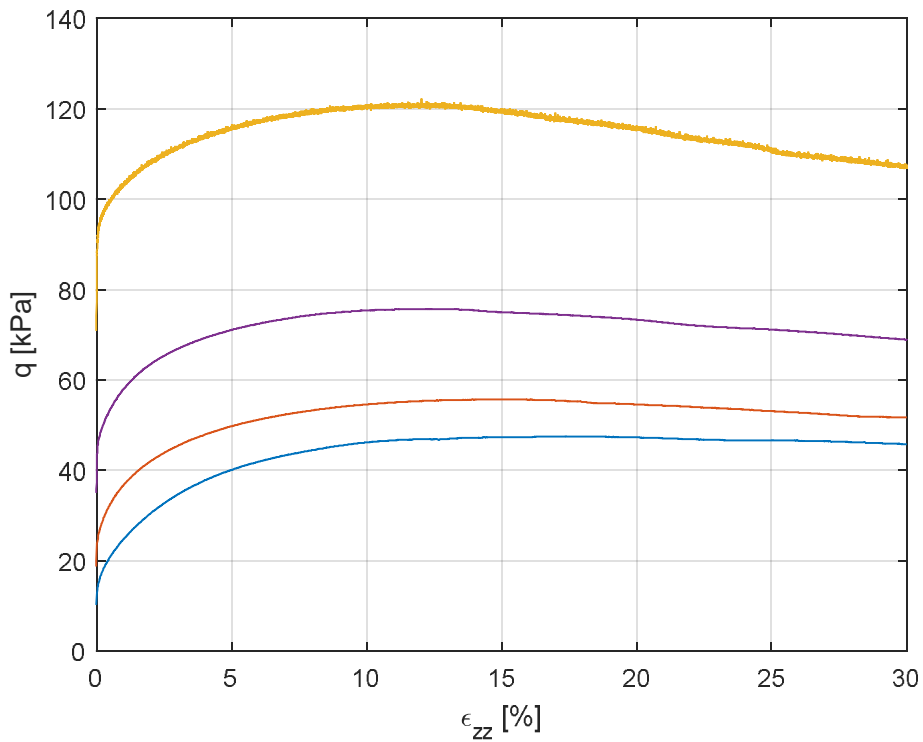


Figure 3.4 Development of deviator stress during shearing

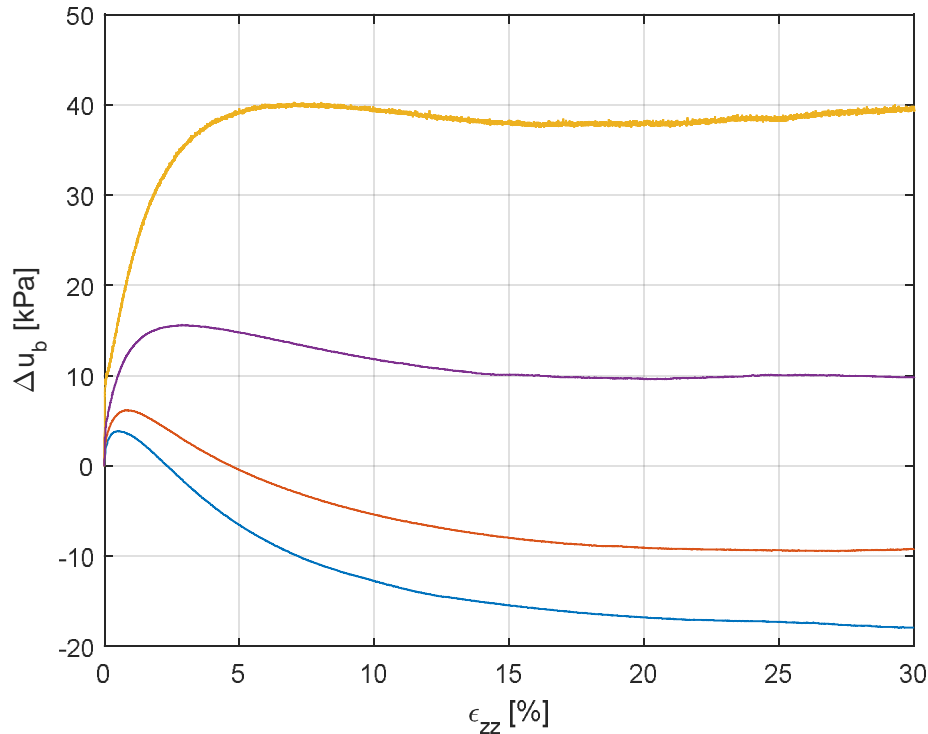


Figure 3.5 Change in water pressure measured at the bottom of the sample during shearing

3.3 Preparation method

The sand models or layers are prepared by pluviation of dry sand in a partially water-filled container. This method results in a fully saturated soil model. In order to compare the results from different soil models the same preparation technique is applied for homogenous sand models as for the layered soil models. By continuously raining sand close to the water surface and controlling the free water height between 1.5 and 2.5 cm, a loose state is achieved. A medium dense state is achieved by periodically gently tamping the sand surface during pluviation (Van der Linden 2016, Van der Linden 2017, De Lange et al. 2016). During preparation the bulk density was closely monitored by measuring the sample height and weight.

Table 3.4 compares the measured density index with the target density index. The density index is based on the whole model in case of reference models and on the thick top and bottom layers in case of layered models. The measurements give good confidence in the preparation methods. The average density index of all loose and medium dense models is equal to respectively 33% and 59%. Deviations from the target up to 11% are found.

Soil model	1	2	3	4	5	6	7	8	9	10
Target I_D [%]	30	30	30	60	60	30	30	60	30	< 30
Measured I_D [%]	36	29	28	54	60	41	32	61	28	18

Table 3.4 Comparison between target and achieved density index

For the layered soil models, clay layers were placed after trimming prefabricated clay bricks to the required dimensions. The Vingerling K147 clay is delivered by Sibelco in bricks of approximately 12.5 x 12.5 x 32 cm sealed in plastic. First the brick are trimmed into bricks of

10 x 10 x 25 cm with a steel wire. This mitigates possible disturbance due to shipping and handling. Then thinner slices are cut from the reshaped brick and are placed on the sand. The slices are pushed gently together to prevent formation of air pockets between the bricks as much as possible. The clay slices are placed in such way that the cone penetrates at sufficient distance from an interface between slices, see Figure 3.6.

By lowering the water table below the surface level of the sand but keeping it above the level required to prevent air entry into the sand model, suction forces due to capillary action provides additional strength to the sand. This additional strength ensures minimal disturbance of the sand skeleton during placement of the clay slices. The influence of lowering the water table is investigated and it is concluded that this action has no significant influence on the porosity. This technique was validated by Van Der Linden (2016), who didn't observe swell of the clay layers after several days.

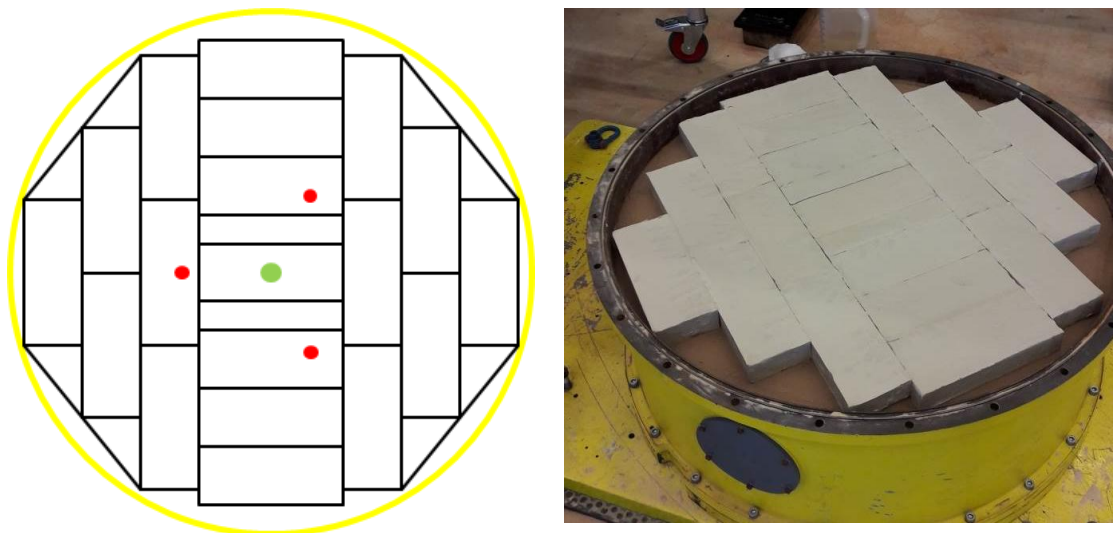


Figure 3.6 Layout of clay slices from a schematic top-view (left) and photographed during preparation (right)

3.4 Preparation accuracy

The bulk density is used to determine the density index of the prepared models. For large volumes this is a robust method: propagation of uncertainty shows that the error in estimating the bulk relative density of the 0.96 m high soil model is better than 2.5% I_D (EA-4/02, 2013). The uncertainty strongly depends on the sample height, since diameter and mass of the sample are accurately known compared to the sample height.

While this method works well for large volumes, the measurement uncertainty in sand layer height begins to govern the estimated density for thinner layers. E.g. when considering a layer thickness of 2 cm, a measurement error of 1 mm can result in an error of 25% in density index. Therefore this method cannot be used to assess the relative density of small layers.

The soil models are prepared in a consistent manner by using the same procedure and technicians. Although local variations may occur, it is reasonable to assume that the bulk density is representative for the local density.

After testing samples are taken during excavation of the model to determine the local density. For these small, but accurately known mass and volume, density measurements the measurement uncertainty is assessed to be about 6% I_D . The post-test density measurements cannot be directly used to assess the pre-test density, since cone penetration

and altering the stress levels will affect the density. However, these measurements are used to assess local variation.

3.5 Post-test local density measurements

The results of the post-test local density measurements are given in Annex B. A standard deviation in density index of 10% is found for the reference models, which is in line with the measurements during preparation. Based on the pre-tests and post-test measurements it is concluded that this value is a representative upper bound for all the soil models. A higher standard deviation is found for soil model 10 (14%). In this special case it was intended to prepare a very loose model and it turned out that structure was not very stable. Therefore a larger variety is observed in the post-test measurements, which is not representative for the other models.

Figure 3.7 depicts a comparison between the average of the local post-test density measurements and the pre-test bulk density. Higher densities, up to approximately 20% I_D , are found after testing. The results for soil model 9 give an even higher deviation. However, this result is seen as an outlier since the model configuration strongly deviates from the other models. Though the measurements generally show an increase in density after testing, no conclusions can be drawn for the thin layers, since the clay layers influence what is happening in the interbedded thin sand layers.

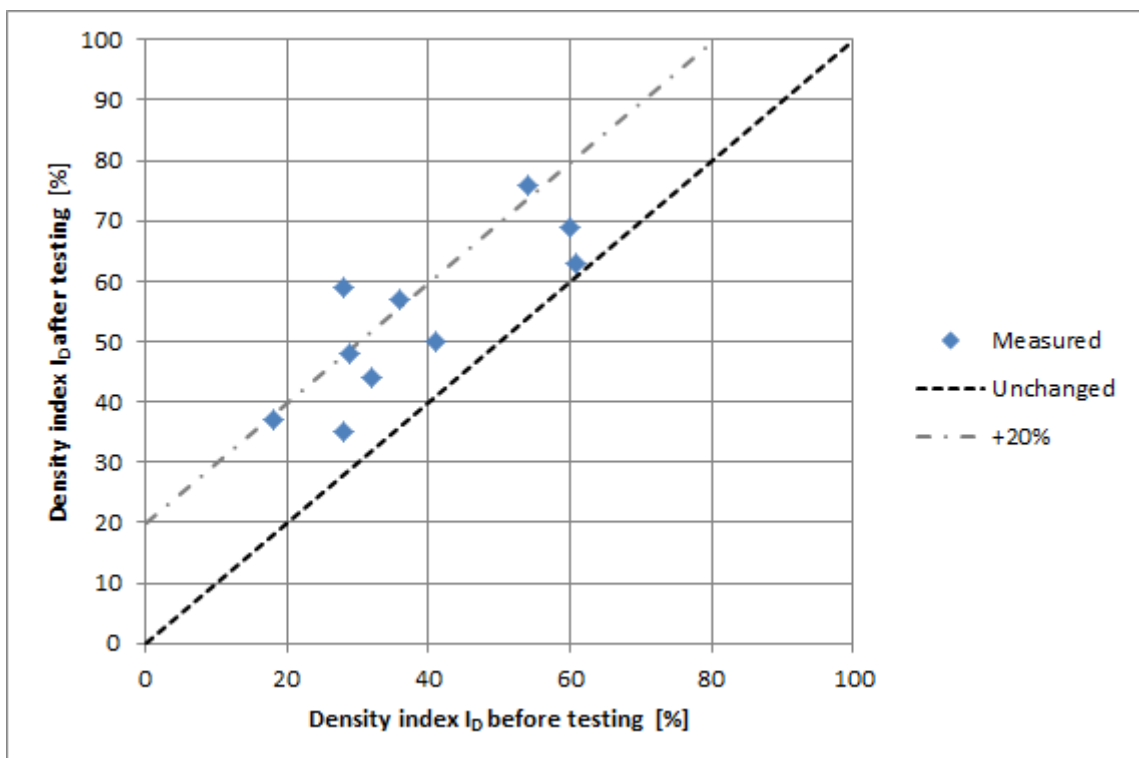


Figure 3.7 Comparison between measured bulk density before testing and average of local densities after testing

4 Test results

4.1 Data processing

The test results are given in Annex A. For each soil model the following four graphs are made:

- The cone resistance q_c as function of depth.
- The sleeve friction as function of depth.
- The friction ratio as function of depth and.
- The soil behaviour type index I_c (Robertson, 2009) as function of depth.

Data processing is limited to shifting the baseline values of the sensors to zero at the start of the test. The depth presented in the graphs is the level of the cone base. The friction ratio is defined as the ratio of the sleeve friction and the q_c at the same level as the middle of the friction sleeve. The reference depth is determined by looking where the q_c starts to increase. The positions of the clay layers are indicated by grey areas. Some discrepancies between the indicated level and the actual level of the clay layers may exist, since the reference depth may deviate from the real surface level depth, due to effects from the tubes which are placed to protect the cushion.

4.2 General remarks on the tests

The test series has been executed successfully and the test setup proved to work properly. Some remarks on the test are given to get a better understanding of the results:

- Leakage of the cushion occurred for pressures higher than 100 kPa during cone penetration testing in soil model 1 and 2. Therefore the third CPT in soil model 1 was performed under an overburden pressure of 100 kPa (instead of 200 kPa) and only two CPTs are performed in soil model 2 (instead of 3).
- Many results show an initial peak in cone resistance at about 5 cm depth. This is an artefact of the tubes which are placed to protect the cushion. The tubes are initially moving along with the cone, affecting the cone resistance and sleeve friction. The most extreme examples are found for the first CPT in the first soil model, where the tube moved along with the cone up to 20 cm and for the first CPT in soil model 9, where the tube moved along with the cone up over the whole depth. Therefore the results over these specific depths should be ignored. Therefore, CPT 1 in soil model 9 is not given in Annex A.
- Local variety in void ratio is observed from the post-test local density measurements (see Annex B). A lower density index at a depth of about 40 to 45 cm below surface level compared to the rest of the model is found for soil model 5. This clearly affects the cone resistance at the same depth. Similarly, based on the cone resistances measured in model 1, a lower density index is expected at a depth of about 30 to 35 cm below surface level. However, not such a clear correlation with the local density measurements is found for this case. Another explanation for the observed trend in cone resistance can be a possible non-uniform lateral stress level during the first tests whereby the horizontal stress is controlled.
- For soil model 10 a large variety in void ratio is observed from the post-test local density measurements. It was intended to prepare a very loose soil model. However, from the post-test local density measurements higher densities are found at the top and bottom of the sand layers than in the middle of these layers. The very loose structure seems to be

not very stable and therefore it is concluded that the density of the thin layers is probably higher than that of the top and bottom layers.

- During model preparation, classification tests are performed on the clay to assess whether the clay is uniform over all tests. Deviations from the other models are found during preparation of model 9 and 10: higher water contents (around 24.5%) and undrained shear strengths of about 18 kPa were measured (torvane and pocket penetrometer), while strengths of about 24 kPa were measured for the other models. Therefore, the results of test 9 and 10 may differ from the other results.
- The degree of consolidation influences the measured cone resistance. The degree of consolidation of the clay layers is assessed by monitoring the measured volume changes. However, some difference in degree of consolidation cannot be excluded.
- Soil will move along with the cone during installation, which complicates the interpretation of the measurements. After cone penetration testing, sand bulbs are found in the clay layers and clay is smeared along the sleeve and the rod. The jumps in cone resistance in the thicker clay layers of soil model 9 are attributed to the fact that sand is taken along with the cone to a certain depth in the clay layers.
- A somewhat higher lateral pressure is applied for CPT 2 and 3 in soil model 5 compared to CPT 1 (difference of about 1 kPa). Therefore, the observed changes in cone resistance should not be explained by change in void ratio only.

4.3 Example – 36 mm cone tests

Figure 4.1 gives the q_c measured by the 36 mm cone in soil model 6 (reference model, $I_D = 41\%$) and soil model 7 (layered model, layer thickness is 2 cm, $I_D = 32\%$). The q_c -profile in the reference model is quite uniform. Some variation in local density is expected, which is confirmed by the post-test local density measurements.

The q_c -profile in the layered model is affected by the cylindrical tube over the first centimetres, while it is moving along with the cone. For deeper levels the measurement is not influenced by the tube. The effects of the layered part on the q_c -profile are clearly visible. The layered part is sensed by the cone at a certain distance and the resistance is decreasing to an almost constant value over the layered part. The individual thin sand layers can be hardly distinguished from the profile. Low contrast is found since the ratio of layer height over cone size is relatively small ($H/d_{cone} = 0.56$). After leaving the layered part, the resistance develops again in the thicker bottom sand layer.

The measured resistances in the thin sand layers show a big difference with the reference model. However, a direct comparison cannot be made, since a difference in density is observed during model preparation. It also should be noted that the resistance measured in the thicker top and bottom sand layers may be influenced by the clay layers of the layered part.

Figure 4.2 gives the measured sleeve friction during the same tests. An almost constant value is measured in the reference model. Higher friction is measured in the layered part of the layered model. During penetration in the thicker bottom sand layer of the layered model, the friction is higher than in the reference test. Possibly, clay that is taken along with the friction sleeve influences the measurement. See also the photographs in Annex B and C.

Figure 4.3 gives the soil behaviour type index I_c (Robertson, 2009) as function of depth. The reference model 6 behaves like silty sand, while the thicker upper and bottom of the layered model behave like a “sand mixture”: silty sand to sandy silt. The layered part behaves like

silty clay to clay. No distinction between the thin layers is found by means of the soil behaviour type index I_c .

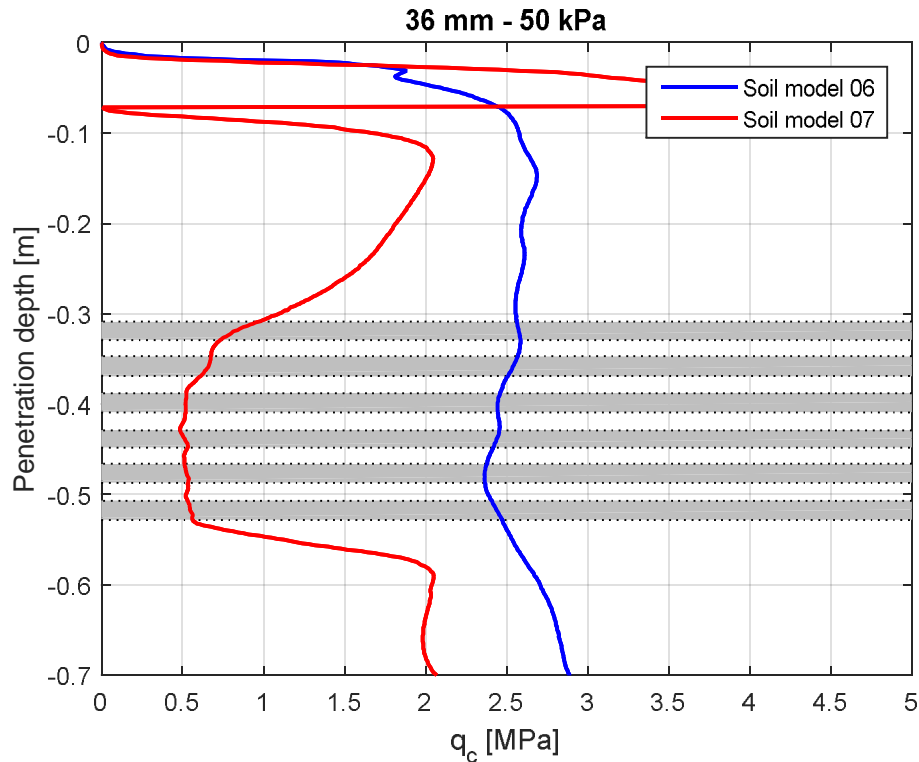


Figure 4.1 Measured cone resistance over depth

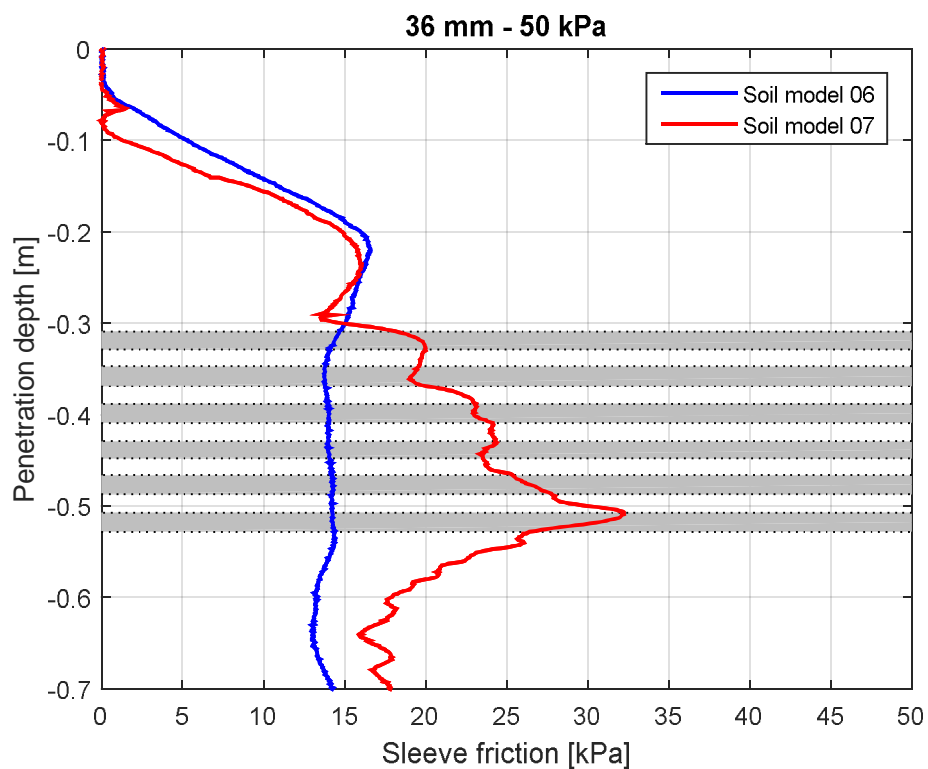


Figure 4.2 Measured sleeve friction over depth

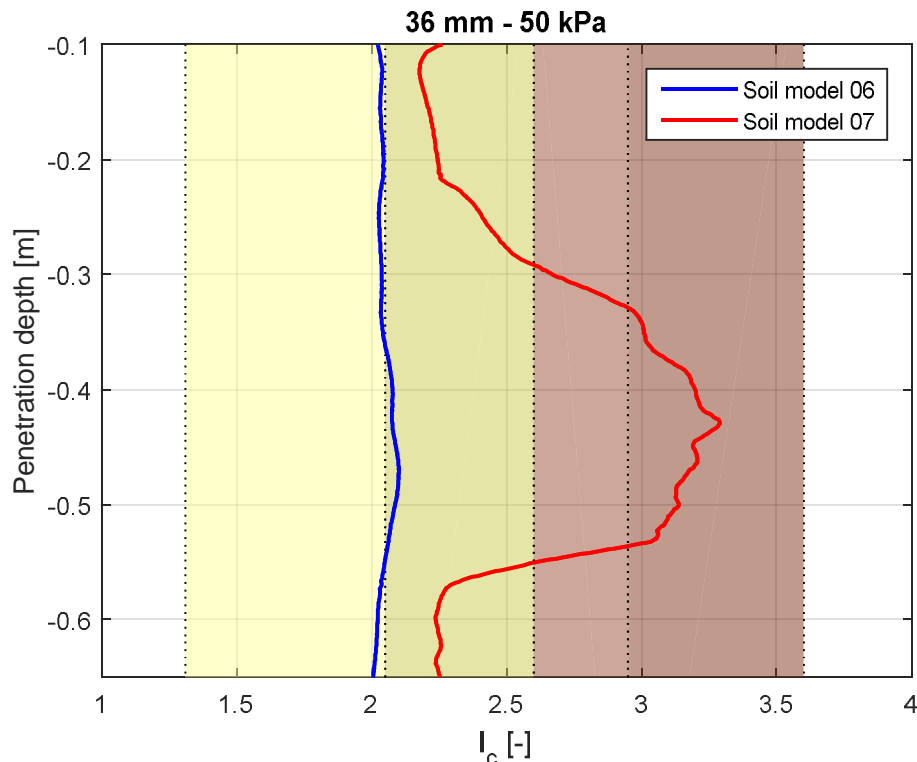


Figure 4.3 Soil behaviour type index I_c (Robertson, 2009) as function of depth

4.4 General observations layered soil models

Figure 4.4, Figure 4.5, Figure 4.6 and Figure 4.7 give results from two different soil models to show the influence of layer thickness and sand density. The presented tests are all performed with a 25 mm cone. From these figures the following conclusions are drawn:

- Greater contrast between cone resistance of the thin stronger and weaker layers is found for higher sand density, higher stress level and larger layer thickness.
- Only little contrast is found for the loose layers of 2 cm thickness. This is also observed for the 36 mm cone, see Section 4.3. The layered part of the soil model behaves in these cases almost like a uniform mixture of sand and clay and individual layers cannot be distinguished at the presented scale.
- The resistance measured in the clay layers is clearly affected by the sand density, while the layer thickness seems to have a smaller influence.

It should be realized that there is some variation in layer thickness, sand density and clay properties. However, the above conclusions remain unchanged with this in mind.

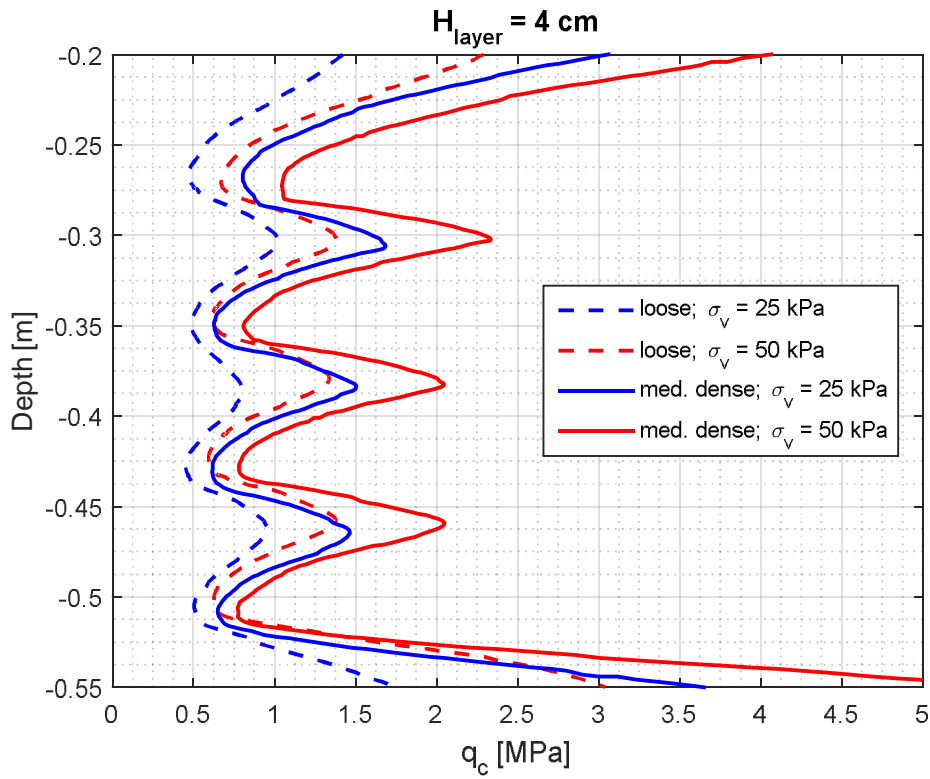


Figure 4.4 Results from soil model 2 and 4 (depths are shifted for comparison purposes)

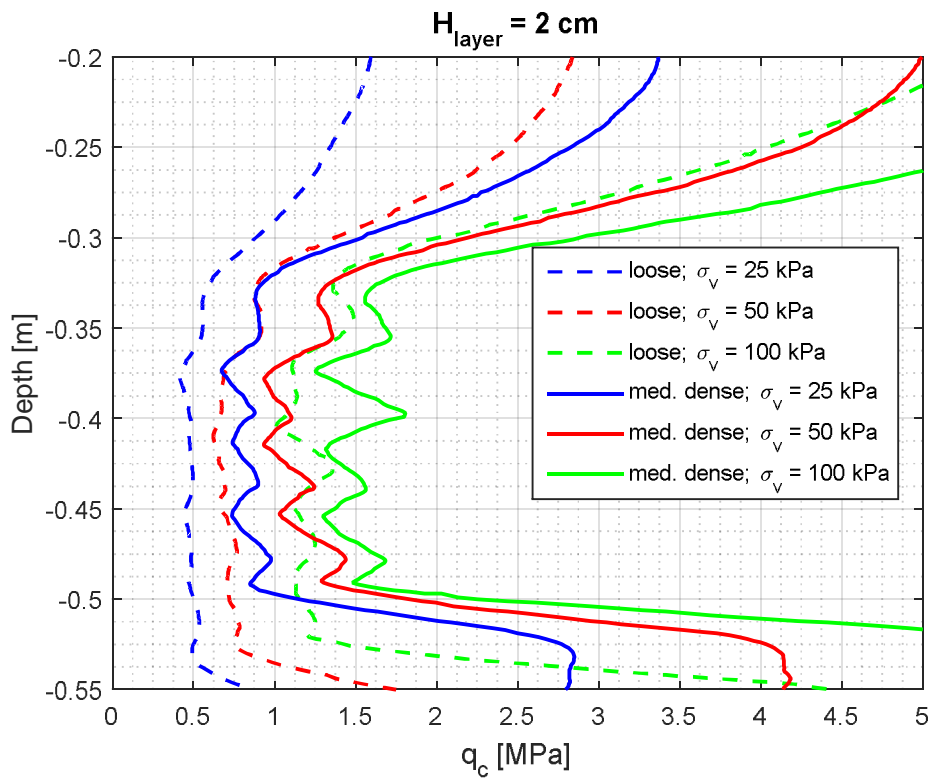


Figure 4.5 Results from soil model 3 and 8 (depths are shifted for comparison purposes)

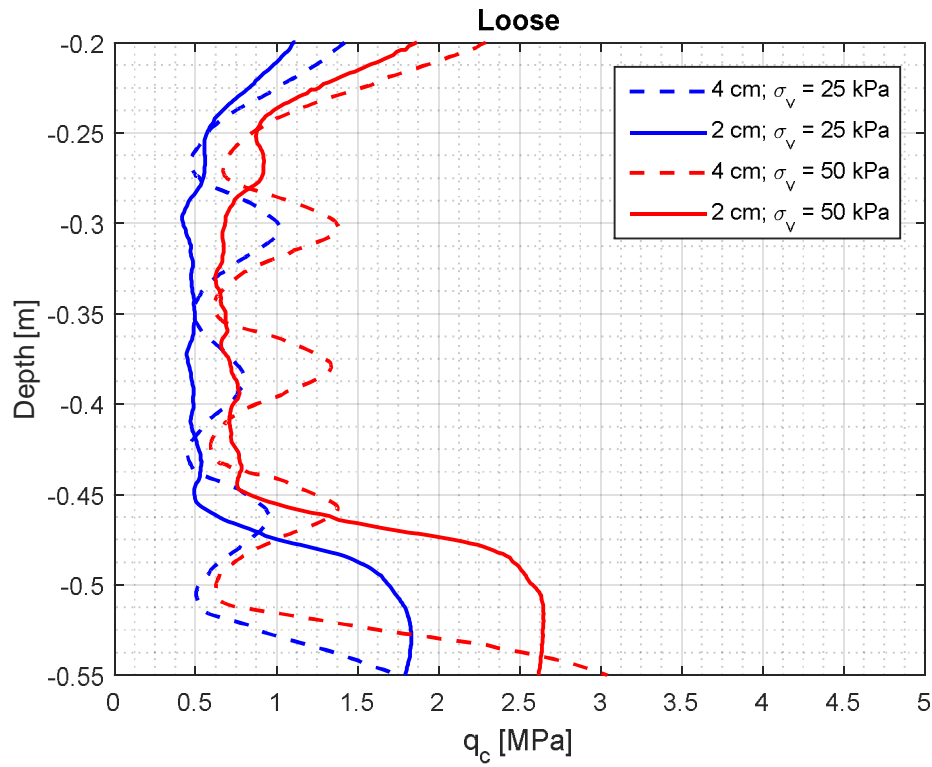


Figure 4.6 Results from soil model 2 and 3 (depths are shifted for comparison purposes)

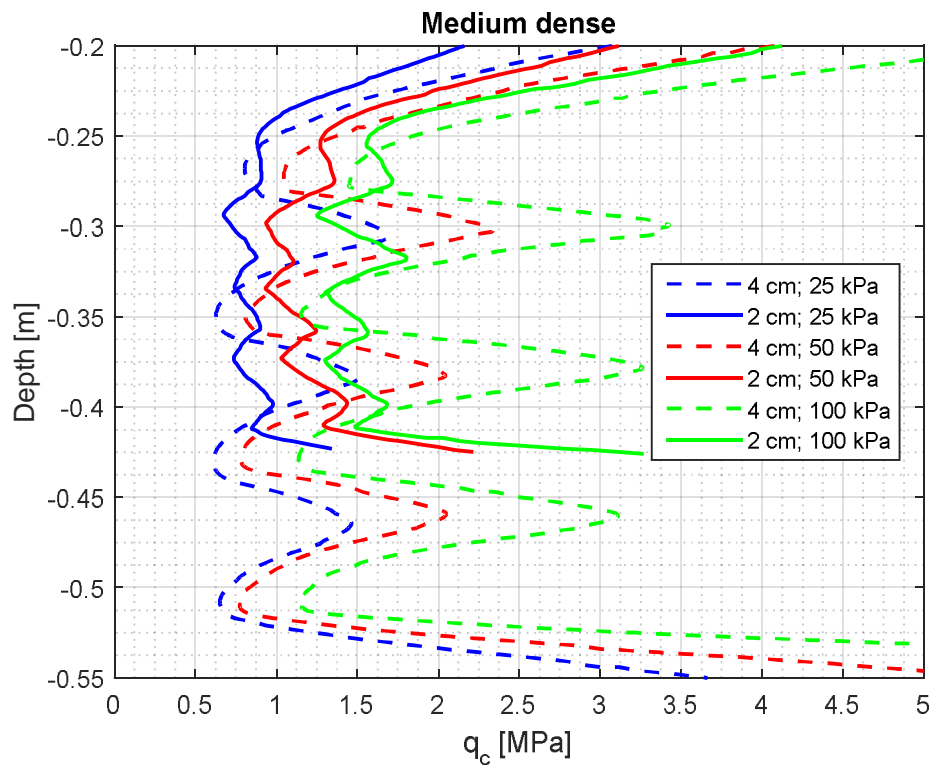


Figure 4.7 Results from soil model 4 and 8 (depths are shifted for comparison purposes)

5 Multiple thin layer correction

5.1 Introduction

For engineering practice, a straight forward manner to correct the measured cone resistance in thin interbedded sand layers is to apply a correction factor on the measurements. In this chapter correction factors for multiple thin interbedded sand layers are derived based on the test results. The thin layer correction factor K_H for a stronger layer in between weaker layers is defined as:

$$K_H = \frac{q_{c;"true"}}{q_{c;m:layer;max}}$$

in which:

- $q_{c;"true"}$ the cone resistance that would have been measured in this same soil if the measurement was not influenced by the overlying and underlying weaker soil.
- $q_{c;m:layer;max}$ the maximum value of the cone resistance measured in the stronger layer.

For the interbedded thin weaker layers a similar correction factor can be derived. Since the layers are relatively thin, $q_{c;"true"}$, determined by applying K_H for the maximum or minimum measured q_c , applies for the whole layer, see Figure 5.1.

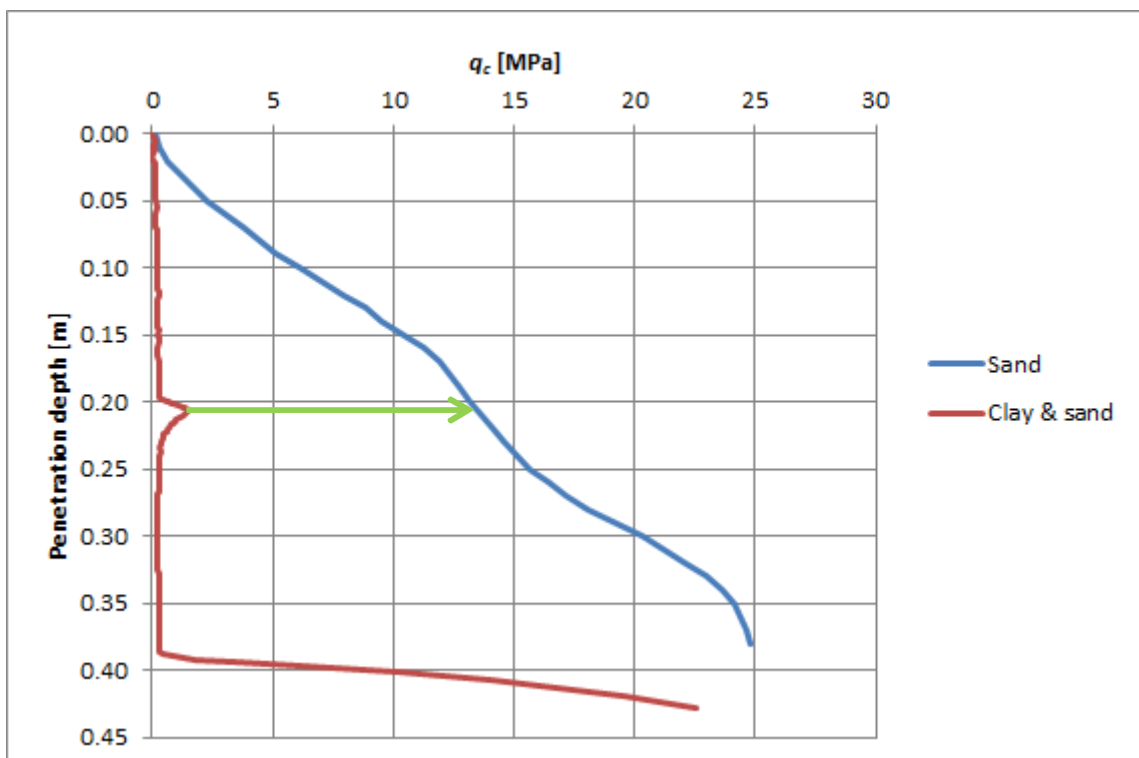


Figure 5.1 Example of thin layer correction (indicated with green arrow)

5.2 Reference tests

Three soil models consisted of sand only: number 1, 5 and 6. Table 5.1 gives an overview of the bulk density index I_D after preparation, the number of CPTs, the location of the CPTs, the applied cone diameter d_{cone} and vertical stress levels σ_v during CPT testing for each soil model.

Soil model	I_D [%]	No. of CPTs	Location	d_{cone} [mm]	σ_v [kPa]
1	36	3	15 cm out of centre	25	25; 50; 100
5	60	3	15 cm out of centre	25	100; 100; 100
6	41	1	centre	36	50

Table 5.1 Relative density index after preparation.

The reference tests are meant to determine the “true” cone resistance. However, a relation between σ'_v , I_D and q_c is needed, since the reference tests do not cover all applied combinations of σ'_v and I_D . Therefore, the test results are compared with the relation proposed by Lunne & Christoffersen (1983):

$$q_{c;Lunne \& Christoffersen} = 61 * \sigma'_v{}^{0.71} e^{2.91I_D}$$

Figure 5.2 and Figure 5.3 present the measured q_c , corrected for σ_v , as function of $q_{c;Lunne \& Christoffersen}$. The results in the upper 15 cm are not included. The q_c shows a clear relation with σ'_v and I_D . The dashed line indicates a perfect fit, while the dotted lines indicate a deviation of 20% from the perfect fit. The bulk density index I_D as determined during the preparation of the models has been used to calculate $q_{c;Lunne \& Christoffersen}$. The stress level used to calculate $q_{c;Lunne \& Christoffersen}$ is a function of the surcharge load and the depth using a density of 19.5 kN/m³ that followed from index testing.

The range in measured cone resistance given in Figure 5.2, is attributed to this variation in density over depth. Based on the relation by Lunne & Christoffersen (1983), variation in I_D of $\pm 10\%$ to 12.5% is found.

As can be seen from these plots, the results of the first CPT at soil model 1 and 5 give a reasonable fit with $q_{c;Lunne \& Christoffersen}$ while the third CPT in soil model 1 and the second and third CPT in soil model 5 show the largest deviations. For the tests in soil model 5 this deviation might be caused by the effects from the prior CPTs. These tests are performed in medium dense sand and under a vertical surcharge pressure of 100 kPa. Therefore less effects from prior CPTs is expected for the tests in other soil models. For the test in soil model 1 increasing the surcharge load and/or leakage of the cushion might have played also a role.

The CPT at the centre of soil model 6 shows lower resistances than expected based on the applied relation. The cone diameter and the location of this CPT are different from the other CPTs plotted in the figures.

It is concluded that the relation of Lunne & Christoffersen (1983) provides a representative value for $q_{c;true}$, corrected for the vertical effective stress level, for the CPTs performed 15 cm out of the centre of the soil model with a 25 mm diameter cone. For the CPT performed at the centre of the soil model using a 36 mm diameter cone an additional factor of 0.7 will be applied to determine $q_{c;true}$, see Figure 5.4.

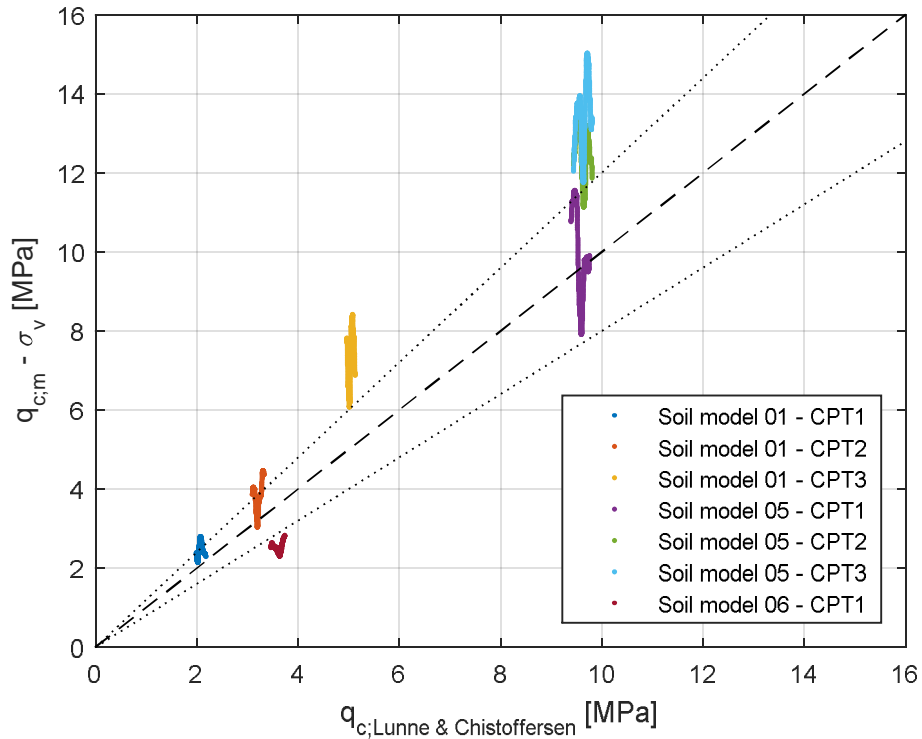


Figure 5.2 The measured cone resistance vs. the results of the relation proposed by Lunne & Christoffersen (1983)

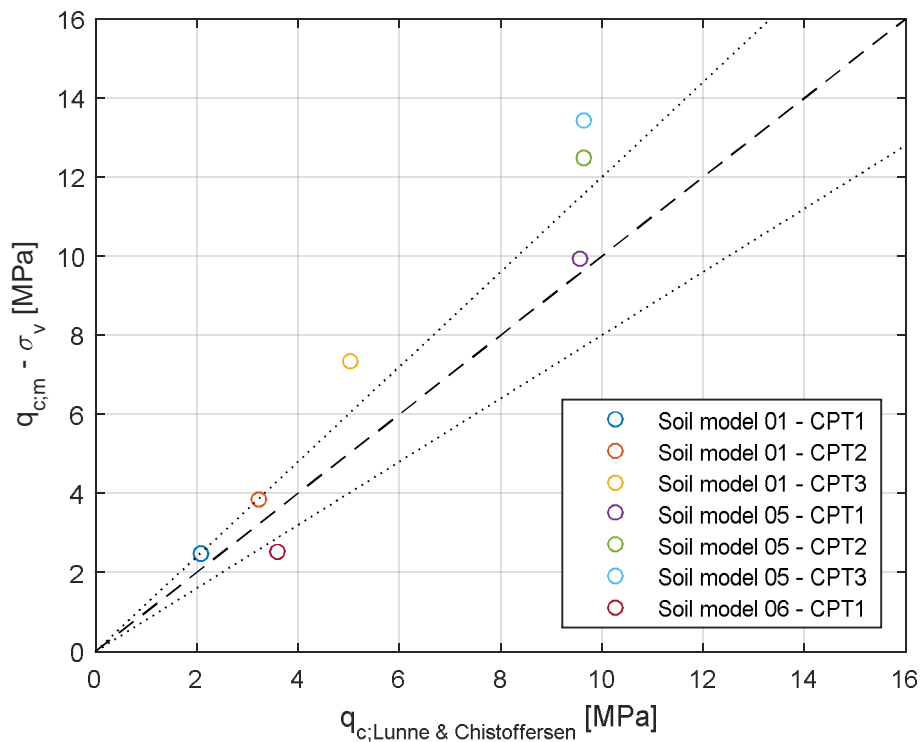


Figure 5.3 The average of the measured cone resistance vs. the results of the relation proposed by Lunne & Christoffersen (1983)

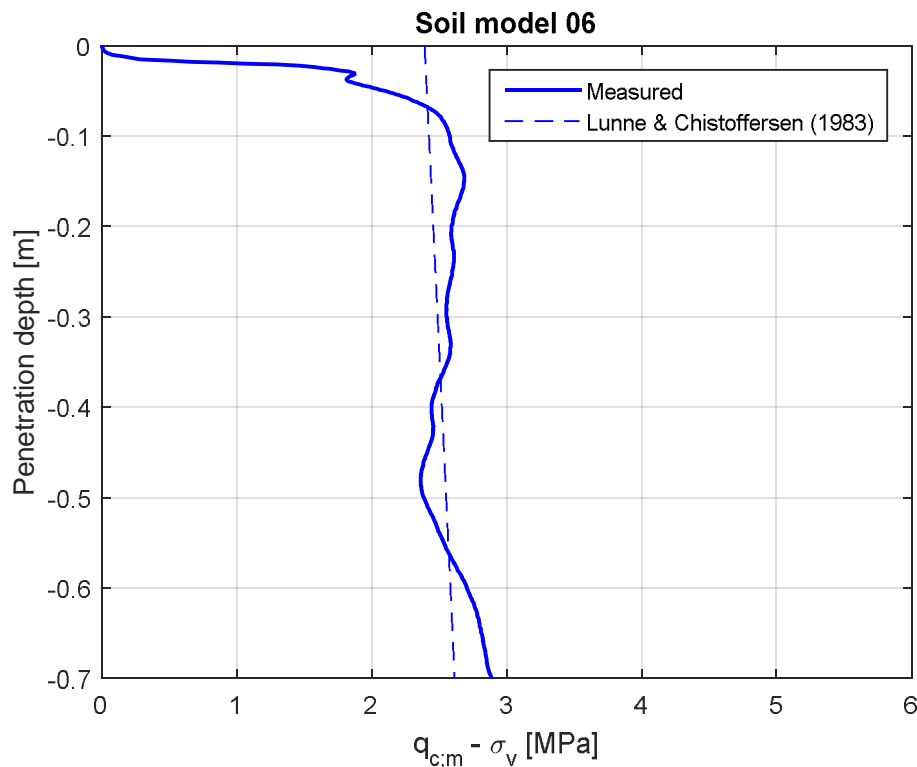


Figure 5.4 Comparison measurement and relation of Lunne & Christoffersen (1983) used for the analysis

5.3 Reliability results layered soil models

It is hard to determine the void ratio (or density index) of the thin interbedded sand layers. Therefore the layered models are assessed based on the measured cone resistance in the layered part. It is expected that the difference between $q_{c;m;layer;max}$ and $q_{c;m;layer;min}$ increases when the density or the stress level increases. Therefore the difference between $q_{c;m;layer;max}$ and $q_{c;m;layer;min}$ (average of both surrounding layers) for all CPTs performed in the layered soil models is plotted as function of $q_{c;Lunne et al.}$, taking both density and stress into account, see Figure 5.5. The results are grouped based on the ratio of the layer thickness H and the cone diameter d_{cone} . The results of the CPTs at soil model 4 of the start-up phase ($H/d_{cone} = 3.2$) are given to give a more complete picture, since a layer thickness of 80 mm wasn't applied in the final test program.

The average difference of the maxima and minima of all separate thin layers for each CPT is used. The measured values are corrected for the vertical stress level. For the calculation of $q_{c;Lunne et al.}$, a I_D of 33% for loose and 59% for medium dense sand layers is used in order to account for the preparation method. Error bars are given to account for the possible deviation in density index. Positive and negative error values of 10% (one standard deviation, see Section 3.5) are used, since the average of all thin layers is given.

The figure gives confidence in the preparation methods, since the results from soil models having different I_D show the same trend. An increase in stress level and I_D leads to an increase in the difference between $q_{c;m;layer;max}$ and $q_{c;m;layer;min}$, while a smaller layer thickness (relative to the cone size) leads to a smaller difference between $q_{c;m;layer;max}$ and $q_{c;m;layer;min}$. Both trends behave as expected. Figure 5.6 gives the same graph for all separate layers, showing the same trends.

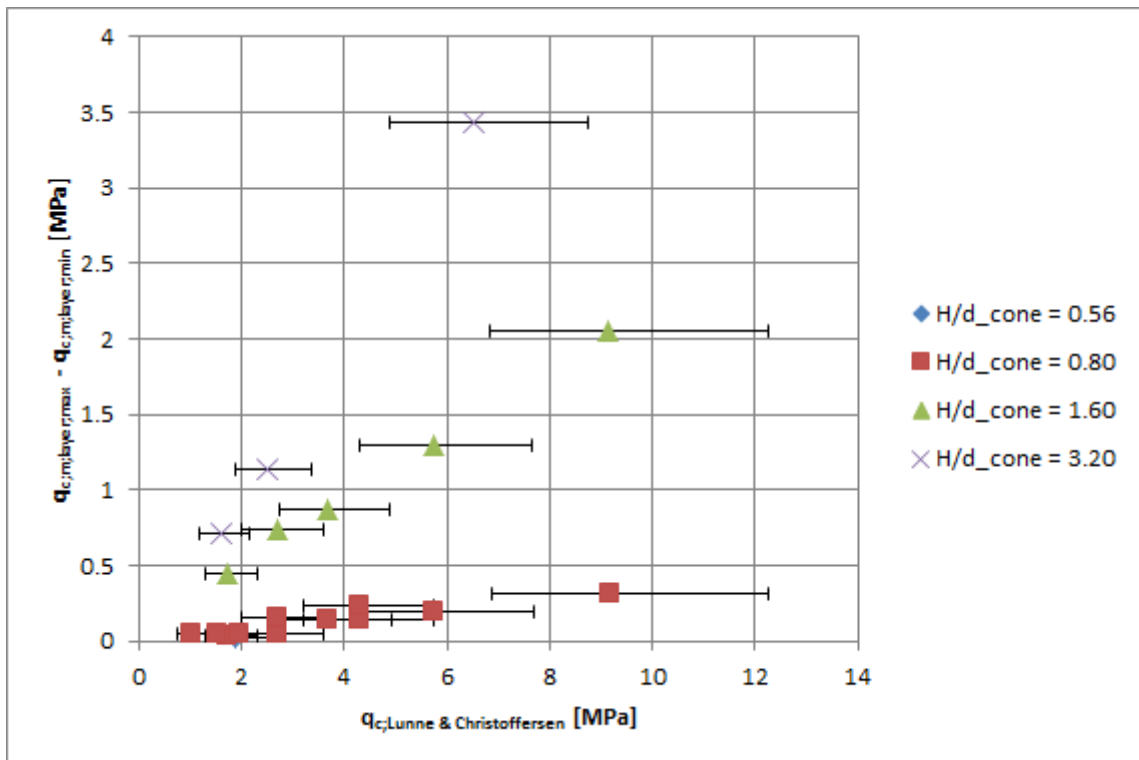


Figure 5.5 The average difference between the maximum and minimum cone resistance of the thin layer part vs. the results of the relation proposed by Lunne & Christoffersen (1983)

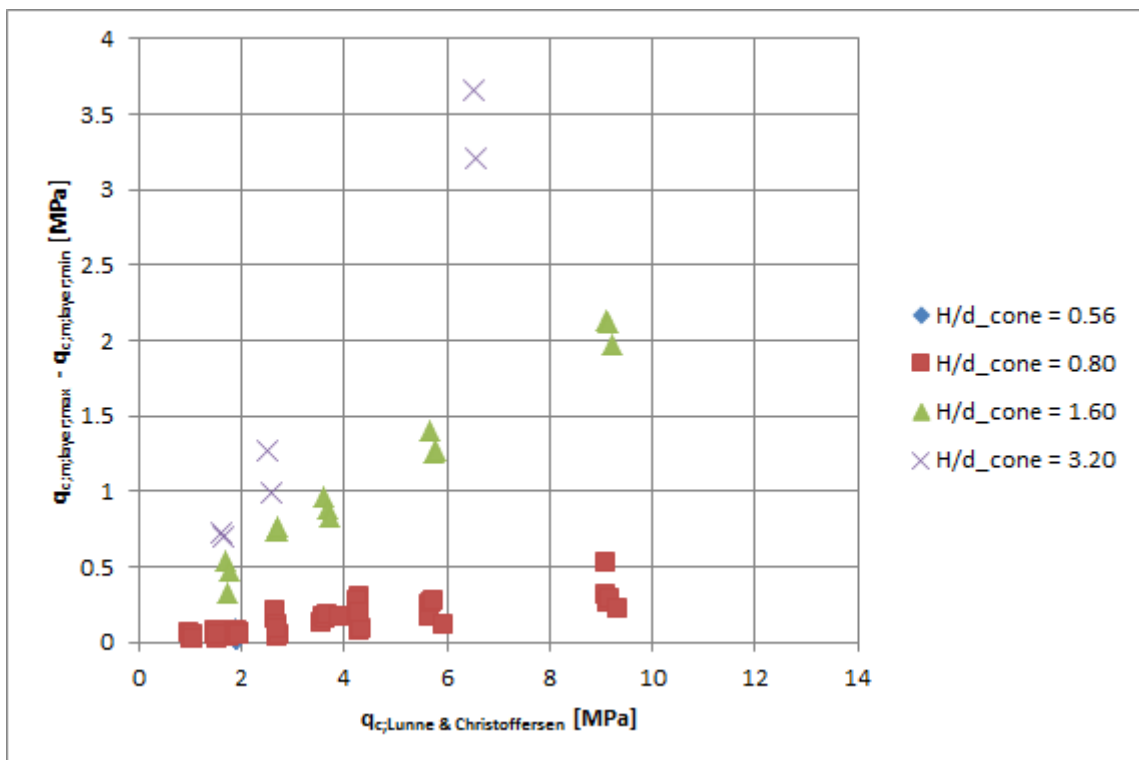


Figure 5.6 The differences between the maximum and minimum cone resistance of the thin layer part vs. the results of the relation proposed by Lunne & Christoffersen (1983)

5.4 Effect of multiple layers

The influence of multiple thin layers can be explained by comparing the results of soil model 3 and 9. The same layer thickness (2 cm), target density (loose) and cone diameter (25 mm) is applied. However, the layered part of model 3 is sandwiched between sand layers, while the layered part of model 9 is sandwiched between clay layers. The results are given in Figure 5.7 for 50 and 100 kPa surcharge load. Distinction can be made between the effects of the layered part as a whole, and the effects of the individual layers. The effects of the layered part as a whole are idealized in Figure 5.8: the layered part is weaker than the surrounding soil in model 3 and stronger in model 9. Besides this, the individual layers are visible in the cone resistance profile. The measurements can be seen as the sum of both effects. This conclusion is confirmed by the q_c measurements in soil model 8 that contains two layered parts with a different number of thin layers, see Figure 5.9.

For the derivation of the correction factors, the maximum value of the cone resistance measured in the stronger thin layers is used. From the description above, it can be concluded that this resistance depends on the position of the layers: the upper and lower thin layers deviate from the layers in the middle of the layered part. This effect is stronger for layer thicknesses smaller than the cone diameter than for layers thicker than the cone diameter.

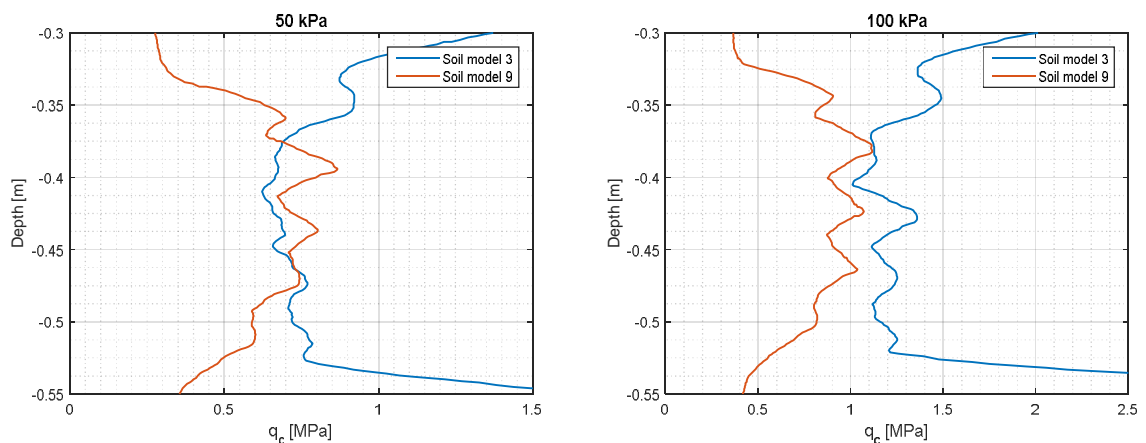


Figure 5.7 Comparison of cone resistance in layered part of soil model 3 and 9 for different surcharge loads

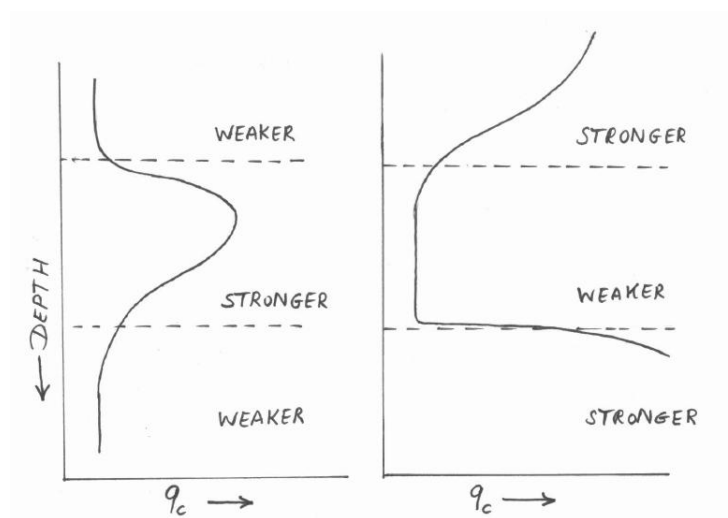


Figure 5.8 Idealisation of cone resistance in a stronger layer interbedded in weaker layers (left) and in a weaker layer interbedded in stronger layers (right)

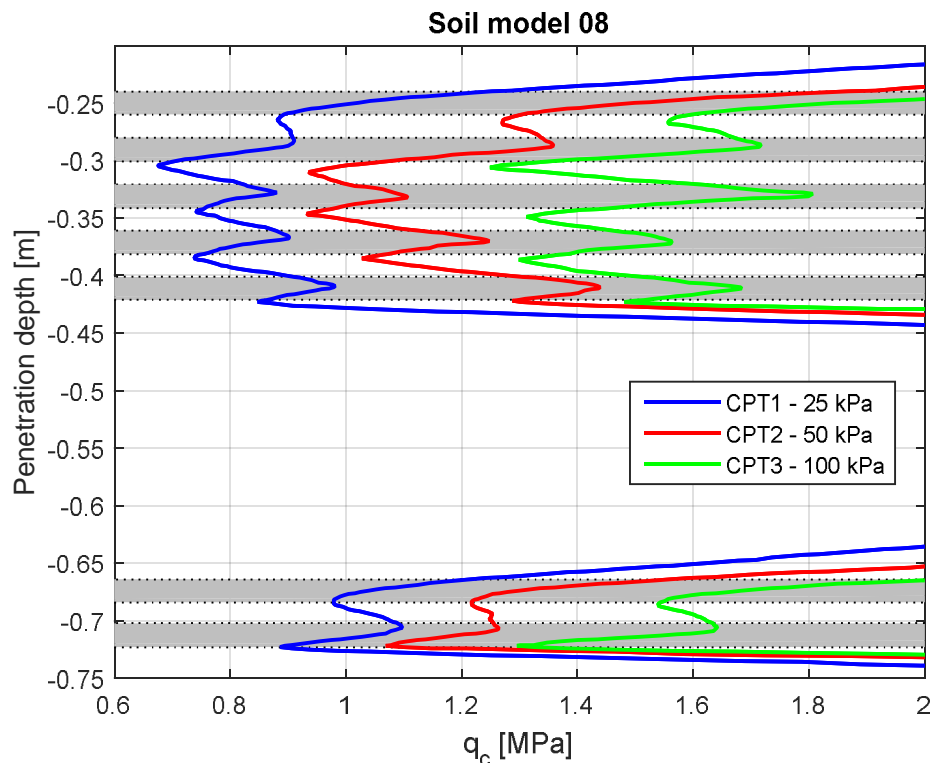


Figure 5.9 Cone resistance profiles measured in soil model 8

5.5 Derived thin layer correction factors

The thin layer correction factor K_H for a stronger thin layer in between weaker thin layers is defined as:

$$K_H = \frac{q_{c: \text{true}} - \sigma_v}{q_{c: \text{m:layer: max}} - \sigma_v}$$

For $q_{c: \text{true}}$ the relation of Lunne & Christoffersen (1983) is used, since the reference tests do not cover all applied combinations of σ'_v and I_D and the resistance measured in the thicker top and bottom sand layers may be influenced by the layered part. As described in Section 5.2, an additional factor of 0.7 is applied for the CPT in soil model 7 (36 mm cone).

The thin layer correction factors for all individual thin layers are given in Figure 5.10 as function of the normalized layer thickness. Higher correction factors and a wider range in correction factors are found for smaller H/d_{cone} ratios. Existing relationships for thin layer correction are also given. The methods of Robertson & Fear (1995) and Youd et al. (2001) give similar results. The given graph of Youd et al. (2001) is the lower bound of an estimated range based on examination of field data. Strong deviations from these relationships are found for small H/d_{cone} ratios, while a good fit is found for a H/d_{cone} ratio of 3.2.

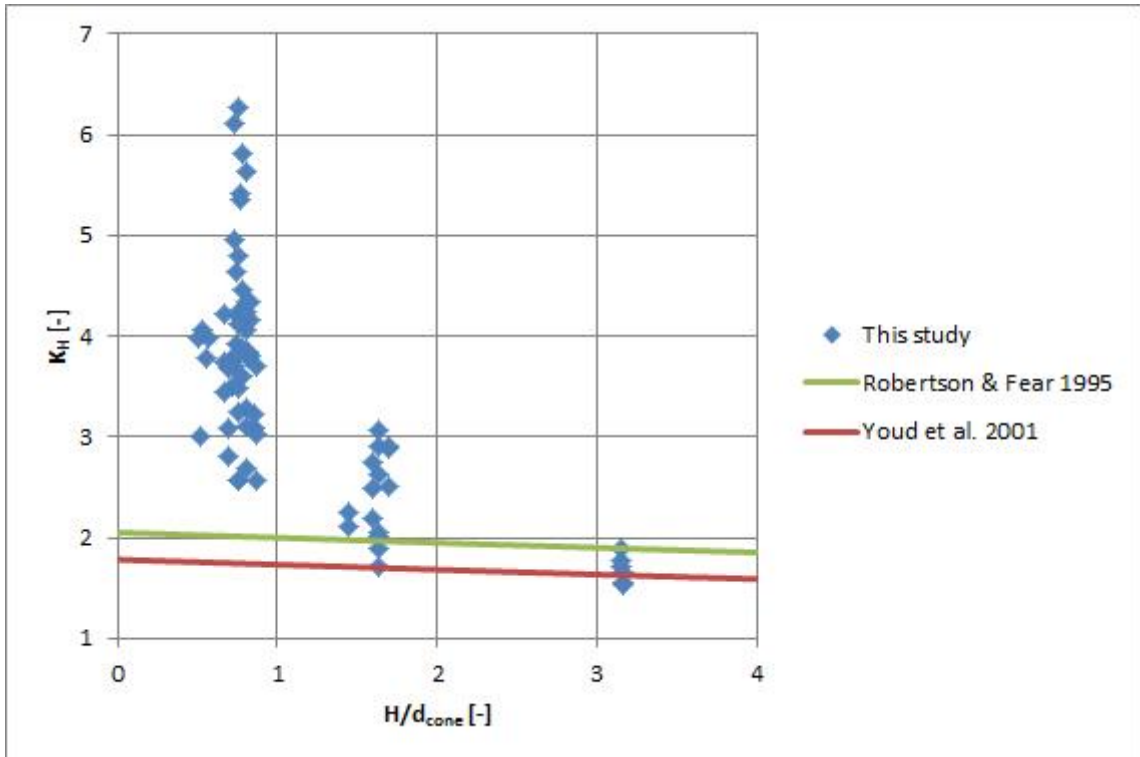


Figure 5.10 Thin layer correction factor as function of the normalized layer thickness

Since the correction factor is not only a function of the normalized layer thickness, but also of the strength and stiffness of the individual layers, other graphs are made to visualize both effects and to better understand the wide range in found correction factors.

In line with Vreugdenhill (1994), Moss et al (2006) and Boulanger & DeJong (2018) the ratio of “true” cone resistance $q_{c;true}$ is determined to have a measure for the influence of the strength and stiffness of the individual layers. For the clay layers, $q_{c;true}$ is calculated based on the undrained shear strength s_u , which is a function of the effective stress level and the degree of consolidation:

$$q_{c;clay;true} - \sigma_v = N_k * s_u$$

The s_u value is determined by triaxial testing, see Section 3.2.2. A N_k factor of 10.4 is applied based on the measured cone resistances in thicker clay layers (soil model 4 of the start-up phase and soil model 2 from Van der Linden (2016)), see Figure 5.11.

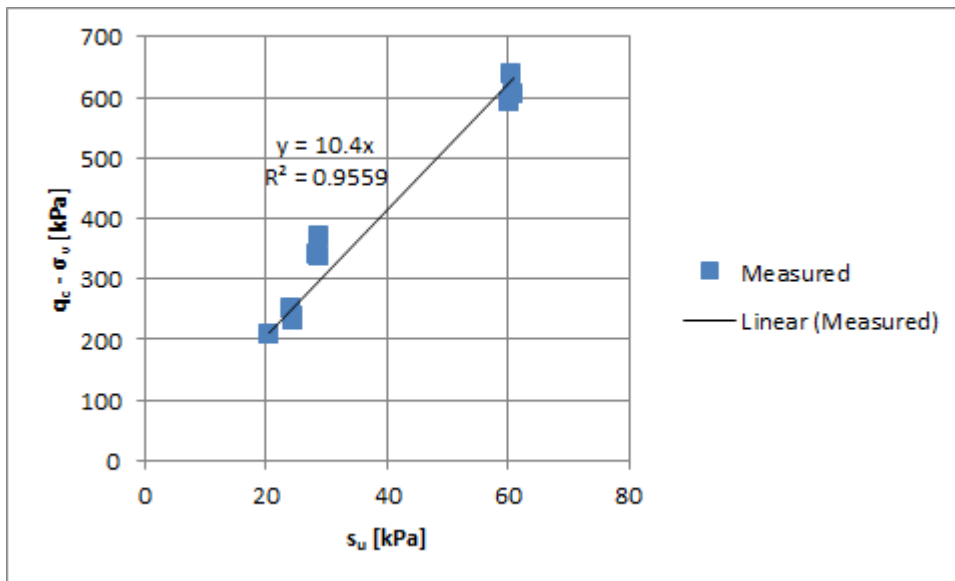


Figure 5.11 Cone resistance corrected for the vertical stress level as function of undrained shear strength

The ratio of “true” cone resistance is defined as:

$$\text{ratio } q_{c; \text{true}} = \frac{q_{c; \text{stronger}; \text{true}}}{q_{c; \text{weaker}; \text{true}}}$$

Figure 5.12 gives the derived correction factors for all individual thin layers as function of $\text{ratio } q_{c; \text{true}}$. Figure 5.13 gives the derived correction factors as function of $\text{ratio } q_{c; \text{true}}$. The average of the maxima of the separate layers is used to determine the correction factor K_H . For the 2 cm layers the upper and the lower layer are neglected, based on the conclusions of Section 5.4. Vertical error bars are given to account for the possible deviation in density index. Positive and negative error values of 10% (one standard deviation, see Section 3.5) are used, since the average of all thin layers is given. Horizontal error bars are given to account for the possible deviation in clay strength ($0.1 * s_u$, based on extensive series of pocket penetrometer and torvane measurements). The factors are grouped based on the ratio of the layer thickness H and the cone diameter d_{cone} .

The relation proposed by Moss et al. (2006) is also given in this figure for the applied H/d_{cone} ratios. A good fit is found for layer thicknesses smaller than the cone diameter, while the relation provides too large correction factors for larger H/d_{cone} ratios. Further, from a physical point of view, the lines should give a correction factor equal to 1 for a $\text{ratio } q_{c; \text{true}}$ of 1.

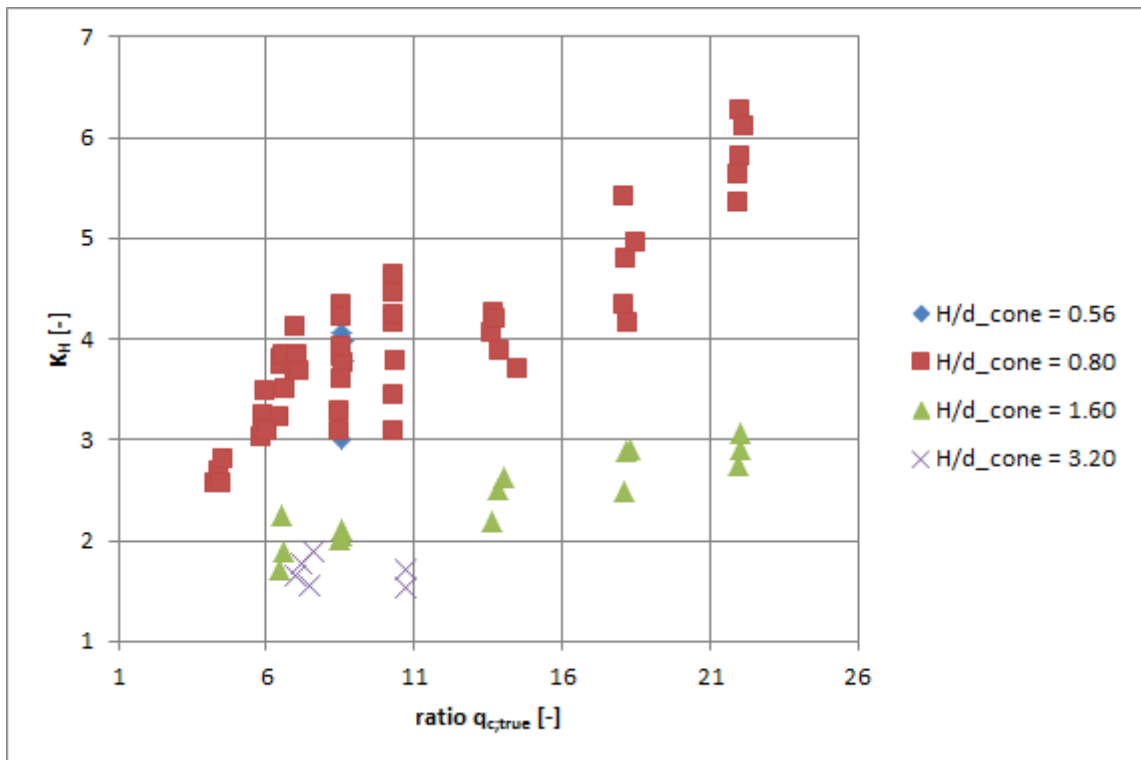


Figure 5.12 Derived correction factors (all individual layers) as function of the ratio of "true" cone resistance

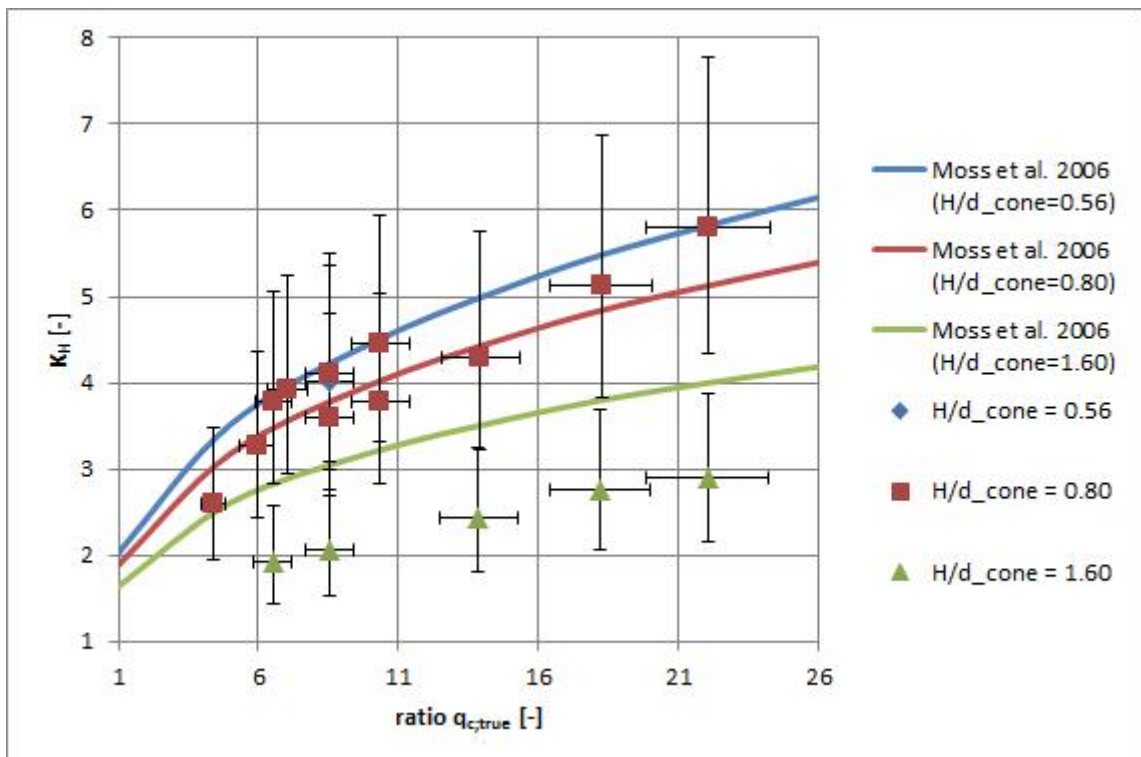


Figure 5.13 Derived correction factors (average values) as function of the ratio of "true" cone resistance

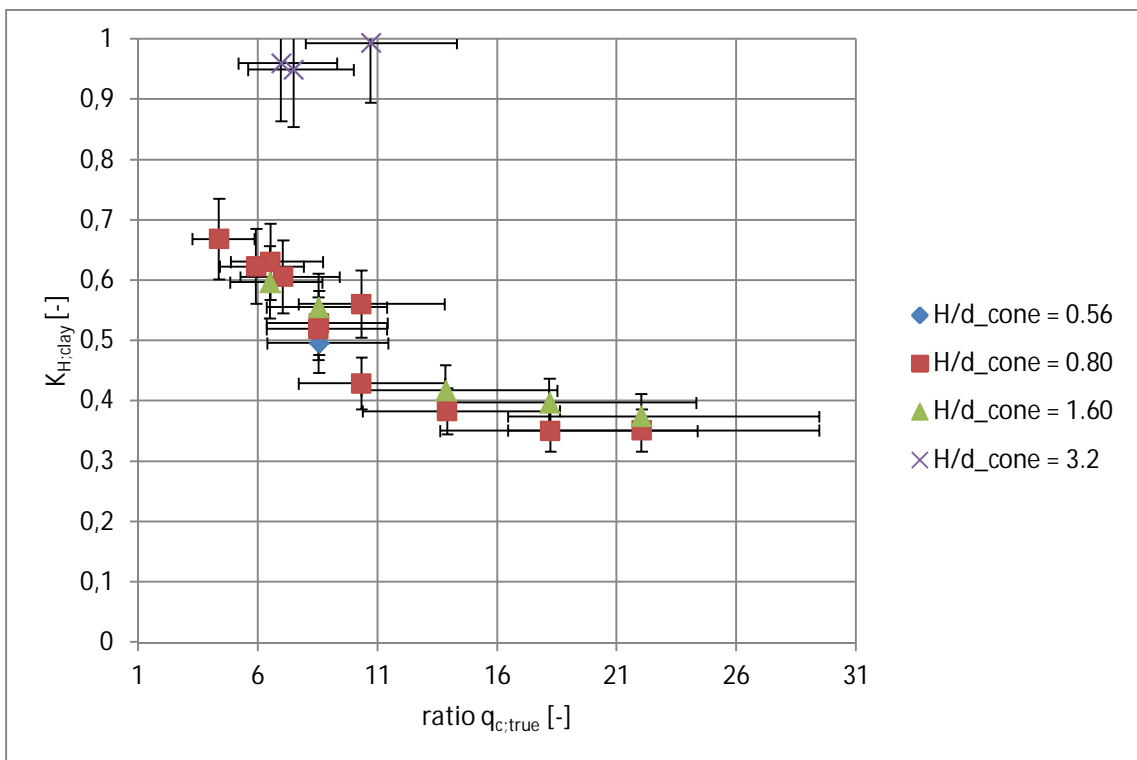


Figure 5.14 Derived correction factors for the thin clay layers as function of the ratio of "true" cone resistance (average values)

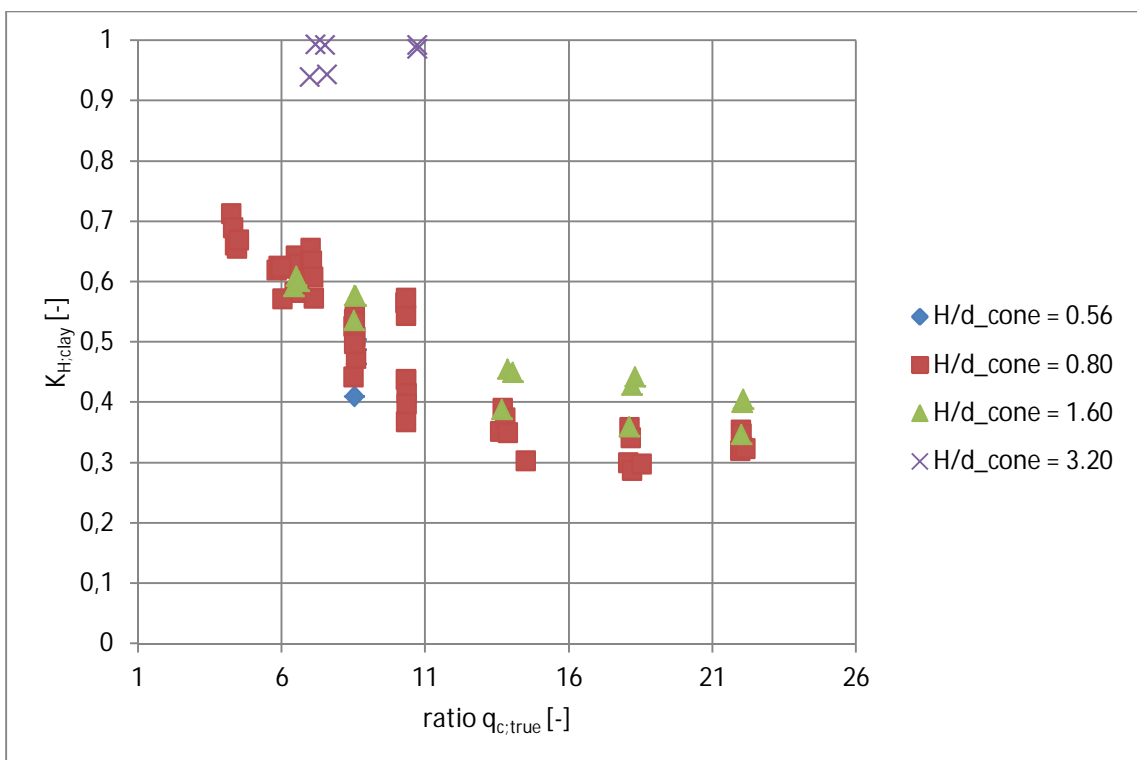


Figure 5.15 Derived correction factors for the thin clay layers as function of the ratio of "true" cone resistance (all individual layers)

The thin layer correction factor K_H for a weaker thin layer in between stronger thin layers is defined as:

$$K_H = \frac{q_{c: \text{true}} - \sigma_v}{q_{c:m: \text{layer: min}} - \sigma_v}$$

Figure 5.14 gives the derived correction factors for the clay layers as function of *ratio* $q_{c: \text{true}}$. The average of the maxima of the separate layers is used to determine the correction factor K_H . Also in this analysis the upper and the lower layers have been neglected for the 2 cm layers. As observed before, the clay resistance is clearly affected by the sand density, while the layer thickness seems to have a smaller influence. However, it should be realized that a correction factor of about 1 is found for a H/d_{cone} ratio of 3.2. Figure 5.15 gives the derived correction factors for all individual clay layers.

5.6 Additional information from the cone resistance profile

Since in the field the ratio of "true" cone resistances is not known, additional information is needed to apply a correct correction factor in a forward situation. Boulanger & DeJong (2018) give an inverse filtering procedure for developing estimates of "true" cone penetration tip resistance from measured cone penetration test data in interlayered soil profiles. However, this procedure cannot yet deal with such thin layers as are currently being investigated in this study.

It is thought that the ratio of $q_{c:m: \text{layer: max}}$ and $q_{c:m: \text{layer: min}}$ may provide additional information, since this can be seen as a measure for *ratio* $q_{c: \text{true}}$. Figure 5.16 gives the average $q_{c:m: \text{layer: min}}$ of the surrounding thin layers as a function of $q_{c:m: \text{layer: max}}$ for all thin sand layers for all cone penetration tests. Although different stress levels and densities have been applied, clear trends are found. These trends seem to be characteristic for a certain layer thicknesses normalized for the cone size. However, it should be noted that only one type of sand and one type of clay have been applied for this study.

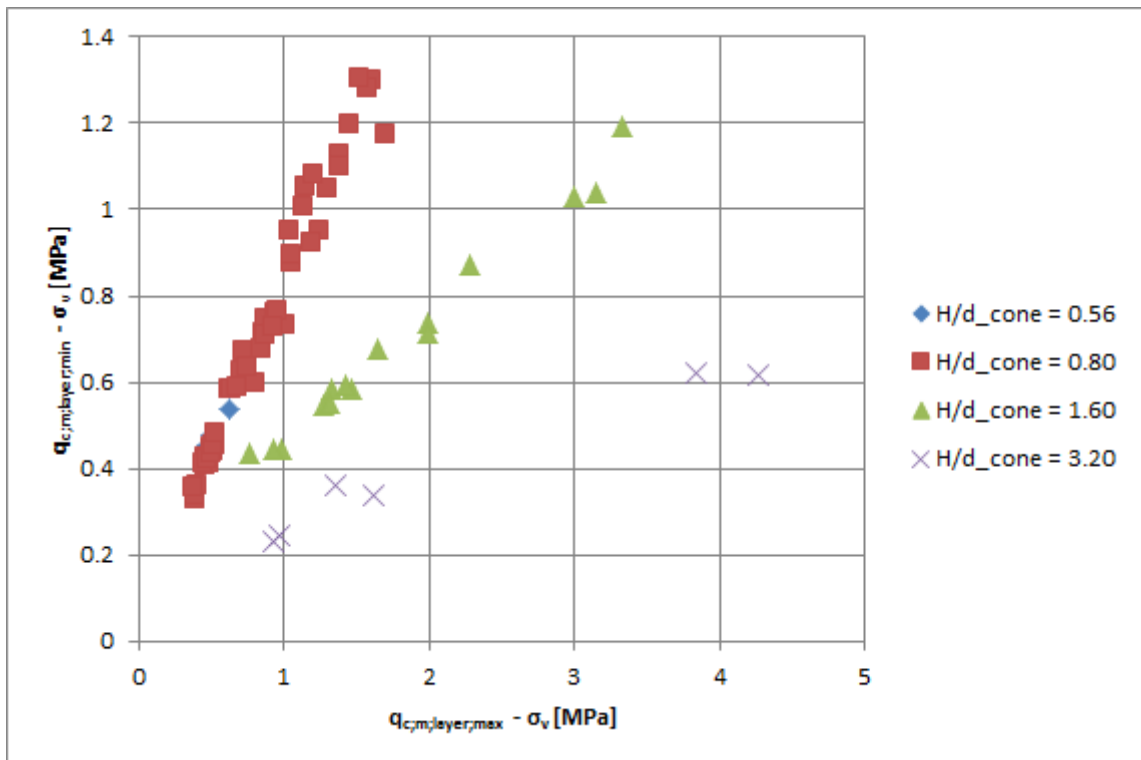


Figure 5.16 Min. cone resistance in thin weak layer vs. max. cone resistance in thin strong layer

Figure 5.17 and Figure 5.18 give the correction factor K_H as function of the ratio of $q_{c,m:layer:max}$ and $q_{c,m:layer:min}$. A logarithmic scale is applied, since little contrast in cone resistance is found for the lowest H/d_{cone} ratios. Figure 5.17 gives the average values with error bars as described in Section 5.5. Figure 5.18 present the correction factors derived for all individual thin sand layers enclosed by thin clay layers. In general, an increase of K_H is found for an increase of the ratio of $q_{c,m:layer:max}$ and $q_{c,m:layer:min}$. The different H/d_{cone} ratios are clearly distinguished and show each an own trend.

However, it should be realized that in current practice many layers with H/d_{cone} ratios smaller or of about 1 won't be recognized, since the standard data sampling interval is 20 mm. This will act as a filter and extreme values may be lost. Therefore, less contrast will be found in the thinly layered deposits and it will be hard to apply a method such as proposed in this section.

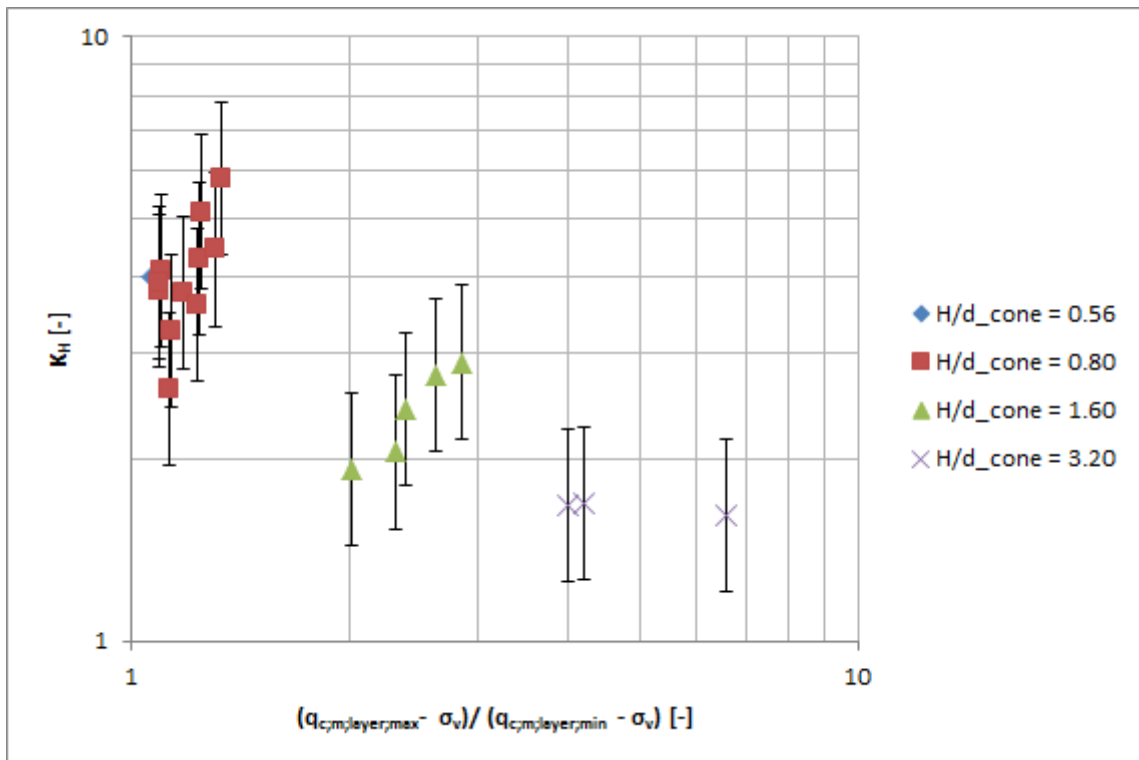


Figure 5.17 Thin layer correction factor as function of ratio of maximum and minimum cone resistance in the layered part (average values)

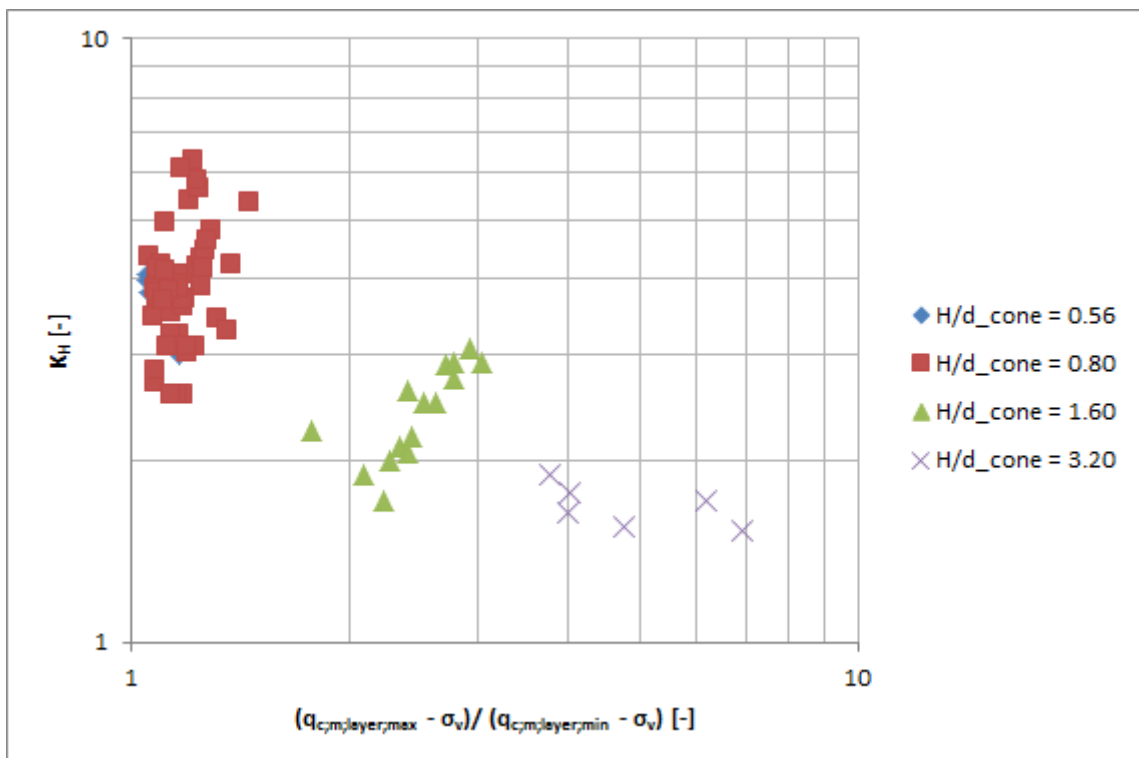


Figure 5.18 Thin layer correction factor as function of ratio of maximum and minimum cone resistance in the layered part (derived from all separate thin sand layers)

6 Numerical simulation

6.1 Analytical methods

The test results are simulated with analytical solutions. Based on Van der Linden (2016), the solution by Joer et al. (1996) and the Dutch pile bearing capacity prediction method of Koppejan are used. The method of Koppejan is described in the Dutch annex of Eurocode 7 (NEN 9997-1). Both methods are adjusted to obtain a better fit with the measurements. Thin layer correction factors are derived from these methods and are compared with the correction factors derived from the test results.

6.1.1 Joer et al. (1996)

The “simple” elastic analysis proposed by Vreugdenhil et al. (1994) has been generalised for multiple layers by Joer et al. (1996). This method determines a weighted average of the shear modulus of the separate layers, depending on the cone tip level. The distance to a layer interface determines the degree of contribution of that layer. Vreugdenhil et al. (1994) assume that the shear modulus of a layer is proportional to the characteristic cone resistance of that layer, meaning that the relative difference in shear modulus represents the relative difference in characteristic cone resistance.

In order to obtain a better fit for the thinly layered parts, parameter a is taken to be equal to the half of the cone radius (instead of the whole radius).

6.1.2 Method of Koppejan

The method of Koppejan considers the variation of the cone resistance in the range of $4D_{eq}$ (the equivalent pile diameter) below and $8D_{eq}$ above the base level and is derived from a combination of empirical data and theoretical influence shapes. The procedure of this method is set up such that a conservative approximation of the path of least resistance will be found.

Three trajectories are defined for which a normative cone resistance has to be determined by averaging, see Figure 6.1. The distance below the pile base over which averaging takes place (trajectory I and II) varies between $0.7D_{eq}$ and $4D_{eq}$, depending on the distance over which the minimum average will be met. The distance above the pile base over which averaging takes place (trajectory III) is fixed at $8D_{eq}$. The procedure to determine the normative cone resistance by averaging over the trajectories II and III (upward directions) is such that the q_c that is taken into account must be equal or lower than the lowest q_c that is found at deeper levels (up to the normative distance below the pile base). If a higher value is met, that value must be replaced by the lowest value. The pile bearing capacity is calculated by:

$$q_{b,max} = \frac{1}{2} \cdot \alpha_p \cdot \beta \cdot s \cdot \left(\frac{q_{c,I,av} + q_{c,II,av}}{2} + q_{c,III,av} \right)$$

The parameters α_p , β and s represent pile type factors, which have been set to 1 for this assessment. Based on the findings of Van der Linden (2016), the distance below the pile base over which averaging takes place (trajectory I and II) is set to vary between $0.7D_{eq}$ and $1.5D_{eq}$ (instead of $4D_{eq}$) to obtain a better fit for the thinly layered parts.

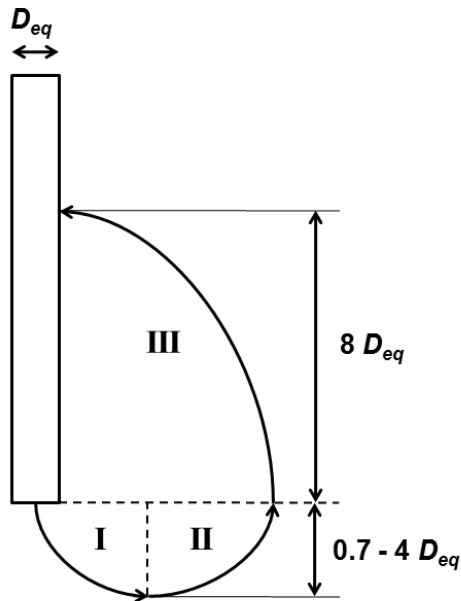


Figure 6.1 Schematization of the trajectories of the method of Koppejan

6.2 Simulation of test results

To simulate the test results, the cone resistance data is normalized in line with Lunne and Christoffersen (1983) by:

$$q_{cN} = \frac{q_c - \sigma_v}{\sigma_v^{0.71}}$$

In this way the results should no longer be dependent on the penetration depth. It should be realized that this way of normalizing is developed for sands and works less well for clays.

“True” cone resistance profiles are created and are used as input for the analytical methods. For the different layer configurations, profiles are created with constant cone resistance over a layer, see Figure 6.2. Table 6.1 gives the applied $q_{cN; \text{“true”}}$ values. The values for the sand layers are calculated by the relation of Lunne and Christoffersen (1983). The value for the clay layer is a pragmatic choice, since the way of normalising doesn’t result in a single value. The average of the values for vertical effective stress levels of 25 and 50 kPa is taken.

Soil layer	$q_{cN; \text{“true”}}$
Loose sand	159
Medium dense sand	340
Clay	21.5

Table 6.1 Applied $q_{cN; \text{“true”}}$ values

For the simulations, the depth is discretised in intervals of 1 mm. A moving average over 27 mm is taken since the cone tip has a height of approximately 27 mm, see Figure 6.3.

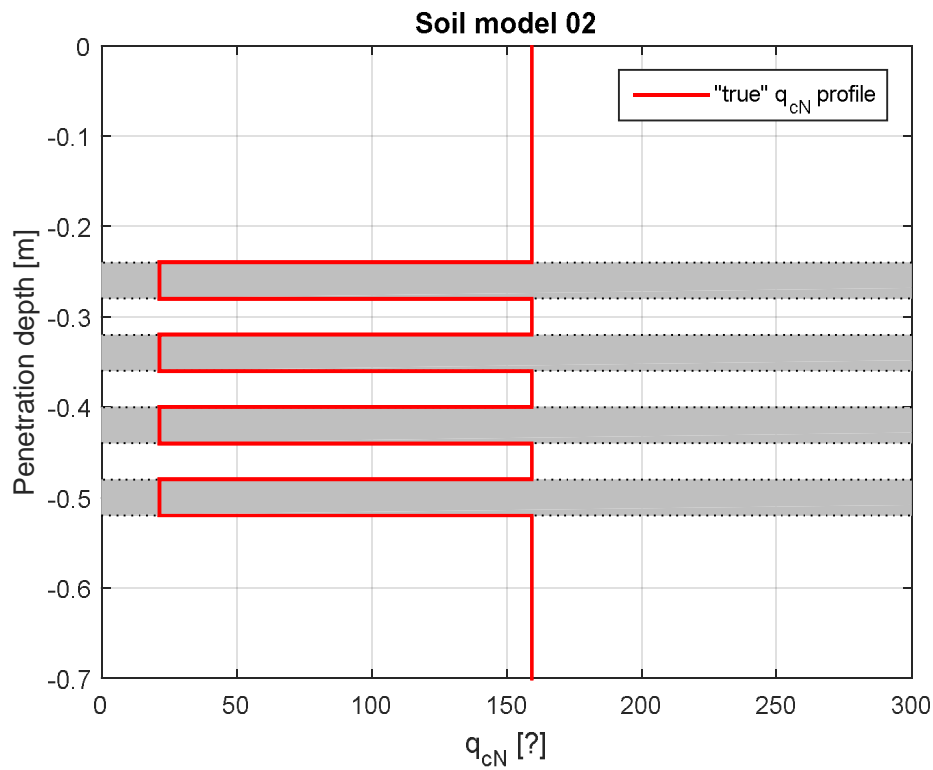


Figure 6.2 Example of "true" cone resistance profile, used as input for the simulations

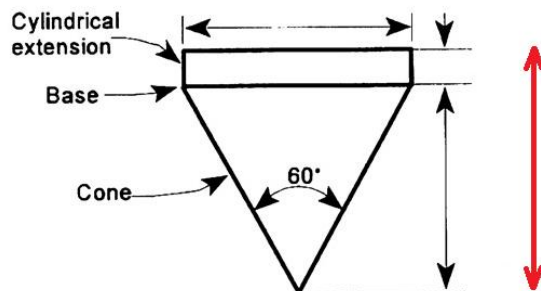


Figure 6.3 Total height of the cone tip (25 mm cone): 21.85 mm + 5 mm = 26.85 mm

The following figures give the simulations of the tests in:

- Soil model 2 and 4 ($H/d_{cone} = 1.6$).
- Soil model 3, 8 and 9 ($H/d_{cone} = 0.8$).
- Soil model 7 ($H/d_{cone} = 0.56$).

From these simulations, it can be concluded that both methods are able to simulate the test results reasonably well. The method of Joer et al. (1996) is partly able to simulate the effects described in Section 5.4, while the method of Koppejan gives the same results for all individual thin layers. The simulations by the method of Koppejan result in general in a larger contrast between the individual layers, compared to the solution of Joer et al. (1996).

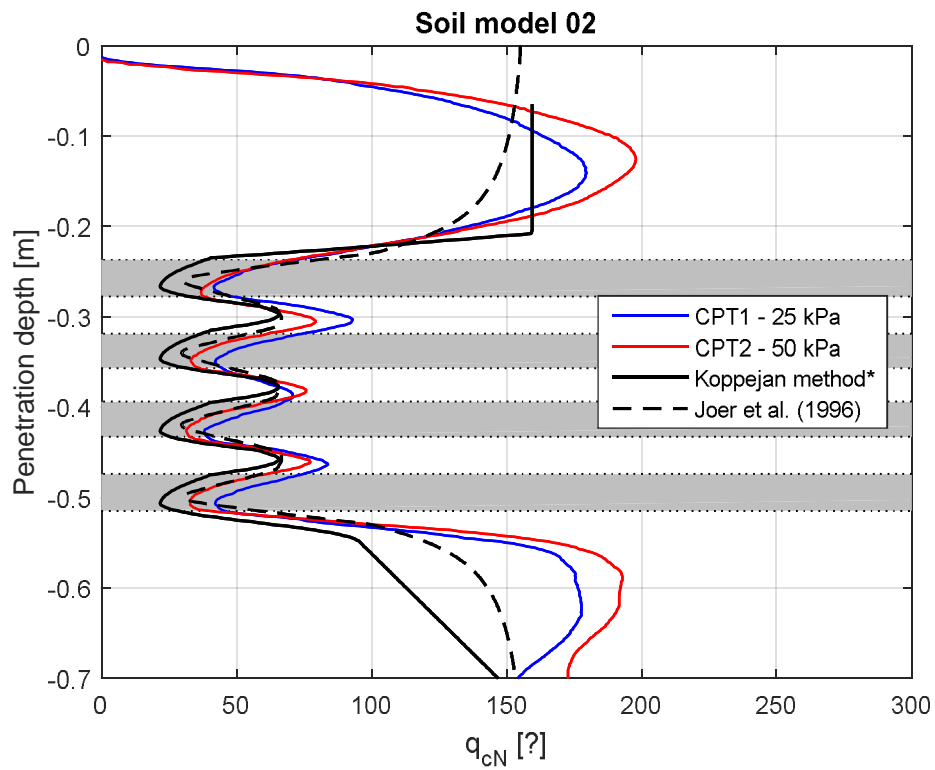


Figure 6.4 Simulations of normalized q_c profiles

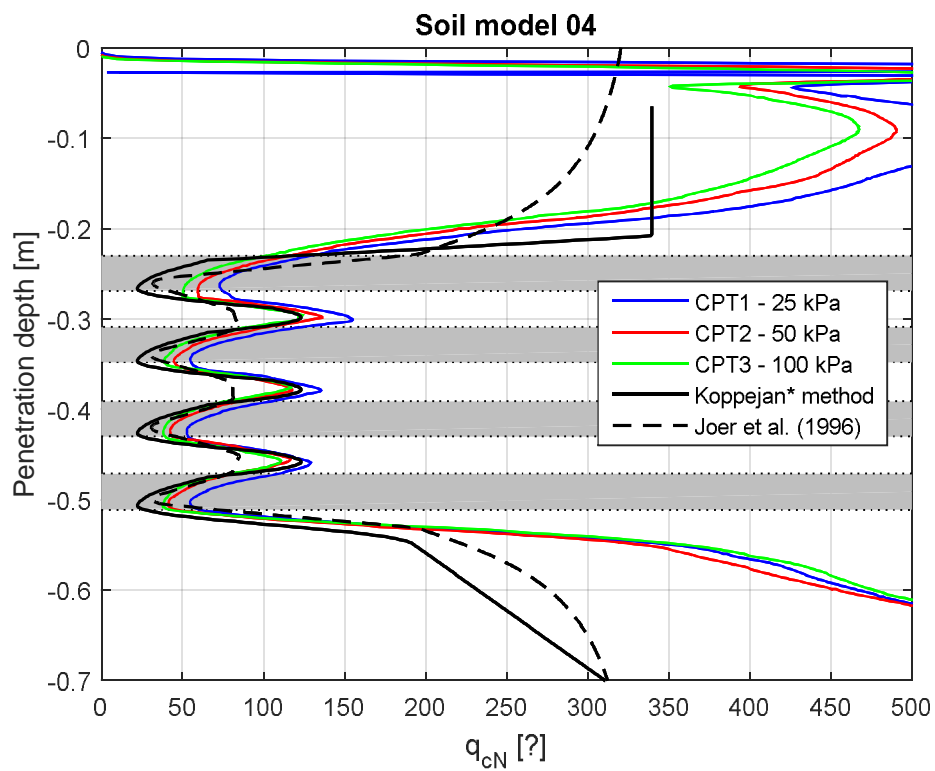


Figure 6.5 Simulations of normalized q_c profiles

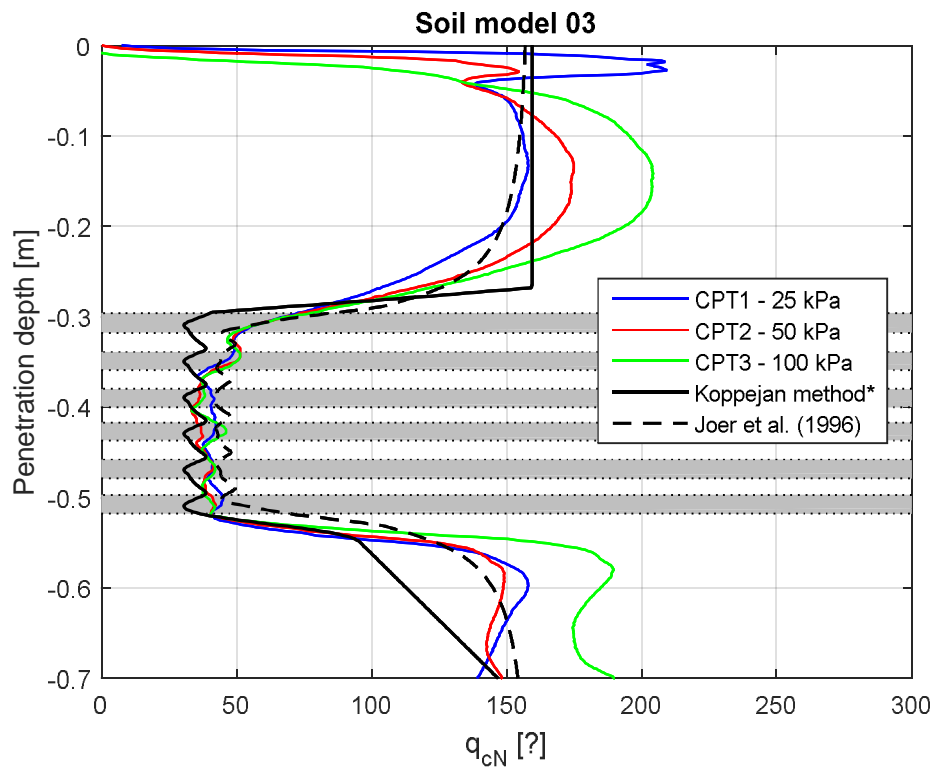


Figure 6.6 Simulations of normalized q_c profiles

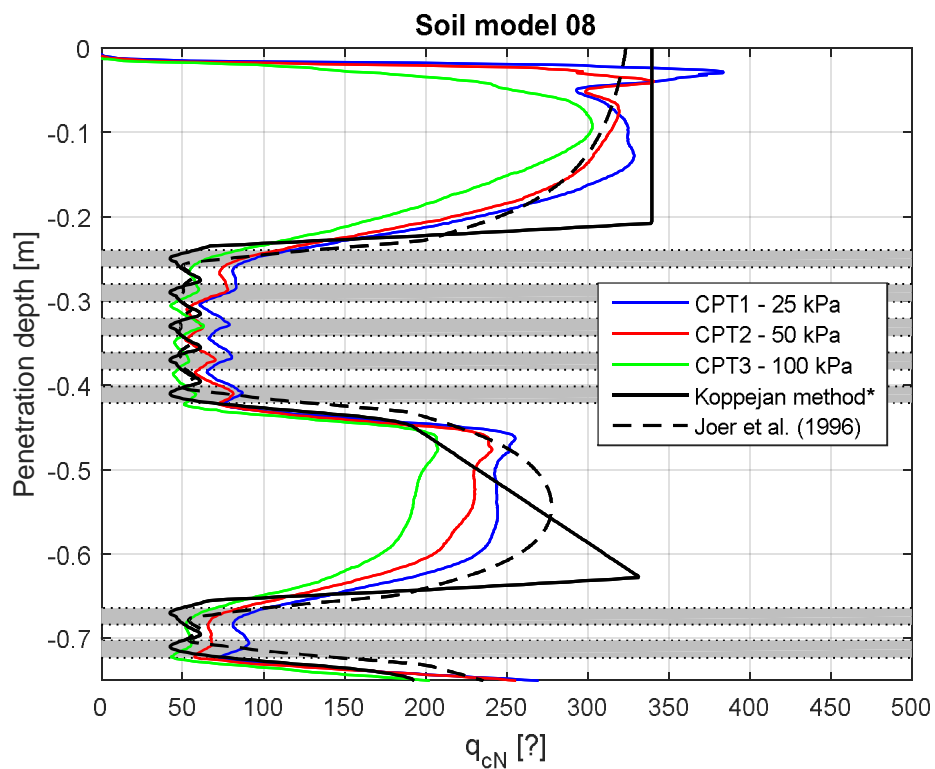


Figure 6.7 Simulations of normalized q_c profiles

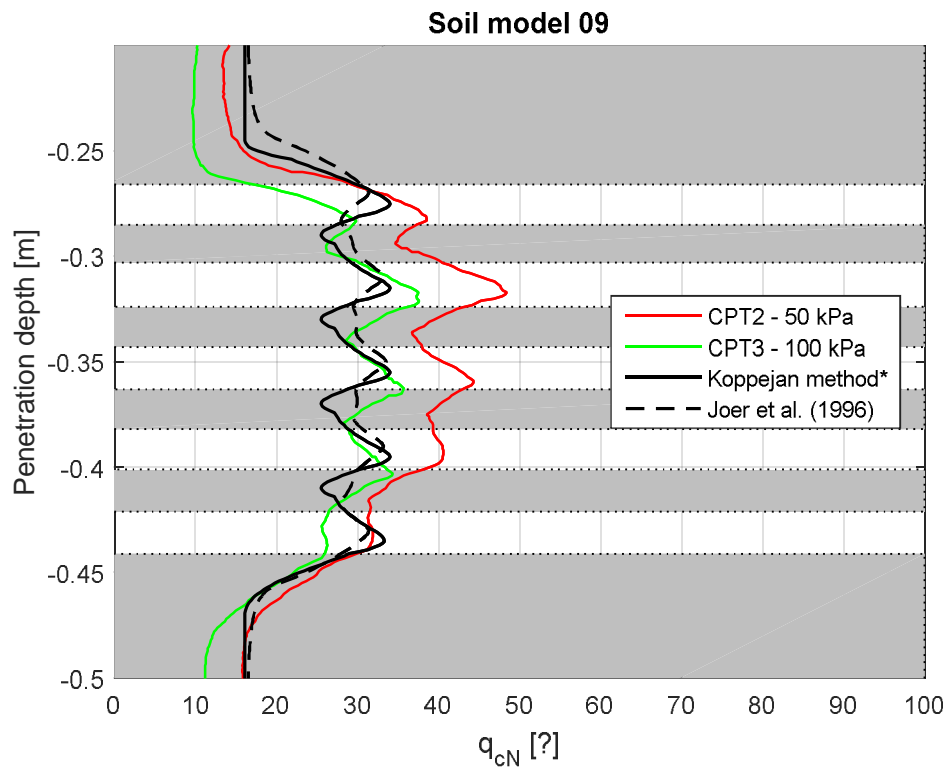


Figure 6.8 Simulations of normalized q_c profiles

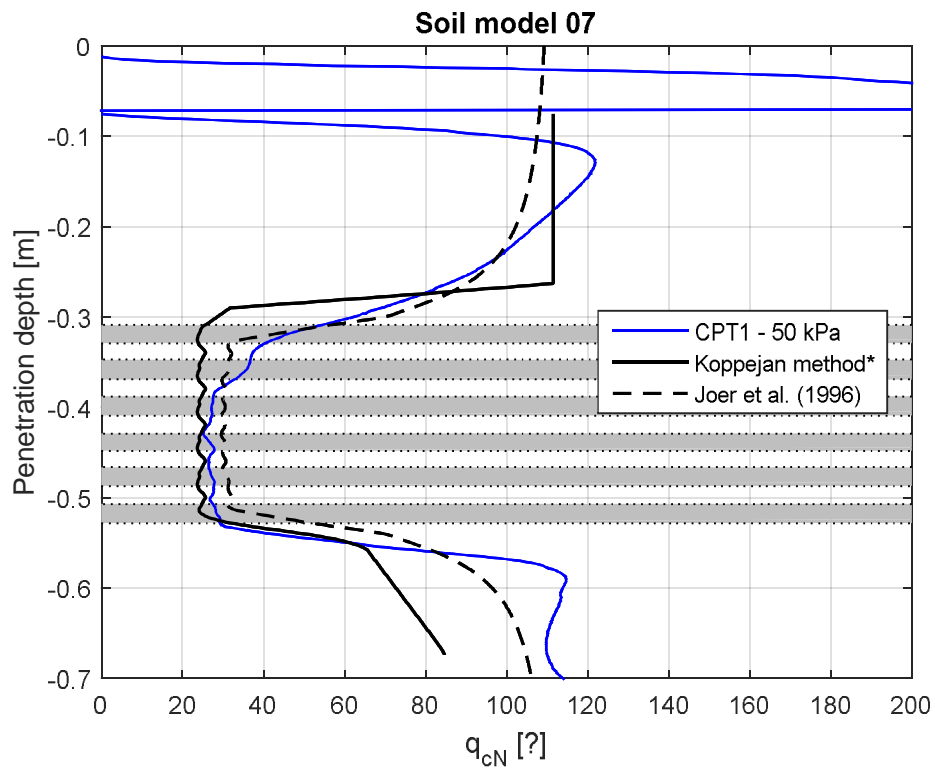


Figure 6.9 Simulations of normalized q_c profiles

From both analytical solutions, thin layer correction factors are derived for a range of combinations of $q_{cN};\text{"true"}$ values (based on the simulation results of the middle sand layer). These factors are compared with the factors derived from the test results (for $H/d_{\text{cone}} = 0.8$ and 1.6). Figure 6.10 presents the derived factors as function of the ratio of $q_{cN};\text{"true"}$ and Figure 6.11 as function of the $q_{cN};\text{layer};\text{max}/q_{cN};\text{layer};\text{min}$ ratio. The methods show different trends. It is concluded that the method of Koppejan results in more realistic trends compared to the linear elastic solution of Joer et al. (1996).

Therefore, thin layer correction factors are also derived for $H/d_{\text{cone}} = 0.5$ and 3.2 by the method of Koppejan. Figure 6.12 presents the derived factors as function of the ratio of $q_{cN};\text{"true"}$ and Figure 6.13 as function of the $q_{cN};\text{layer};\text{max}/q_{cN};\text{layer};\text{min}$ ratio. A reasonable to good fit is found for the factors derived from the test results. The method can be used to derive correction factors for other H/d_{cone} ratios.

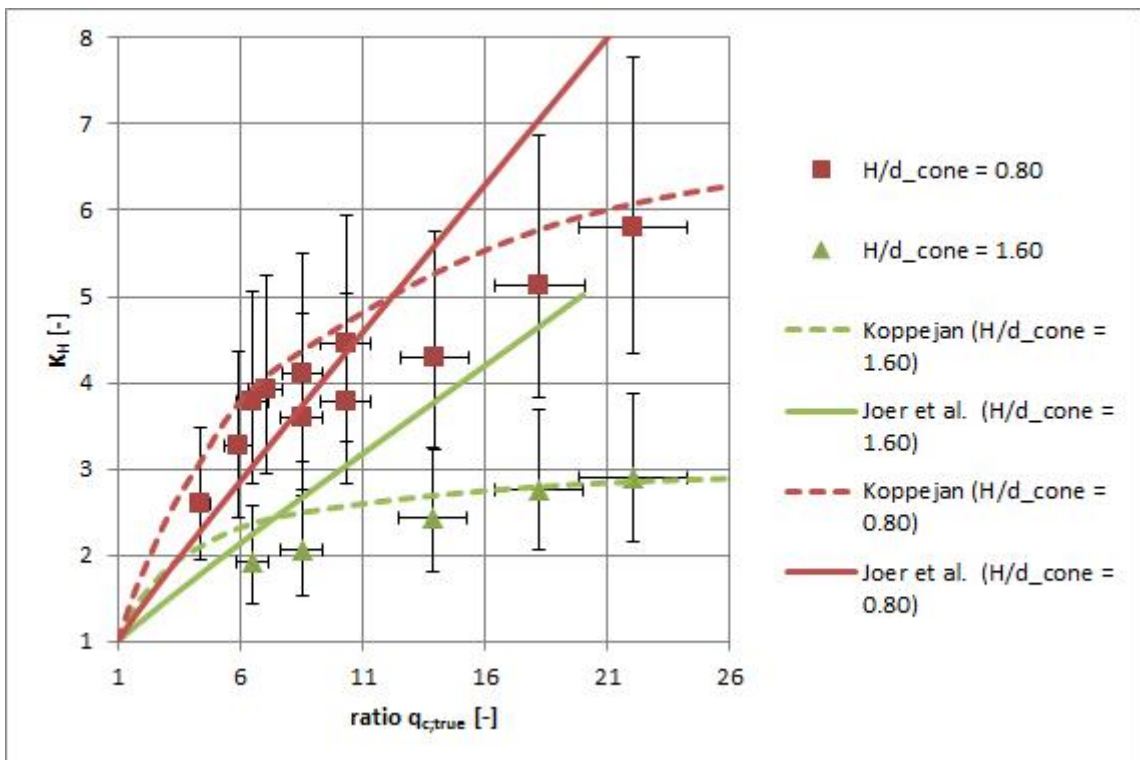


Figure 6.10 Comparison derived correction factors from measurements and from simulations

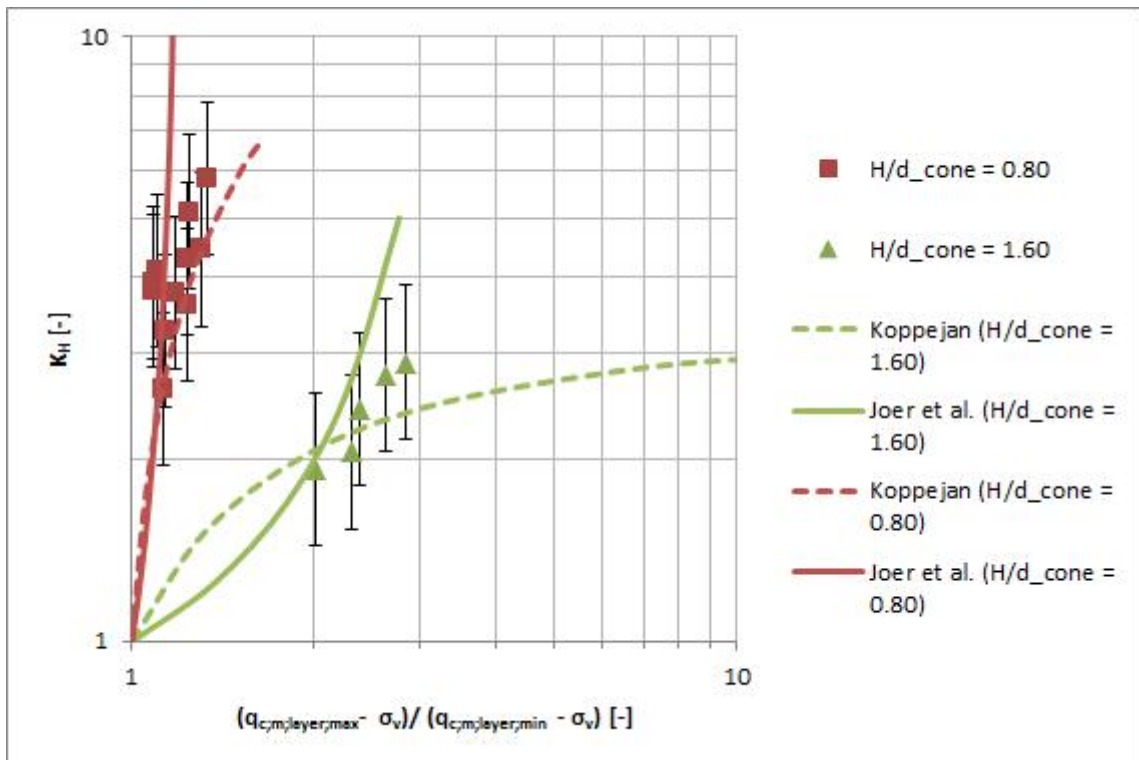


Figure 6.11 Comparison derived correction factors from measurements and from simulations

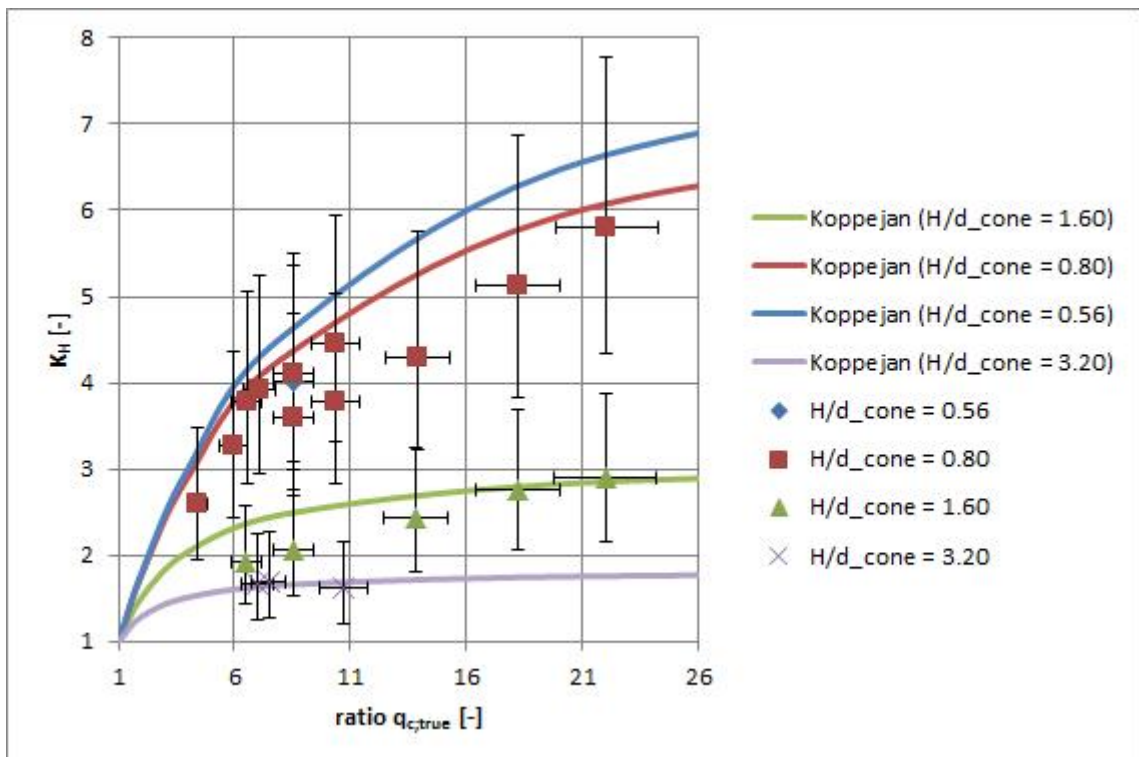


Figure 6.12 Comparison correction factors derived from measurements and from simulations

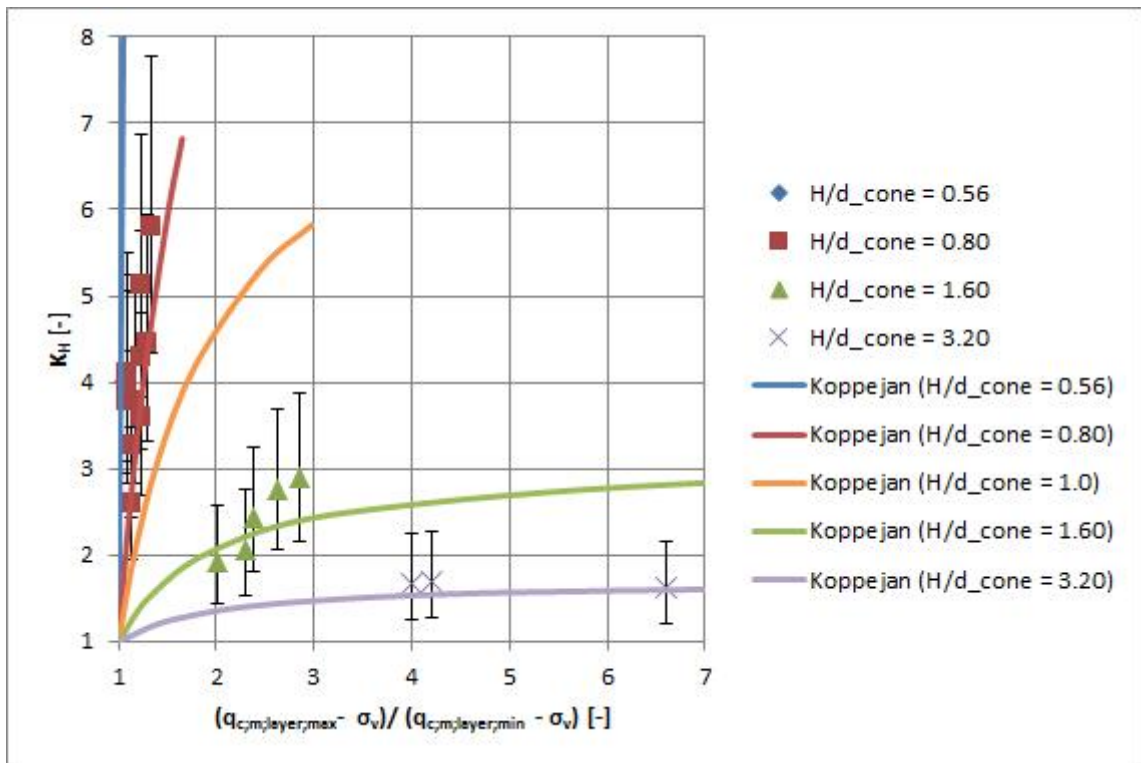


Figure 6.13 Comparison correction factors derived from measurements and from simulations

7 Discussion

Calibration chamber cone penetration tests are performed in artificially built up layered soil to investigate the influence of layer thickness, soil density and stress level. Some aspects with respect to the test results and translation to practice are mentioned in this chapter.

- *Cone size*

A smaller cone (25 mm), than commonly used (36 mm), is applied in most cases, since multiple tests could be performed in one soil model by applying a 25 mm cone and since the model preparation is harder when the layer thickness becomes smaller. Besides 25 mm diameter cones, also the more common 36 mm cone is applied in some soil models. It is not understood why the 36 mm cone resulted in lower cone resistance compared to the 25 mm cones. However, the trend in the cone resistance profile and the derived correction factors are similar for both cone types.

- *Data sampling interval*

The smaller the cone and the smaller the data sampling interval, the more contrast and detail will be measured. A data sampling interval of 1 mm is applied, while an interval of 20 mm is often applied in practice. This will act as a filter for laminated soil deposits which contain thin layers with thicknesses similar or smaller than the cone diameter. Therefore extreme values may be lost.

- *Penetration in layered soil*

In order to achieve a data sampling interval of 1 mm, a penetration rate of 4 mm/s is applied, while a penetration rate of 20 mm/s is applied in practice. Some rate effects, with respect to soil behaviour (drained or (partially) undrained), cannot be excluded. Pore pressures aren't measured. It should be realized that idealized soil profiles, with clear transitions between clean sand and clean clay layers, are tested. In the field such situations probably do not exist, see also Section 1.1. Further, it is observed that clay and sand is taken along with the cone during penetration, which also complicates the interpretation of the measurements, both in the model as well as in practice.

- *Model preparation*

The soil models are prepared in a consistent manner by using the same procedure and technicians. Since it is hard to determine the density of thin layers, due to a relative large contribution of measurement errors, additional analyses are performed to assess the model preparation, see Section 5.3, which give good confidence in the model preparation. Figure 7.1 gives the average cone resistance of the thinly layered parts of the soil models as a function of the relation proposed by Lunne & Christoffersen (1983), which takes the density and the stress level into account. The results are grouped based on the ratio of the layer thickness H and the cone diameter d_{cone} . Also this plot gives good confidence in the model preparation and the test setup. Possible (local) variation in density is taken into account in the analysis of the measurements.

- *Tested configurations*

A range of layer configurations is tested, however not all imaginable configurations are covered. The layered part consisted of multiple thin sand and layers of equal thickness. Besides models where this layered part is enclosed by thicker sand layers, also one model is

prepared where the layered part is enclosed by thicker clay layers (soil model 9). Further, models were prepared with two thin layered parts separated by a thicker sand layer.

- *Derived correction factors*

Since the layers are relatively thin, the determined $q_{c, "true"}$ should apply for the whole layer, assuming uniform properties over the layer height. Thin layer correction factors are derived using the relation of Lunne & Christoffersen (1983). This may have introduced some conservatism. Further, it has to be mentioned that only one, artificial, clay type is applied.

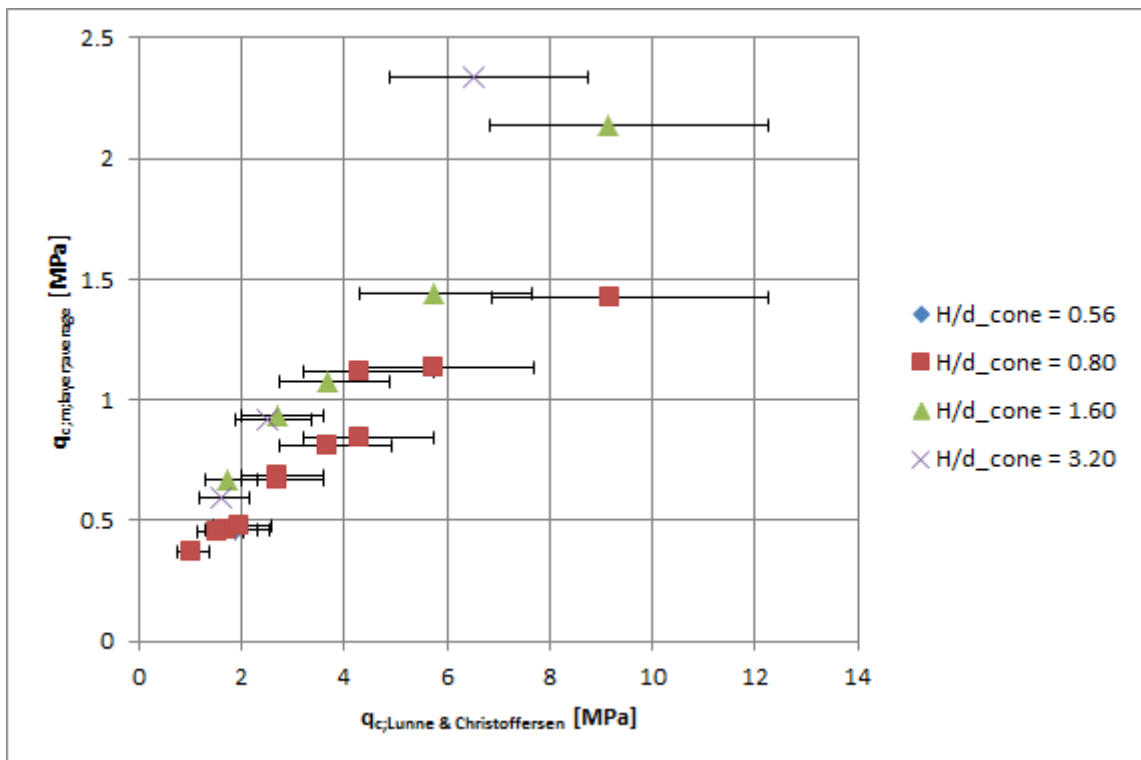


Figure 7.1 Average cone resistance layered part plotted as function of relation of results of the relation proposed by Lunne & Christoffersen (1983)

8 Proposed correction method

In order to propose a correction method for the engineering practice, first some CPT data from locations in the Netherlands where flaser beds are present in the subsoil has been analysed. Only CPT data has been analysed when also a borehole log (photographs) from the same location was available. In this way the levels of the tidal flats are known and the thickness of the individual layers can be estimated. It is observed that the cone resistance in these tidal flat deposits in general is higher and shows more contrast, at a frequency which does not correspond to the layer thickness observed in the borehole logs, compared to the tests results. It is concluded that the observed spatial frequency and contrast in cone resistance is not representative for the small individual layers and cannot be used directly to derive the correction factors.

Therefore a statistical analysis is performed on the derived correction factors of all individual layers grouped by the H/d_{cone} -ratio (0.8, 1.6 and 3.2). The correction factors for the 0.8 H/d_{cone} -ratio are log-normally distributed, while a normal distribution fits well for the other two groups. The derived correction factors are plotted as function of the H/d_{cone} -ratio in Figure 8.1. The values of the individual layers are presented in blue; the average values are given in orange. Five lines are plotted which connect the mean value (solid line), the 15% upper and lower bound (striped) and the 5% upper and lower bound (dotted) of the three H/d_{cone} -ratios. The lines are truncated for H/d_{cone} -ratios smaller than 0.8, since the few results from the 0.56 H/d_{cone} -ratio test are in line with the results from the 0.8 H/d_{cone} -ratio test. These lines can be used to correct CPT data from thinly layered deposits. In order to know the layer thickness, an estimate has to be made by a geologist, preferably from a borehole log.

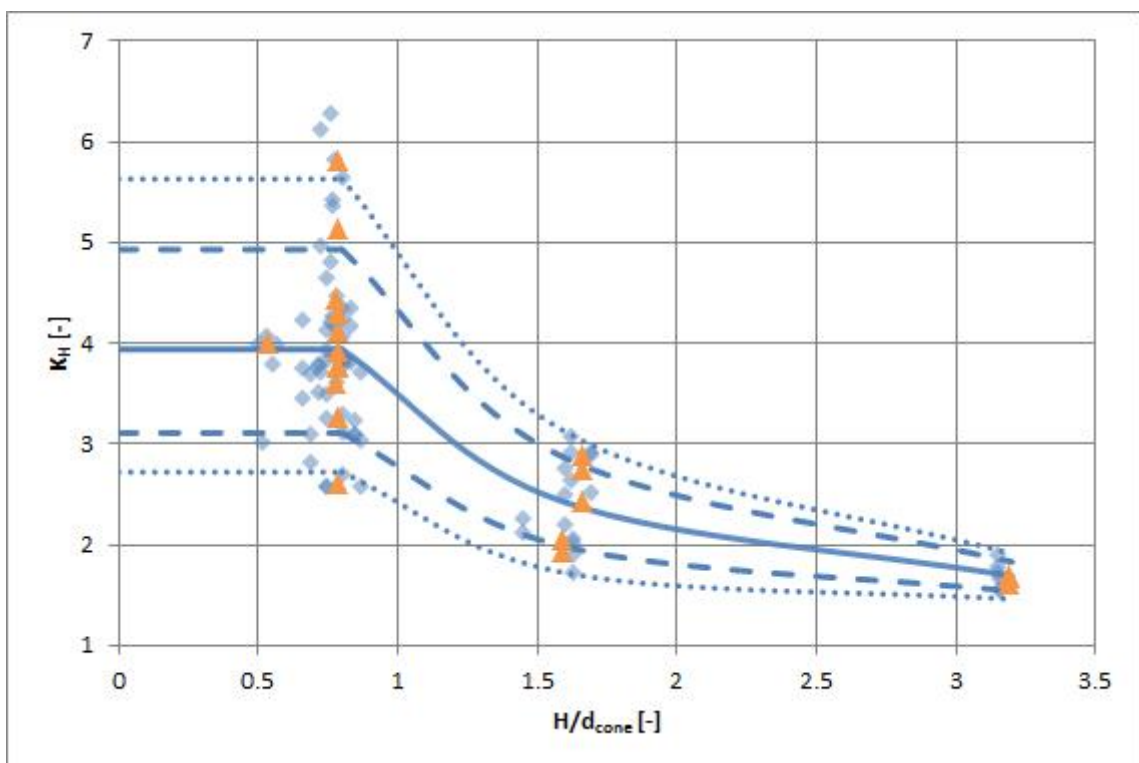


Figure 8.1 Derived correction factors as function of the H/d_{cone} -ratio. The lines connect the mean (solid), the 15% upper and lower bound (striped) and the 5% upper and lower bound (dotted) values of three H/d_{cone} -ratios

9 Conclusions

To generate a broader base for thin layer correction for laminated soil deposits which contain multiple layers with thicknesses similar or smaller than the cone diameter calibration chamber tests are performed. Cone penetration tests are performed in artificially built up layered soil. The influence of stress level, soil density and layer thickness is investigated. Cone penetration tests are performed at vertical effective stress levels up to 100 kPa. Besides 25 mm diameter cones, also the more common 36 mm cone is applied in some soil models.

Several soil models have been created, having different layer configurations and/or densities. The layered models contain multiple thin layers of equal thickness. Loose and medium dense sand layers are prepared to model the stronger layers. Since it is hard to determine the density of thin layers, due to a relative large contribution of measurement errors, additional analyses are performed to assess the model preparation. These analyses give good confidence in the preparation methods.

Based on the measured cone resistance profiles, distinction can be made between the effects of the layered part as a whole, relative to the surrounding soil, and the effects of the individual thin layers. Greater contrast in cone resistance of the thin stronger and weaker layers is found for higher sand density, higher stress level and larger layer thickness. The resistance measured in the thin clay layers is also affected by the sand density and the stress level, while the layer thickness (up to 4 cm for a 25 mm cone) seems to have a smaller influence.

Besides layered models, also homogeneous sand models were prepared to measure the “true” sand cone resistance. The results show a reasonable fit with the relation proposed by Lunne and Christoffersen (1983), which is used to derive thin layer correction factors for laminated soil deposits which contain multiple layers with thicknesses similar or smaller than the cone diameter.

Correction factors between 1.5 and 6 are found. The derived correction factors show clear dependency of layer thickness relative to the cone size, sand density and stress level. A good fit with the lower bound of an estimated range based on examination of field data of Youd et al. (2001) is found for layer thicknesses of 1.6 and 3.2 times the cone diameter, while the relation proposed by Moss et al. (2006) provides a good estimate of the correction factors derived for layer thicknesses of 0.56 and 0.8 times the cone diameter. Besides correction factors for sand layers, also correction factors are derived for clay layers.

The test results are simulated by existing analytical methods. The slightly adjusted method of Koppejan shows a good fit for the factors derived from the test results. The method can be used to derive correction factors for other H/d_{cone} ratios.

After analysing some CPT data from the field, a method for application in practice is proposed based on a statistical analysis of the test results.

10 References

Ahmadi, M.M. and Robertson, P.K. (2005). Thin-layer Effects on the CPT qc Measurement. Canadian Geotechnical Journal 42, pp. 1302–1317.

Bolton, M. and Gui, M. (1993). The study of relative density and boundary effects for cone penetration tests in centrifuge. Research report: CUED/D-SOILS/TR256.

Boulanger, R. W., and DeJong, J. T. (2018). “Inverse filtering procedure to correct cone penetration data for thin-layer and transition effects.” Proc., Cone Penetration Testing 2018, Hicks, Pisano, and Peuchen, eds., Delft University of Technology, The Netherlands, 25-44.

EA. 2013. Evaluation of the uncertainty of measurement in calibration, EA-4/02. European Co-operation for Accreditation of Laboratories, 75 p.

Hird, C.C., Johnson, P. and Sills, G.C. (2003). Performance of miniature piezocones in thinly layered soils. Géotechnique 53(10):885-900.

Joer, H.A., Randolph, M.F. and Liew, Y.H. (1996). Interpretation of Cone Resistance in Layered Soils. Proceedings 7th Australia New Zealand Conference on Geomechanics (Jaska MB, Kagawa WS and Cameron DA (eds)). Institution of Engineers, Australia, pp. 92-97.

Lunne, T. and Christoffersen, H.P. (1983). Interpretation of cone penetrometer data for offshore sands. Offshore Technology Conference, paper OT 4464, Houston, USA, May 4-5, 1983.

Mlyranek, Z., Gogolik, S. and Póltorak, J. (2012). The effects of varied stiffness of soils layers on interpretation of CPTU penetration characteristics. Archives of Civil and Mechanical Engineering 12: 253-264.

Mo, P.Q., Marshall, A.M. and Yu, H.S. (2017). Interpretation of Cone Penetration Test Data in Layered Soils Using Cavity Expansion Analysis. Journal of Geotechnical and Geoenvironmental Engineering 143(1), ISSN 1943-5606.

Moss, R. E. S., Seed, R. B., Kayen, R. E., Stewart, J. P., Der Kiureghian, A. (2006) CPT-Based Probabilistic Assessment of Seismic Soil Liquefaction Initiation. PEER Report 2005/15, April 2006.

Poel, J.T., v. & Schenkeveld, F. (1998). A preparation technique for very homogeneous sand models and CPT research. In Proc. of the int. conf. Centrifuge 98, Tokyo, 149–154.

Robertson, P.K. and Fear, C.E. (1995). Liquefaction and its evaluation. Proceedings First International Conference on Earthquake Geotechnical Engineering (Ishihara ed.), Balkema, Rotterdam, pp. 1253-1289.

Robertson P.K. (2009). Interpretation of cone penetration tests – a unified approach. Can. Geotech. J. 46: 1337-1355.

Tehrani, F. S., Arshad, M. I., Prezzi, M., and Salgado, R. (2018). Physical Modeling of Cone Penetration in Layered Sand. To be published in Journal of Geotechnical and Geoenvironmental Engineering Volume 144 Issue 1 - January 2018.

Van den Berg, P., De Borst, R. and Huétink, H. (1996). An Eulerian Finite Element Model for Penetration in Layered Soil. International Journal for Numerical and Analytical Methods in Geomechanics 20:865-886.

Van der Linden, T.I. (2016). Influence of multiple thin soft layers on the cone resistance in intermediate soils. MSc thesis, Delft University of Technology.

Vreugdenhil, R., Davis, R. and Berrill, J. (1994). Interpretation of Cone Penetration Results in Multilayered Soils. International Journal for Numerical and Analytical Methods in Geomechanics 18:585-599.

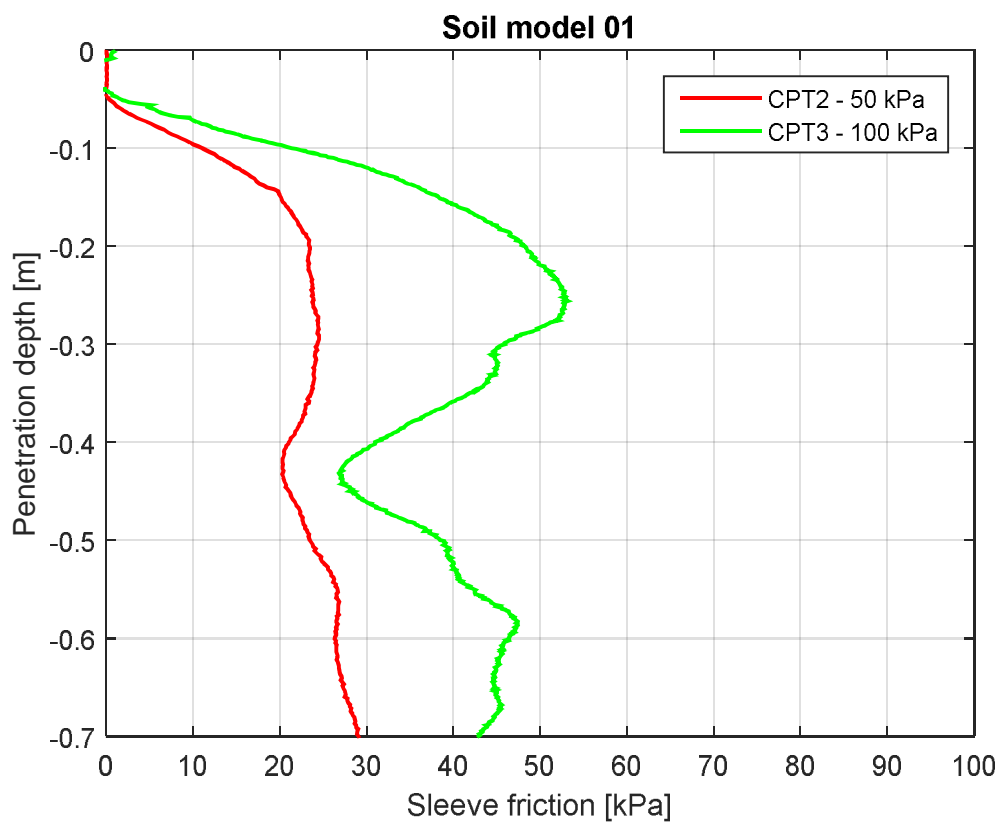
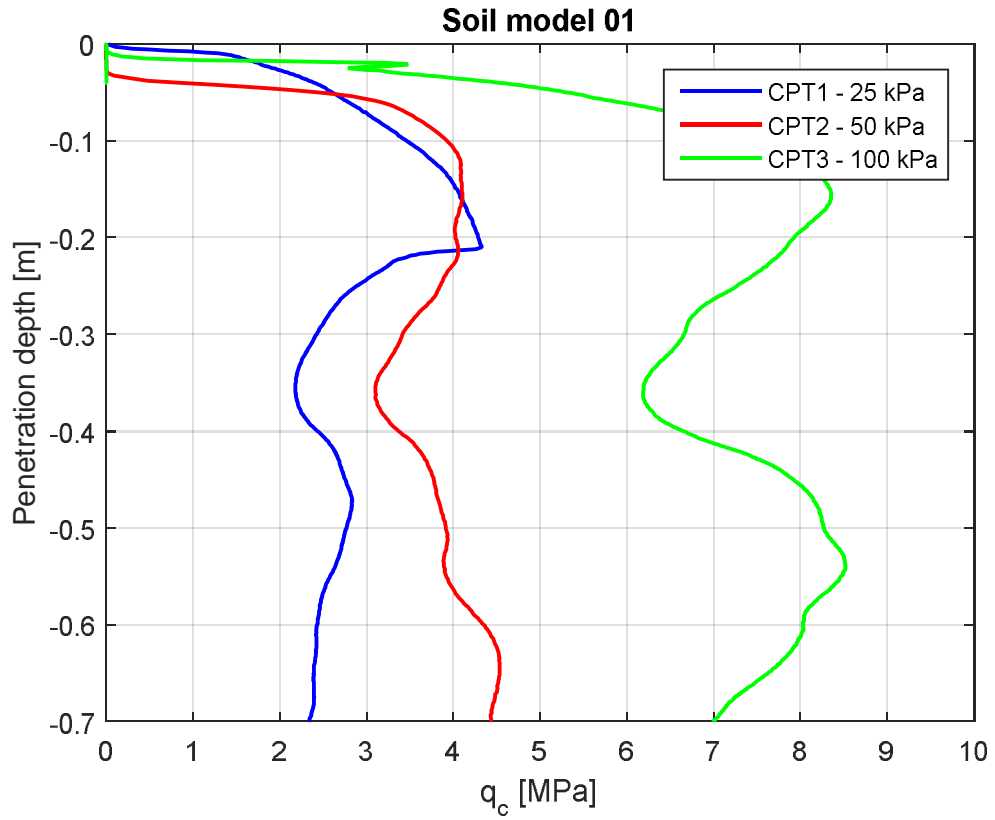
Youd, T., Idriss, I., Andrus, R., Arango, I., Castro, G., Christian, J., Dobry, R., Finn, W., Harder, L., Jr., Hynes, M., Ishihara, K., Koester, J., Liao, S., Marcuson, W., III, Martin, G., Mitchell, J., Moriwaki, Y., Power, M., Robertson, P., Seed, R., and Stokoe, K., II (2001). Liquefaction resistance of soils: Summary report from the 1996 NCEER and 1998 NCEER/NSF workshops on evaluation of liquefaction resistance of soils. J. Geotech. Geoenviron. Eng. , 127 (10), 817–833.

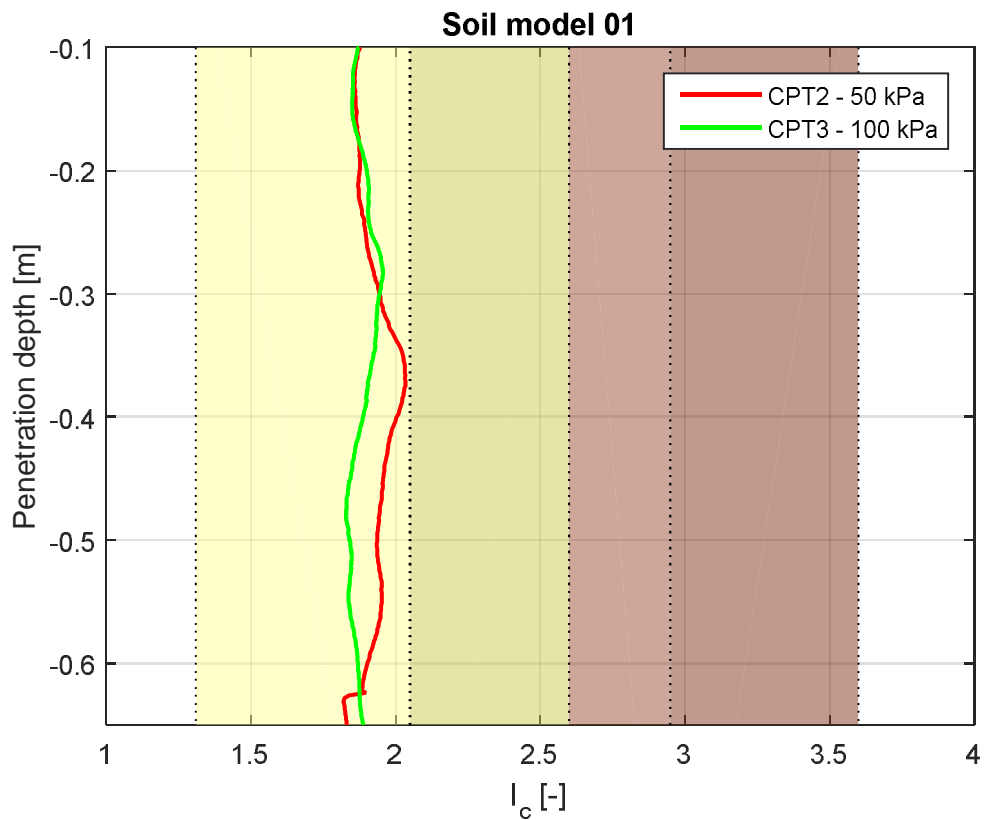
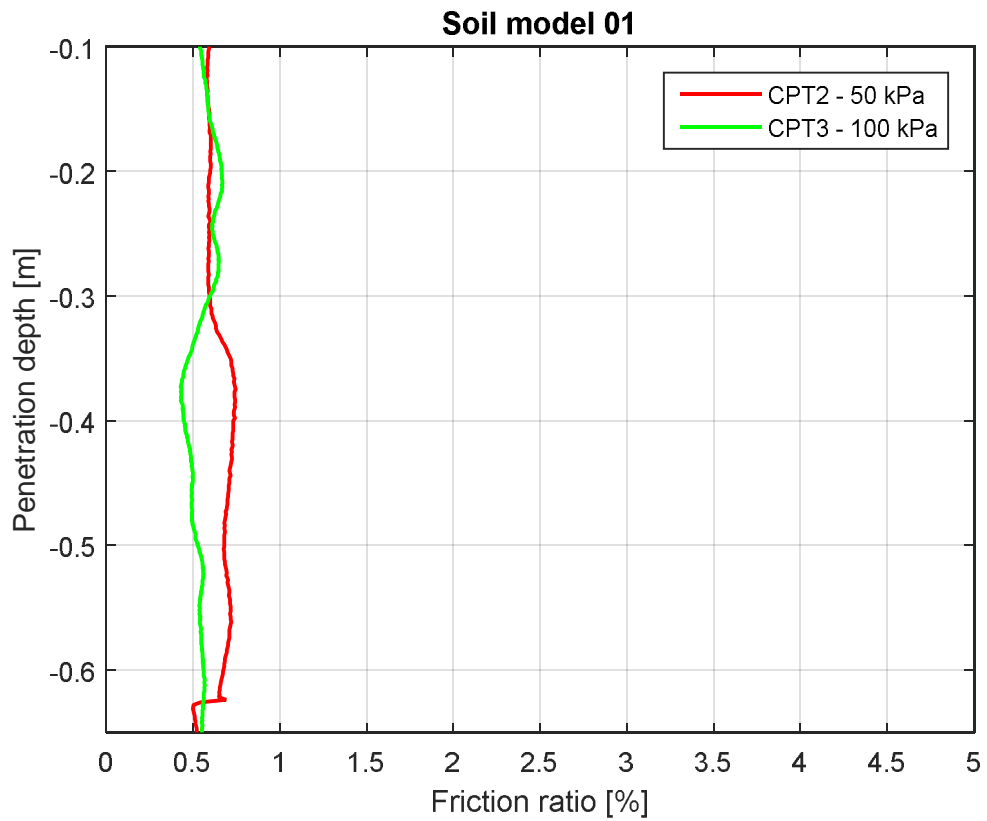
A Test results

For each soil model the following four graphs are given:

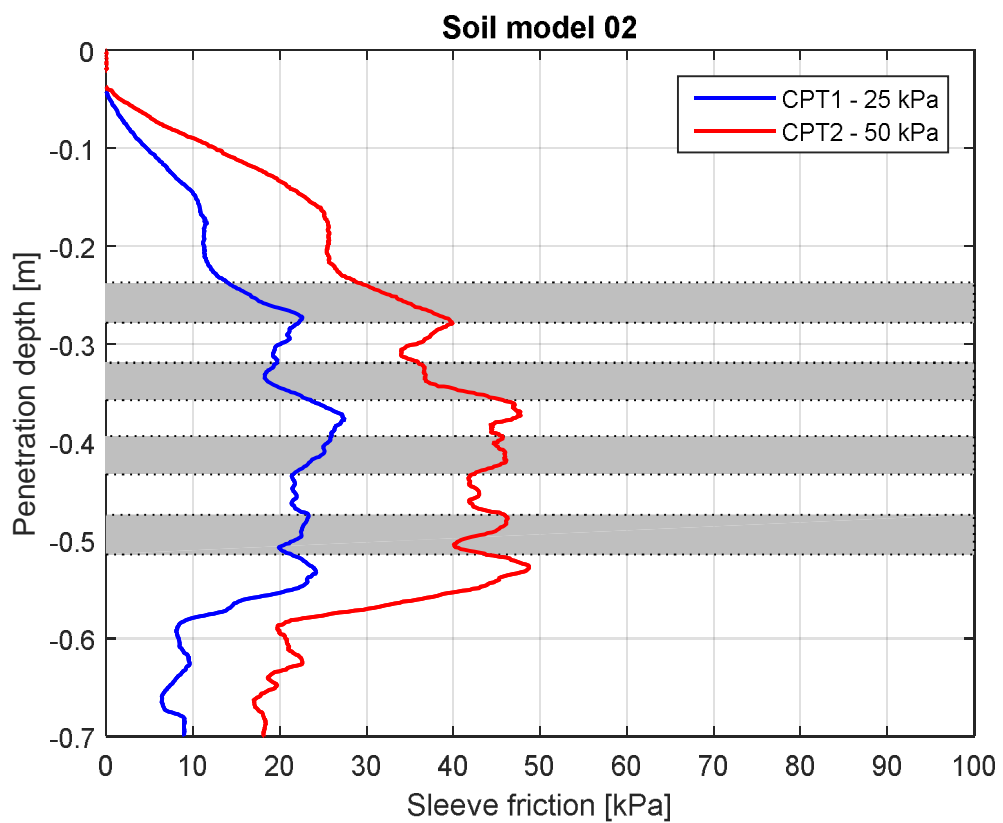
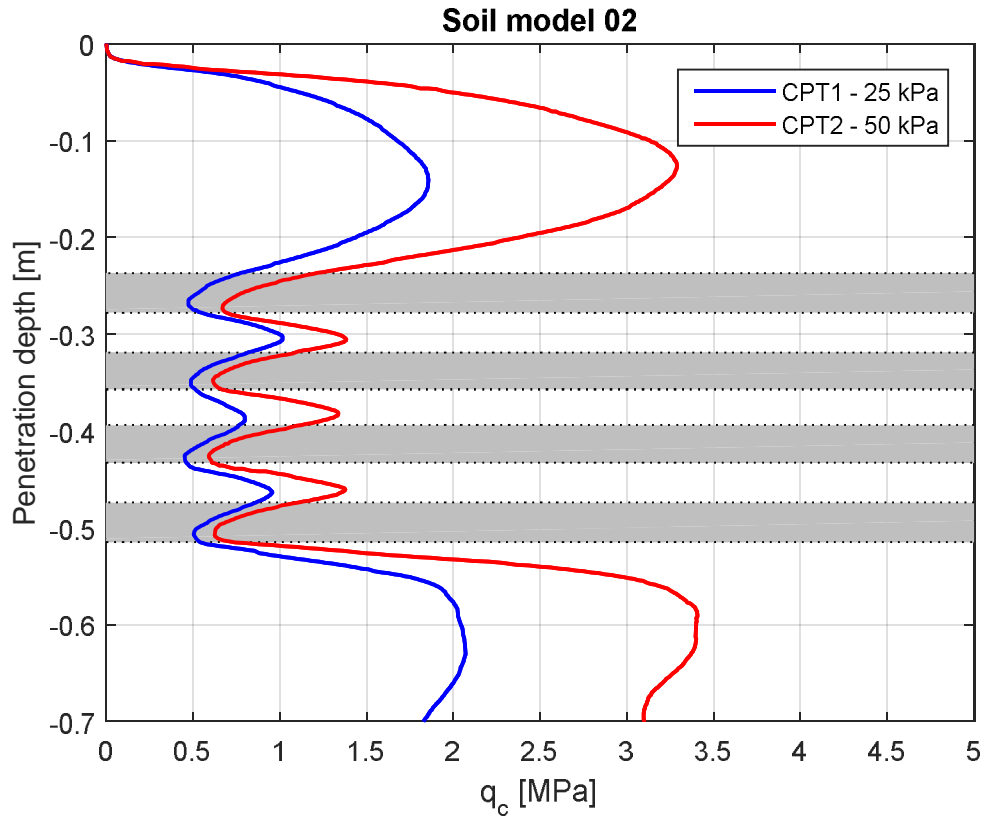
- The cone resistance q_c as function of depth.
- The sleeve friction as function of depth.
- The friction ratio as function of depth.
- The soil behaviour type index I_c (Robertson, 2009) as function of depth.

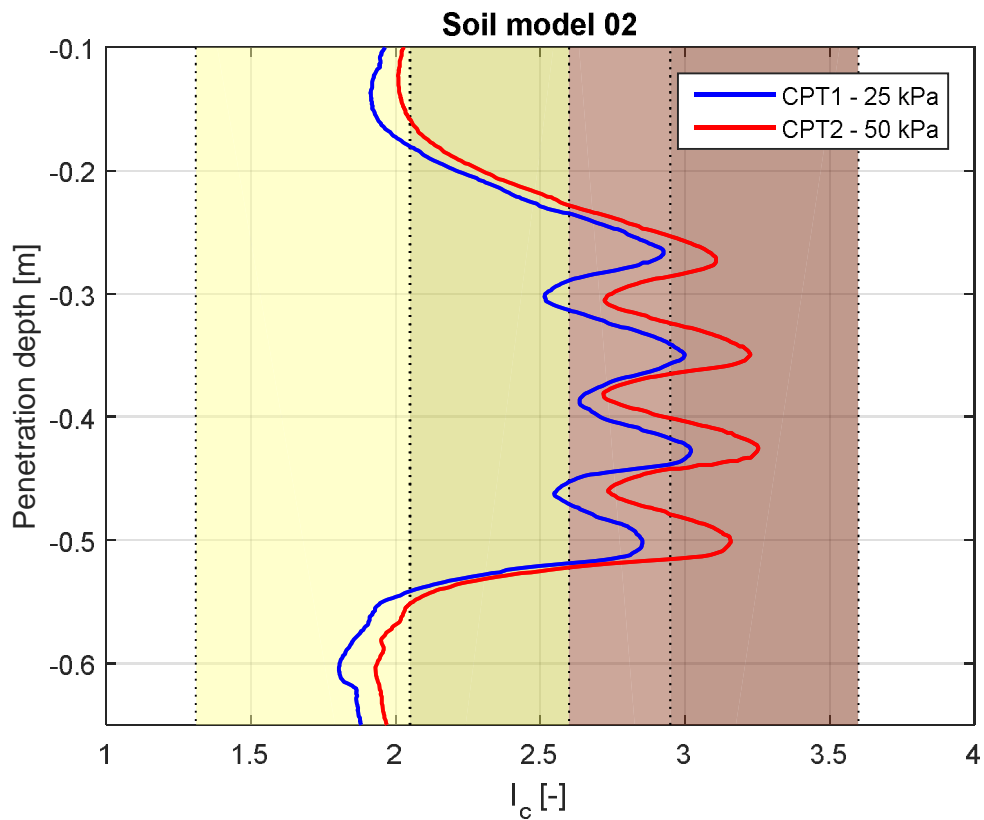
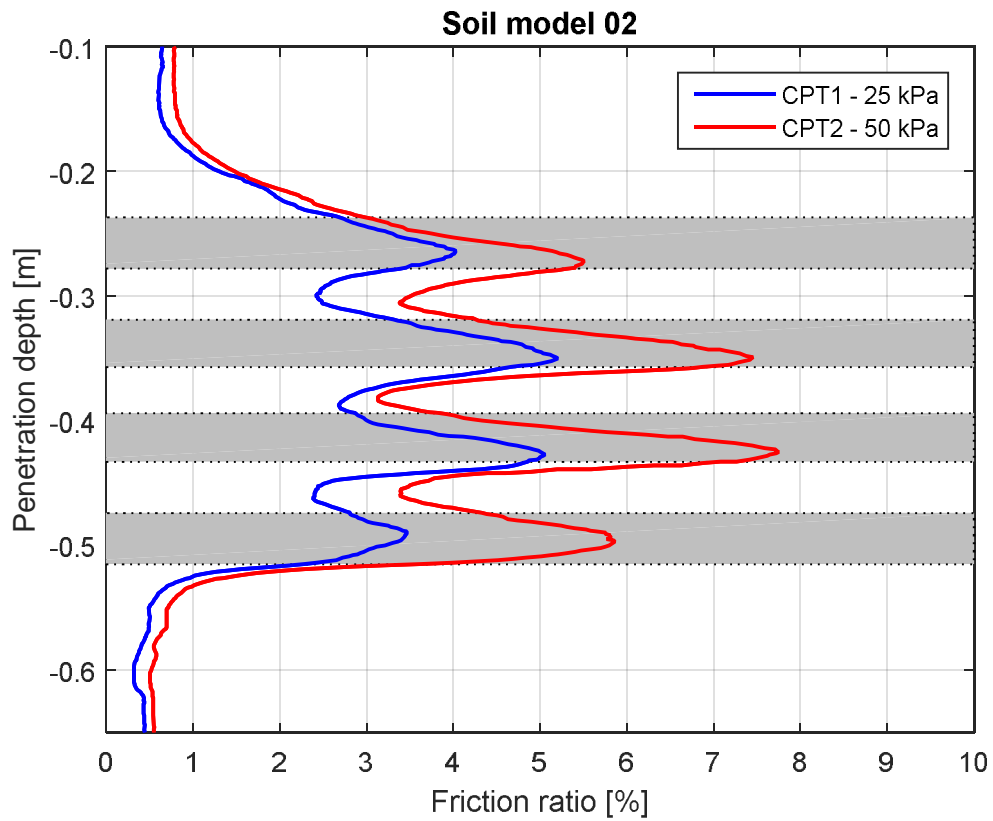
A.1 Soil model 1



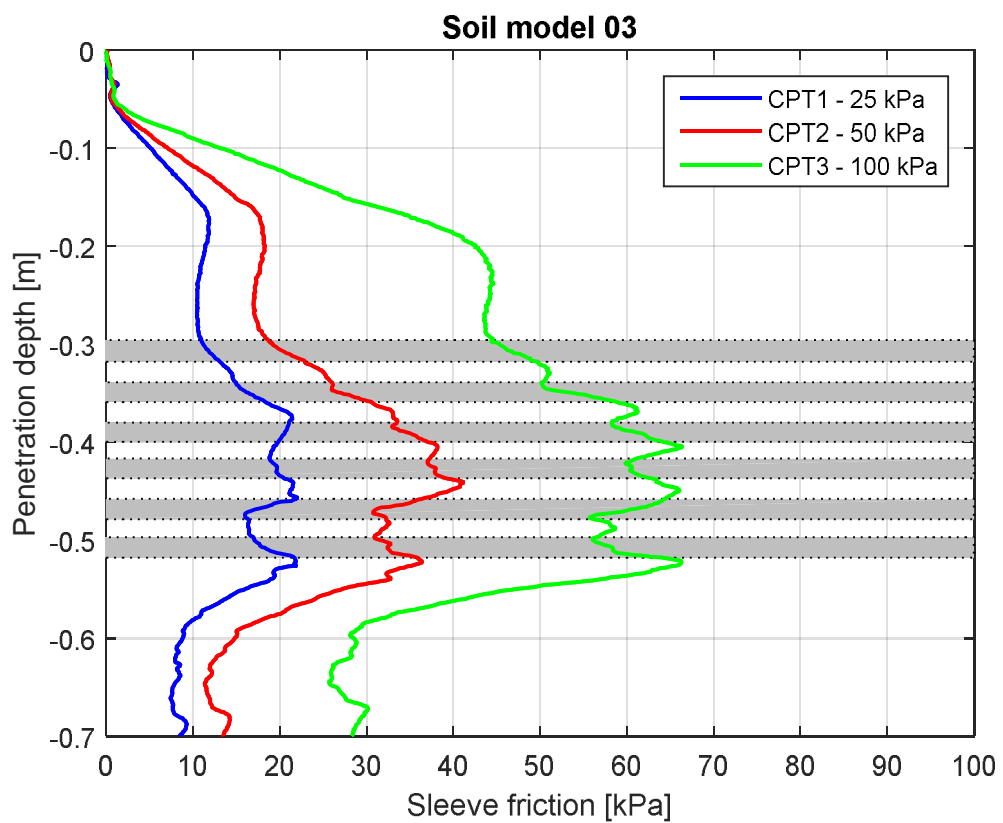
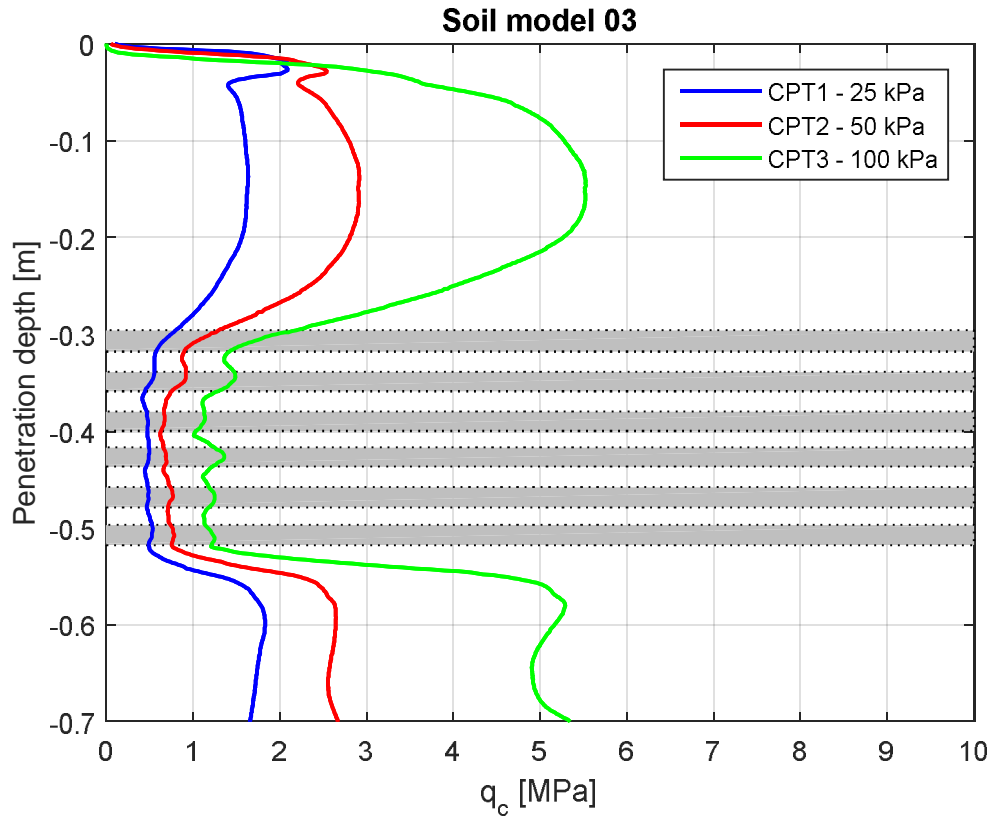


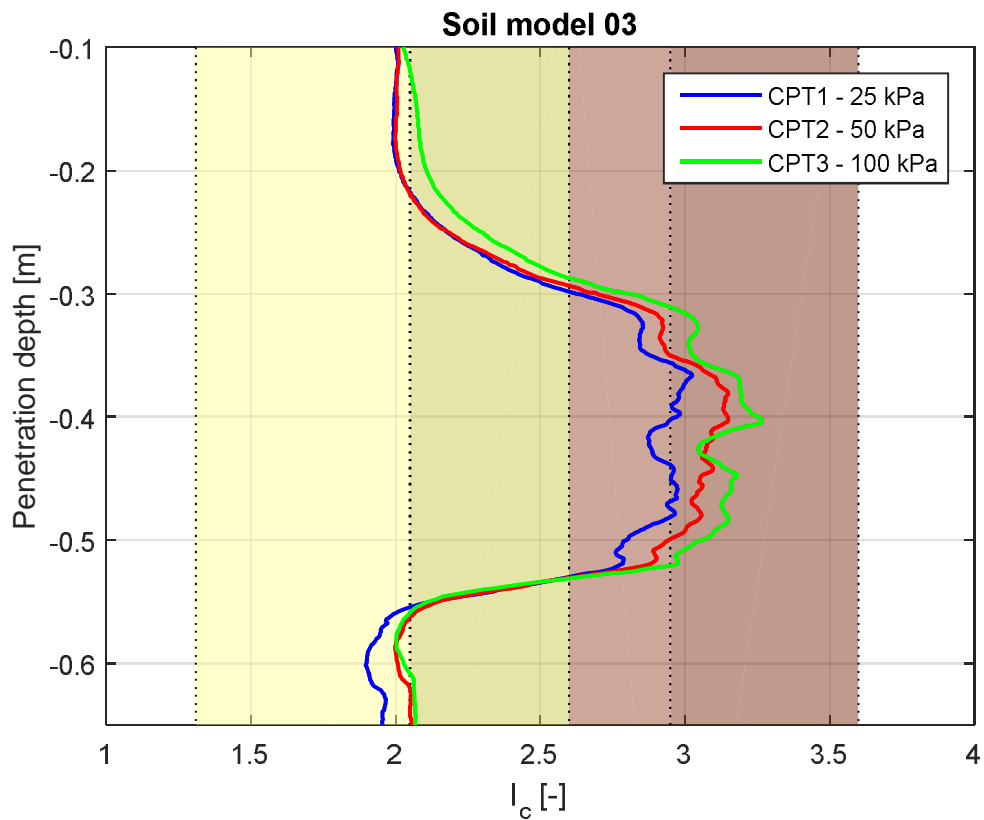
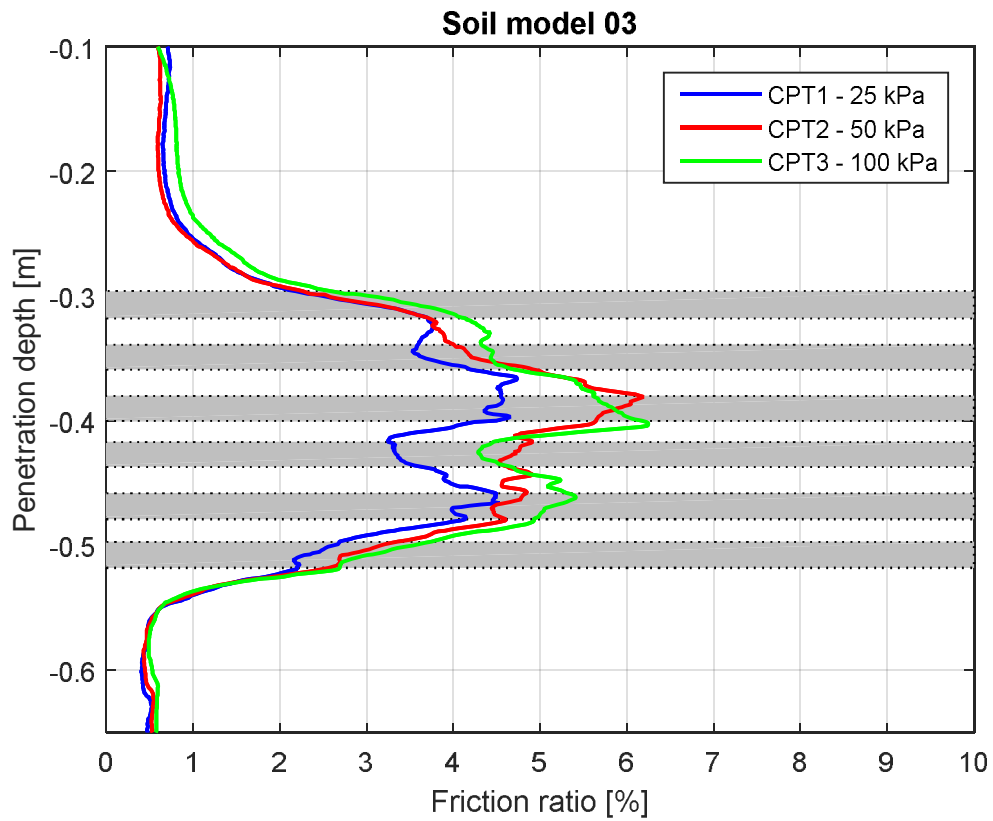
A.2 Soil model 2



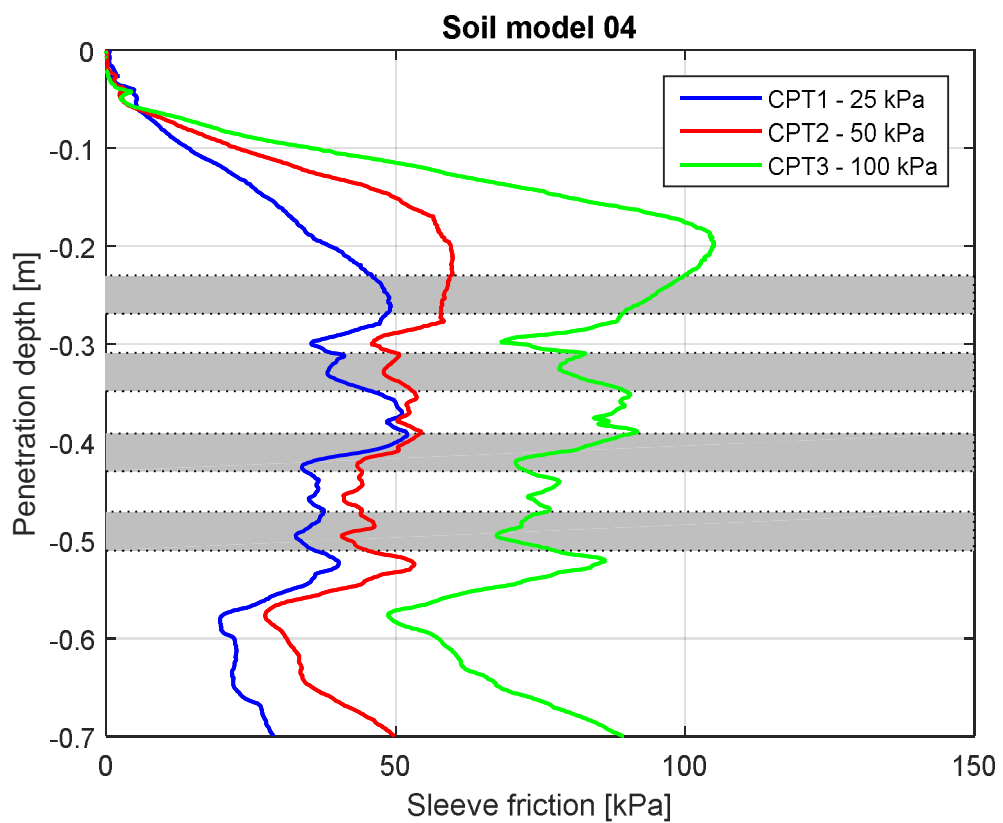
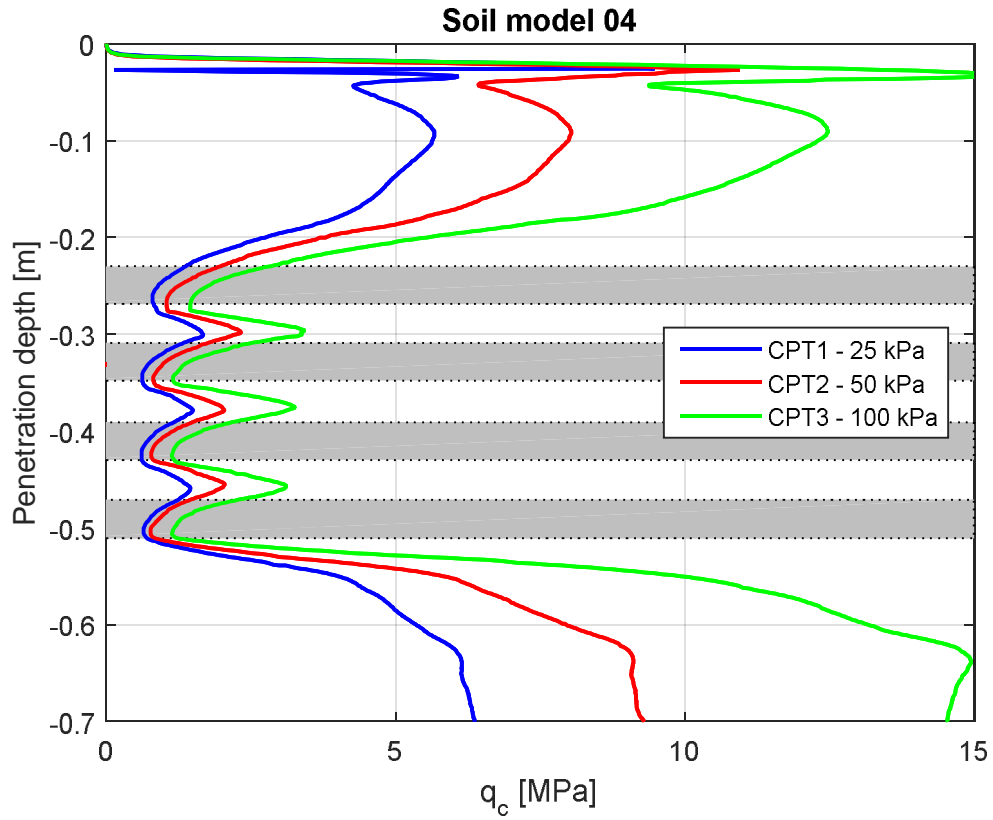


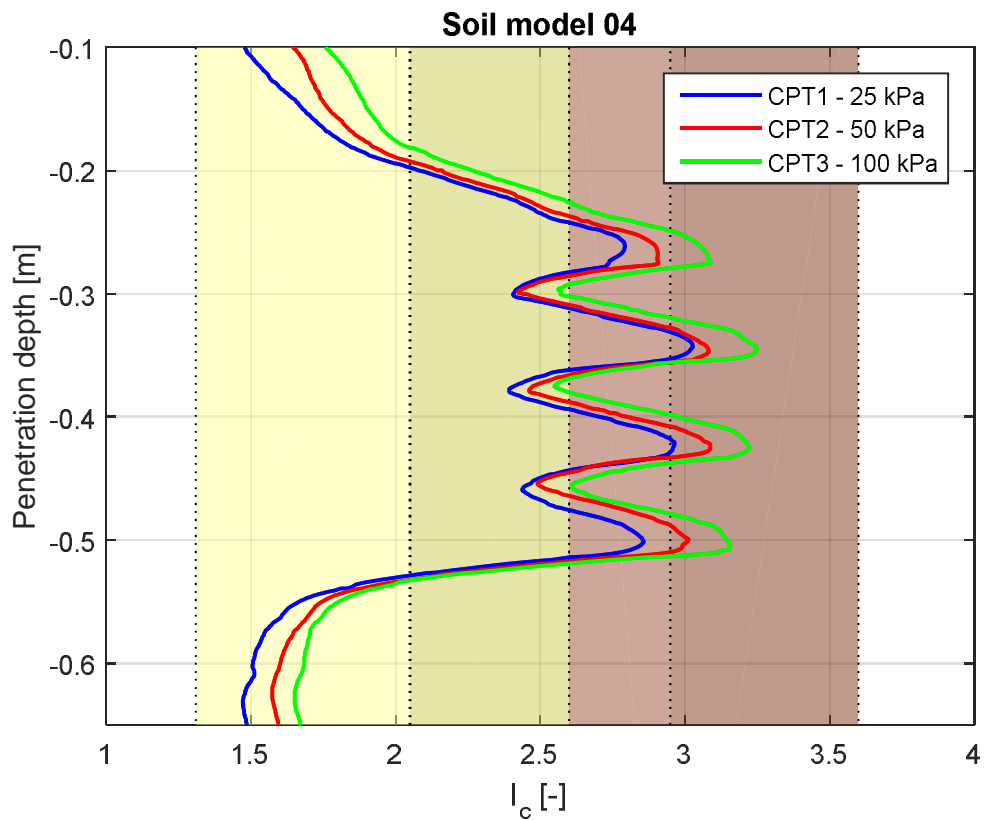
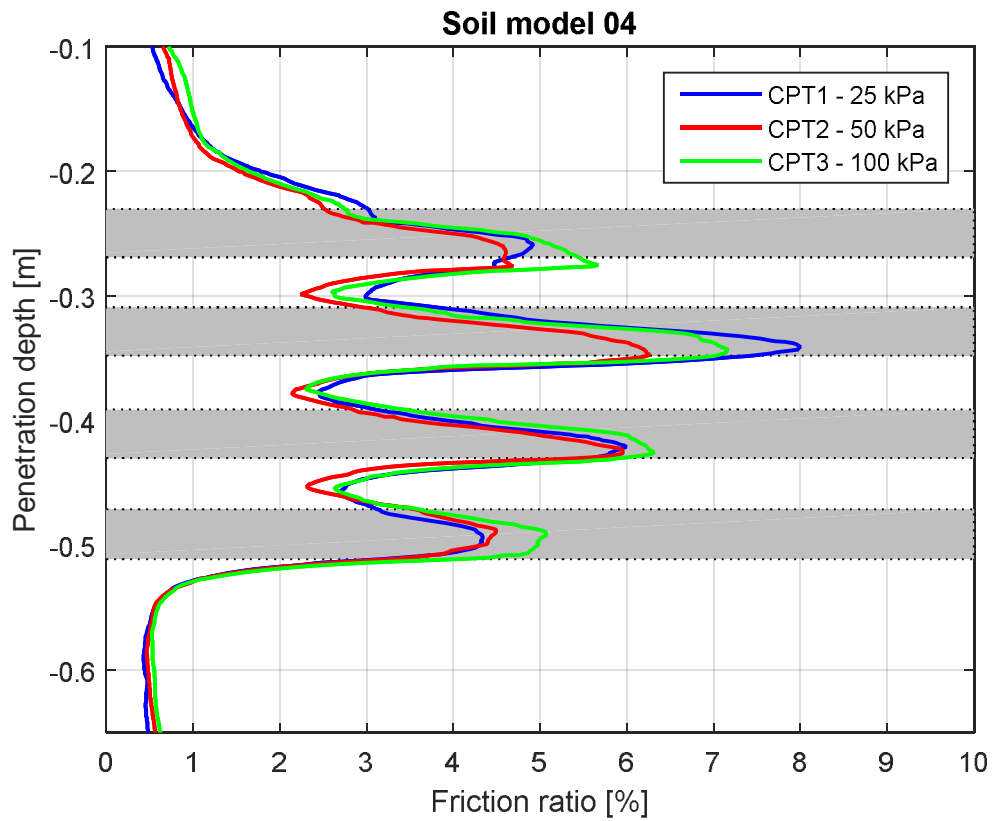
A.3 Soil model 3



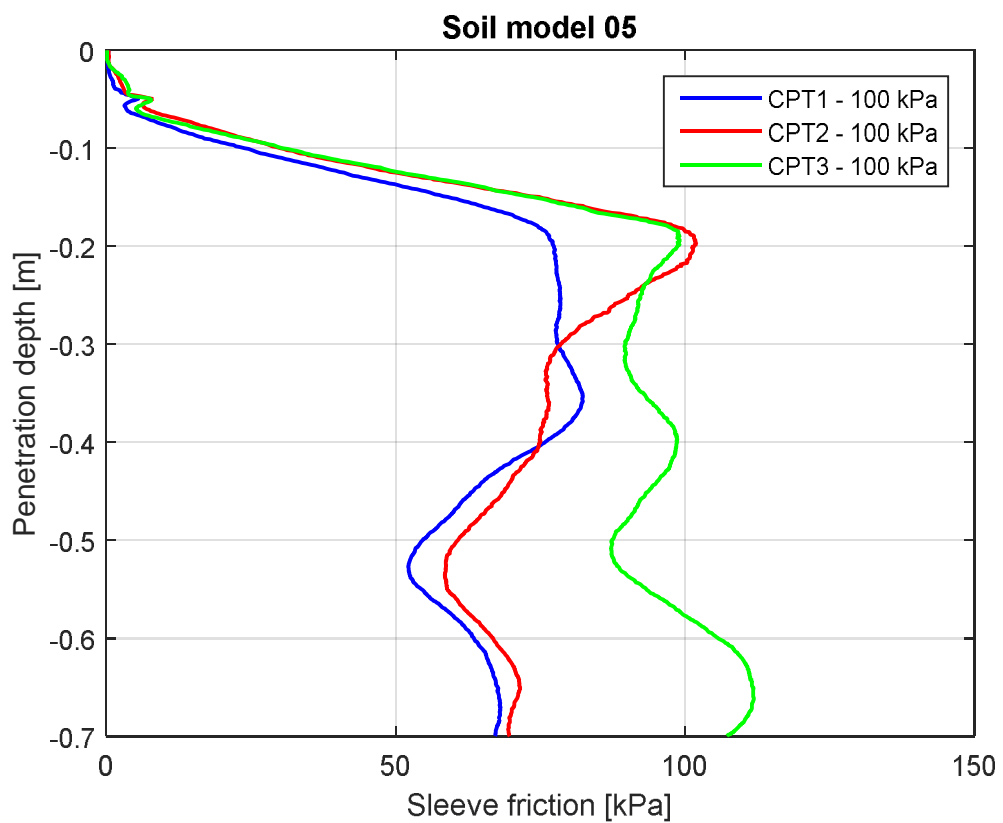
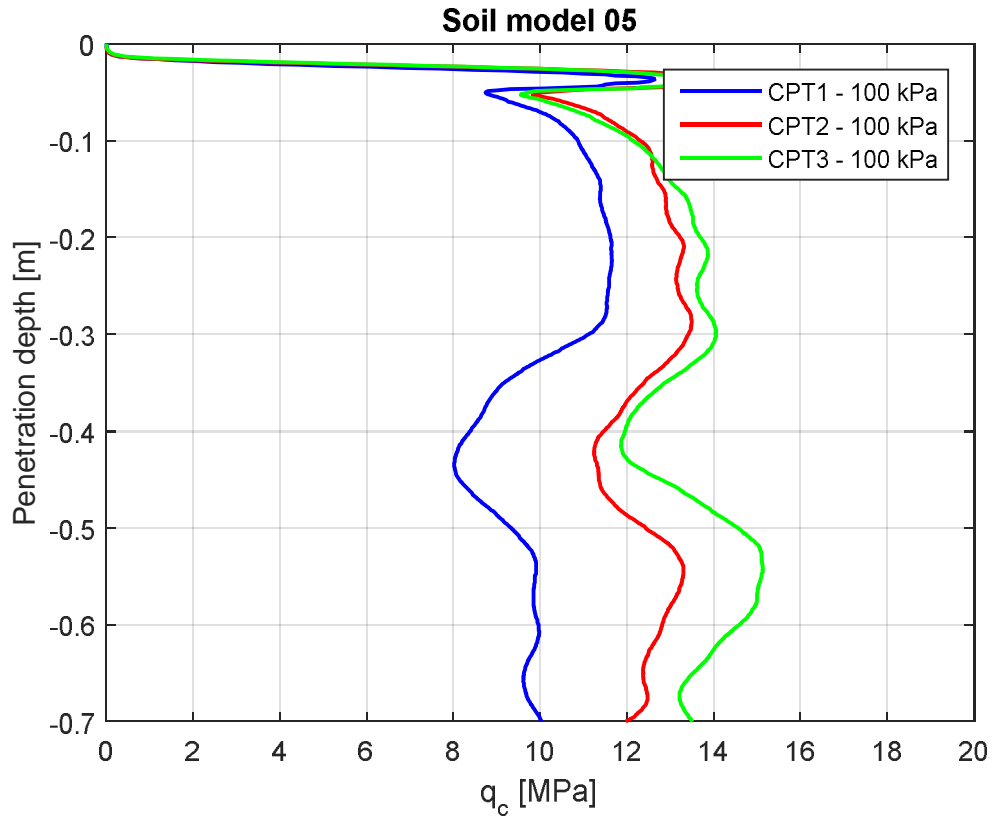


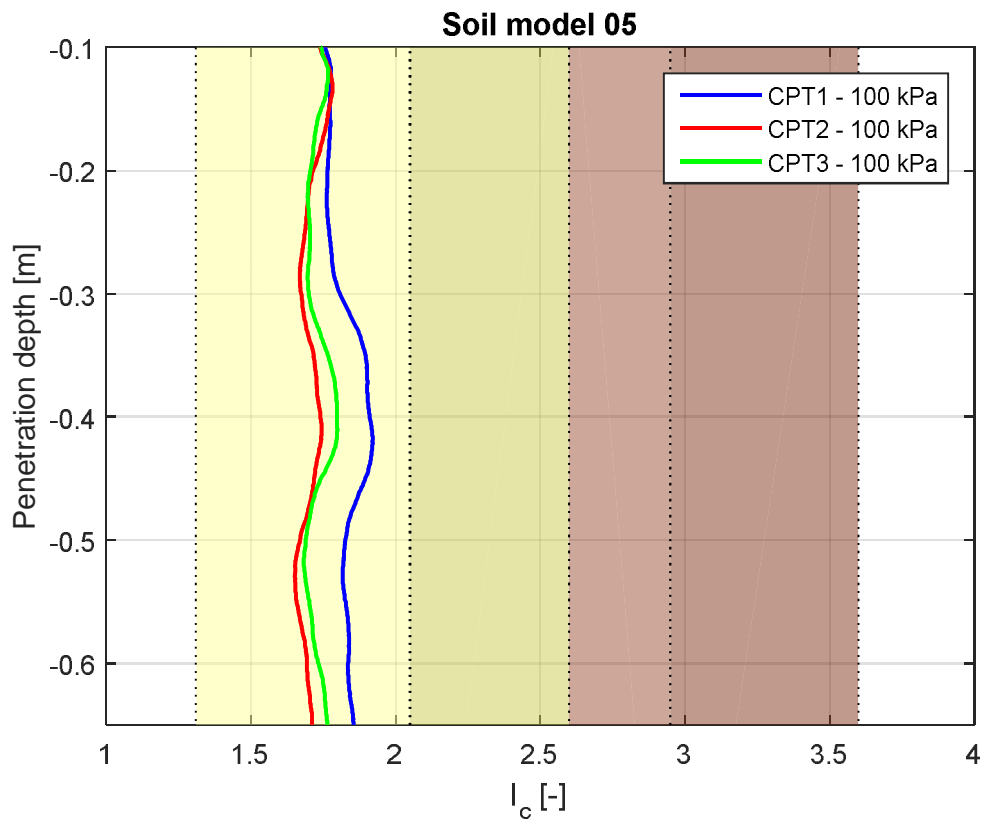
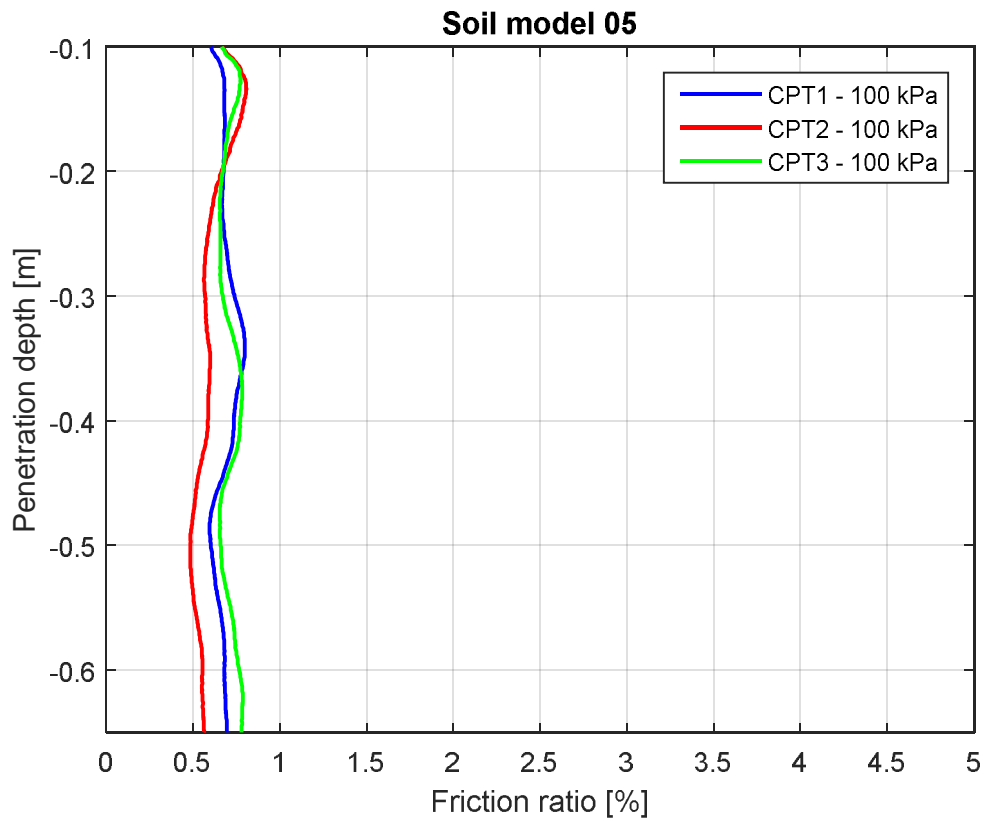
A.4 Soil model 4



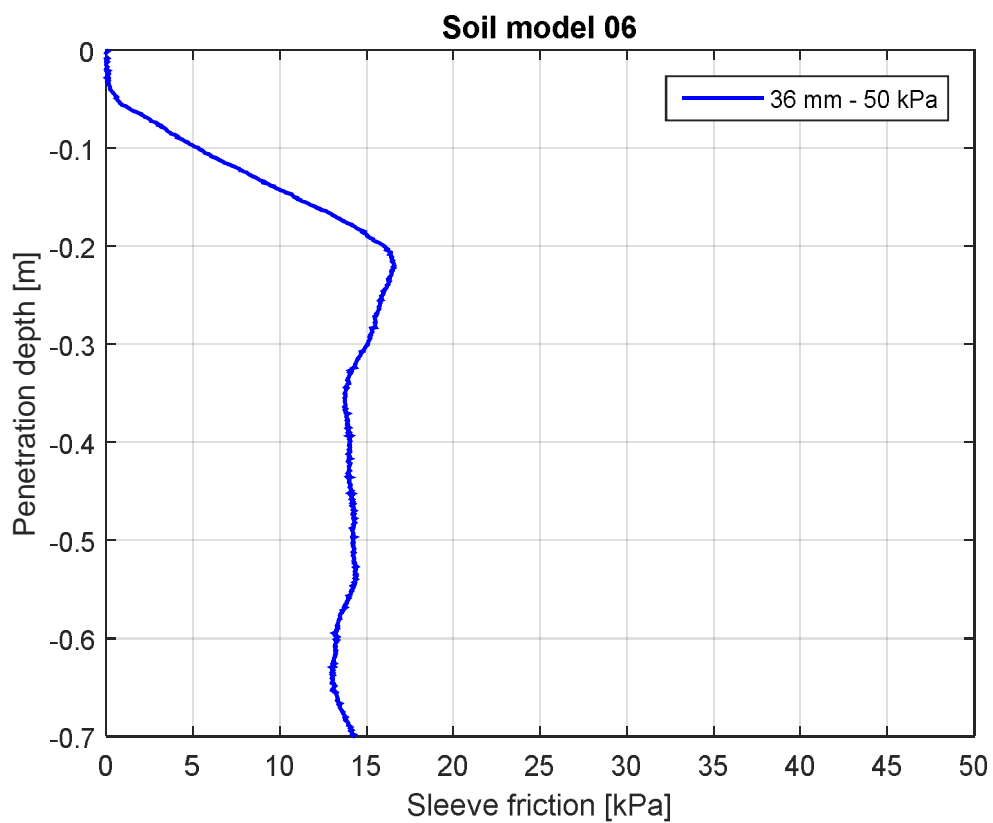
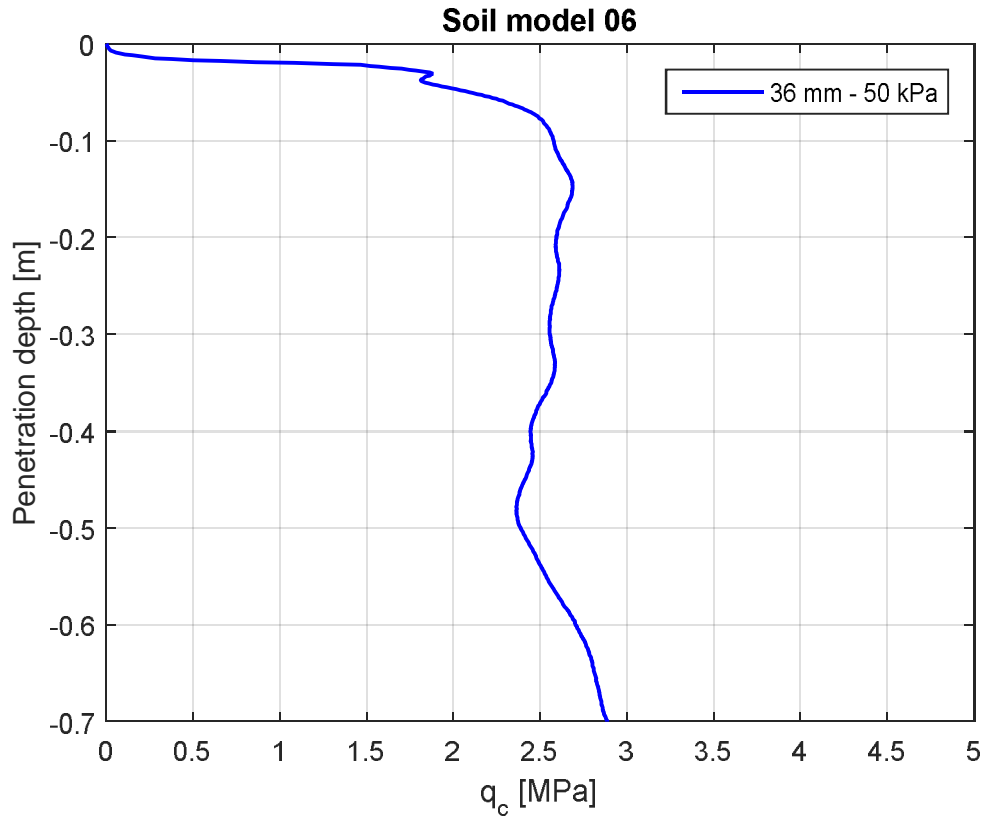


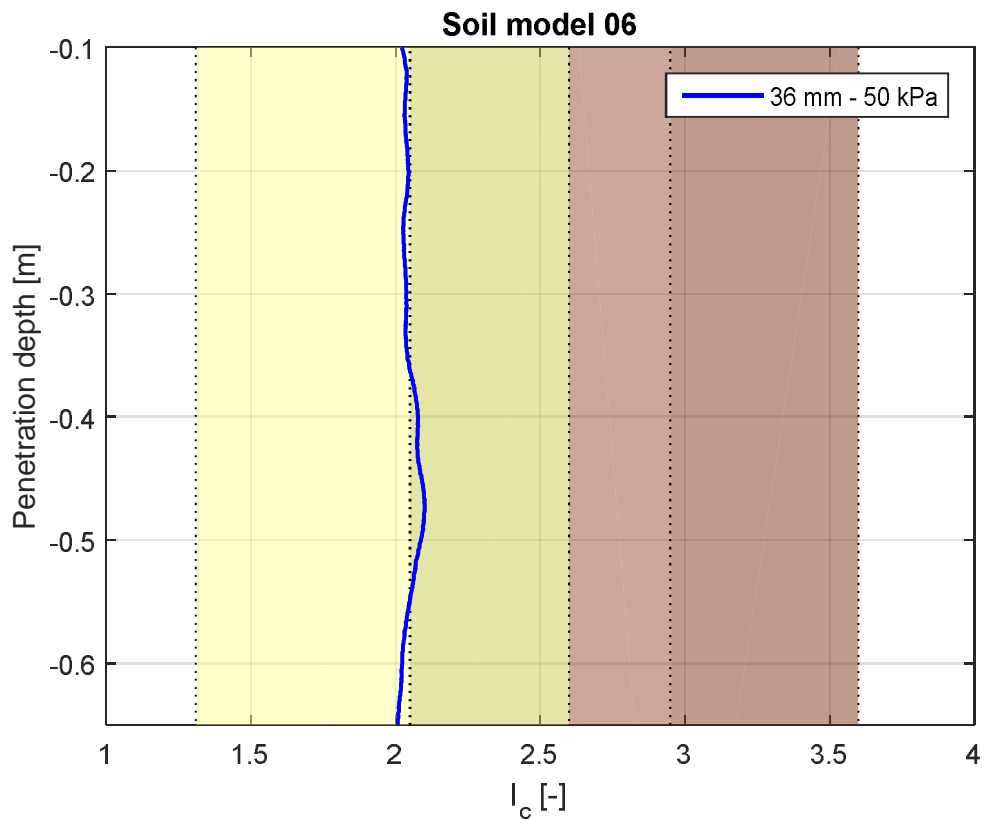
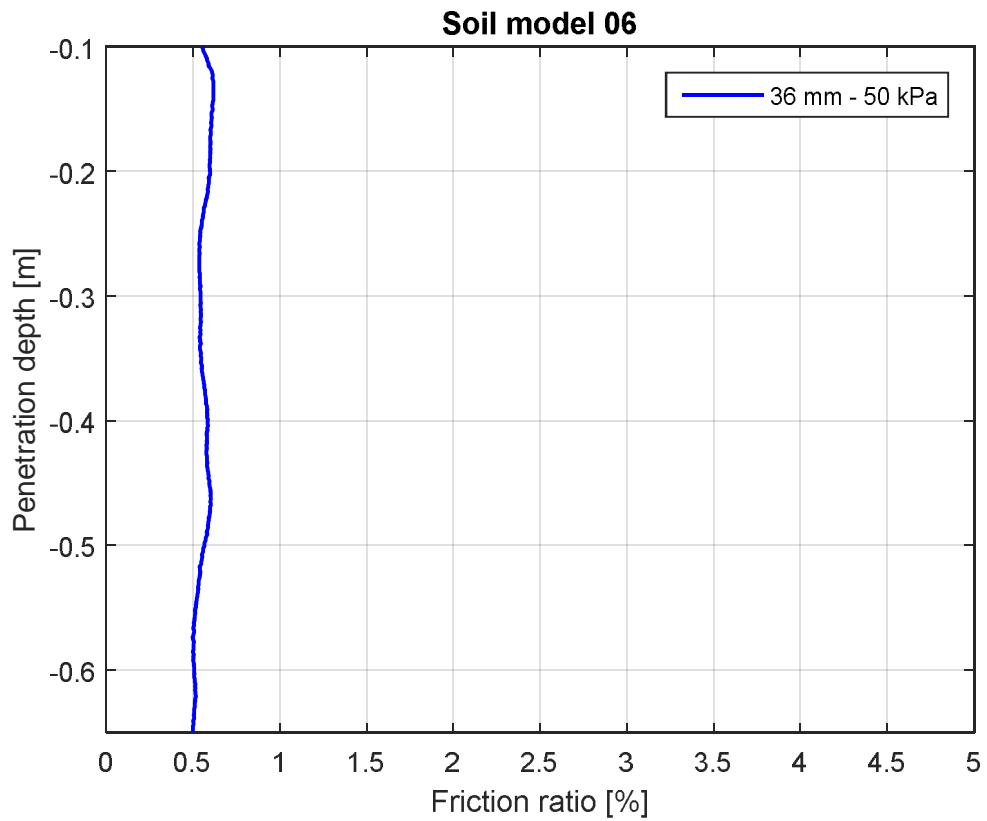
A.5 Soil model 5



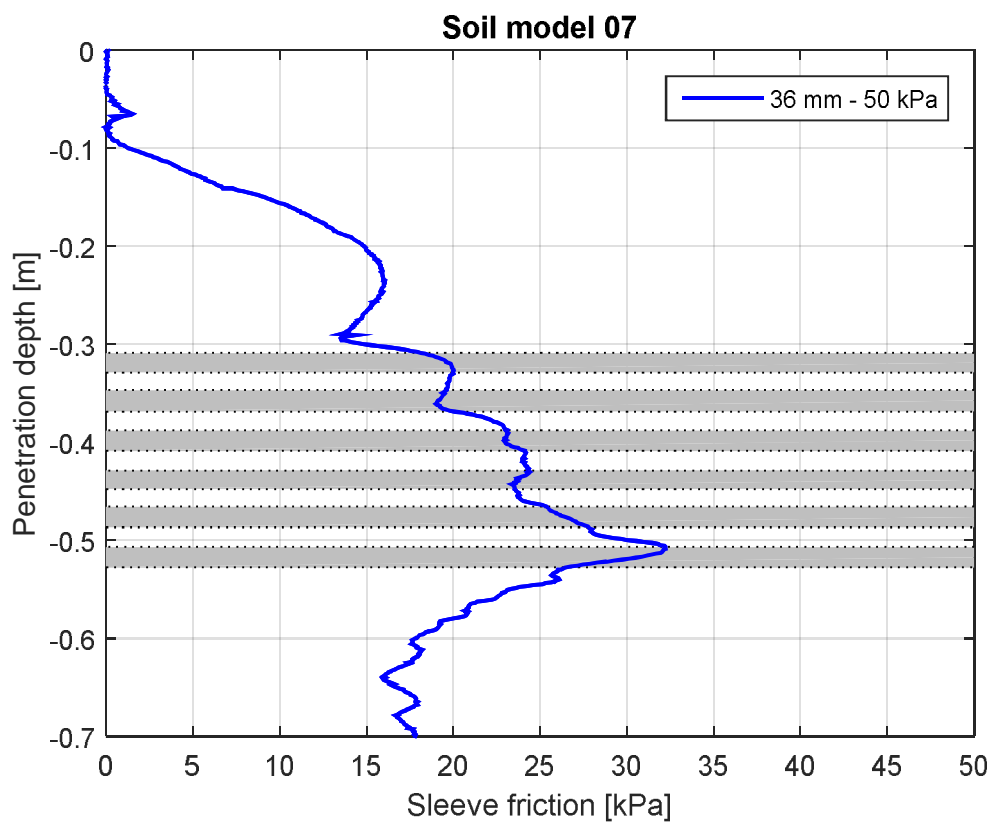
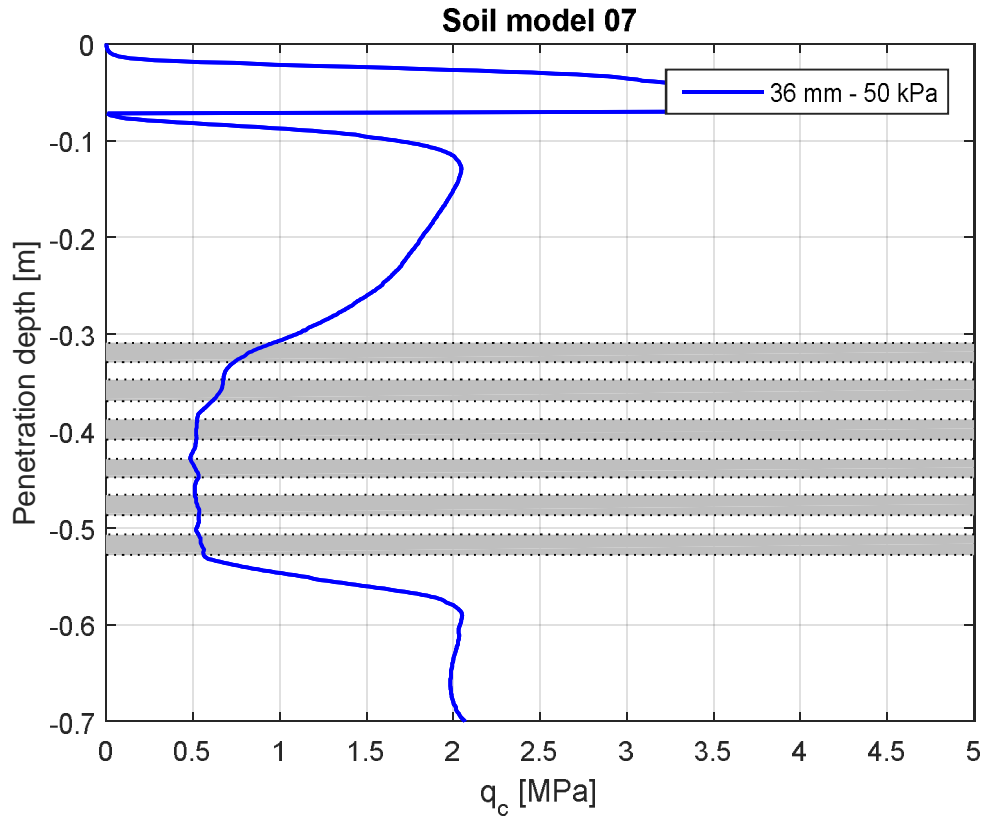


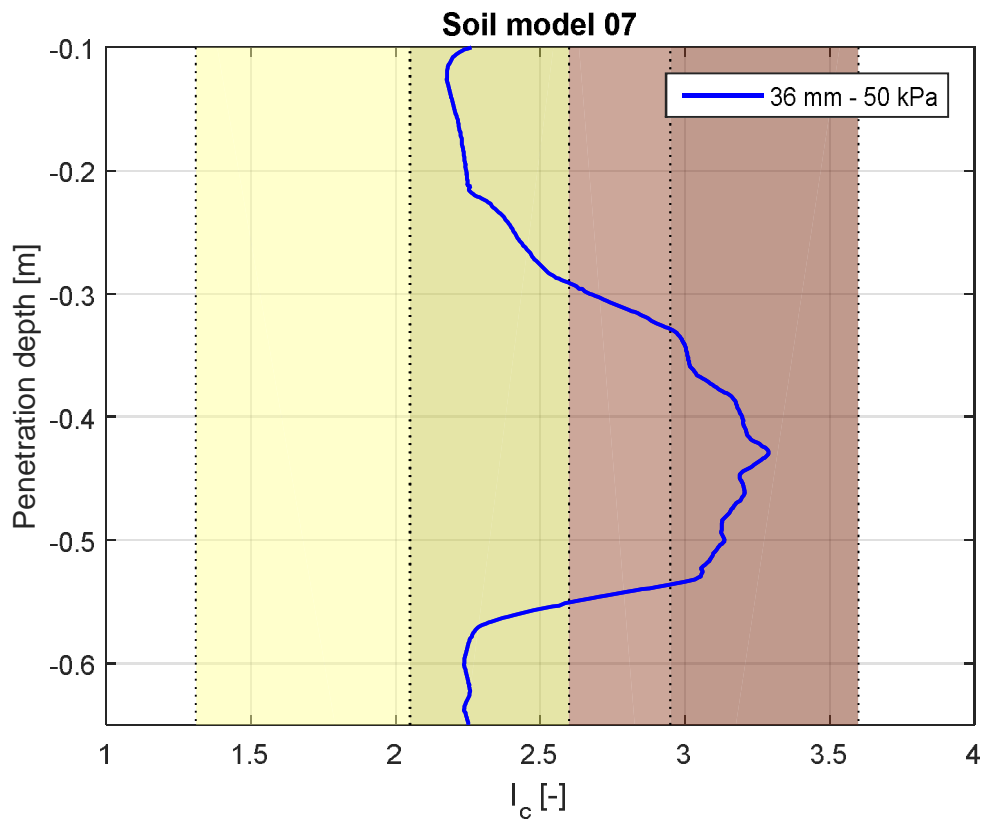
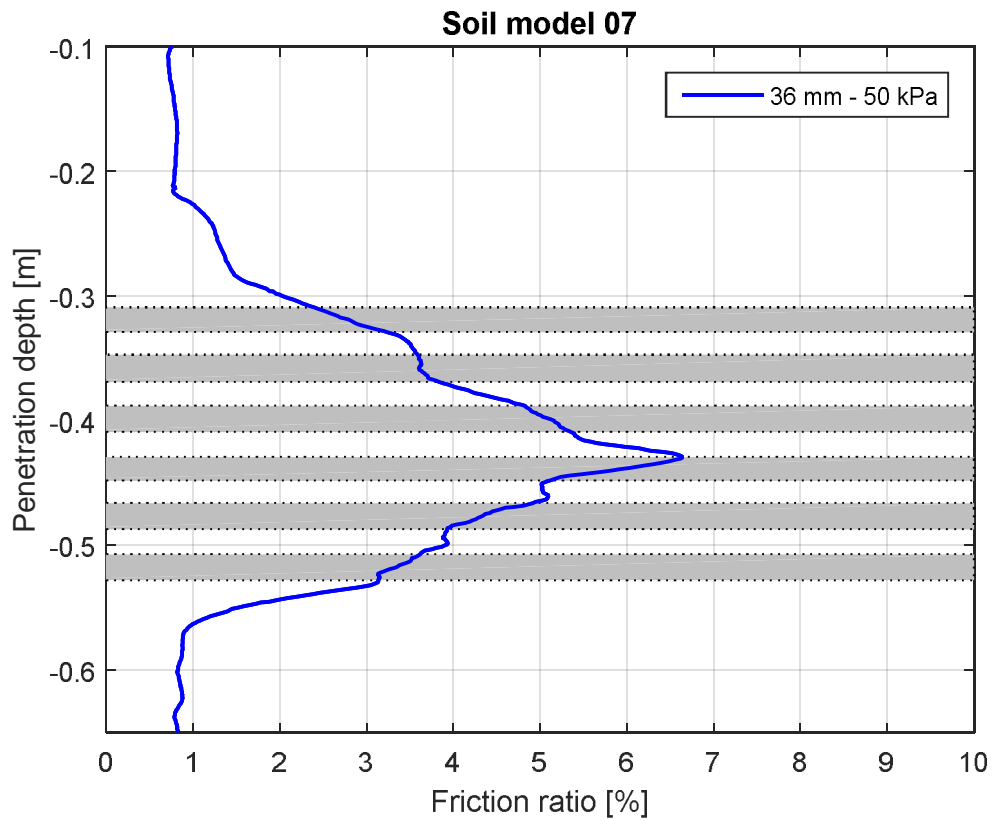
A.6 Soil model 6



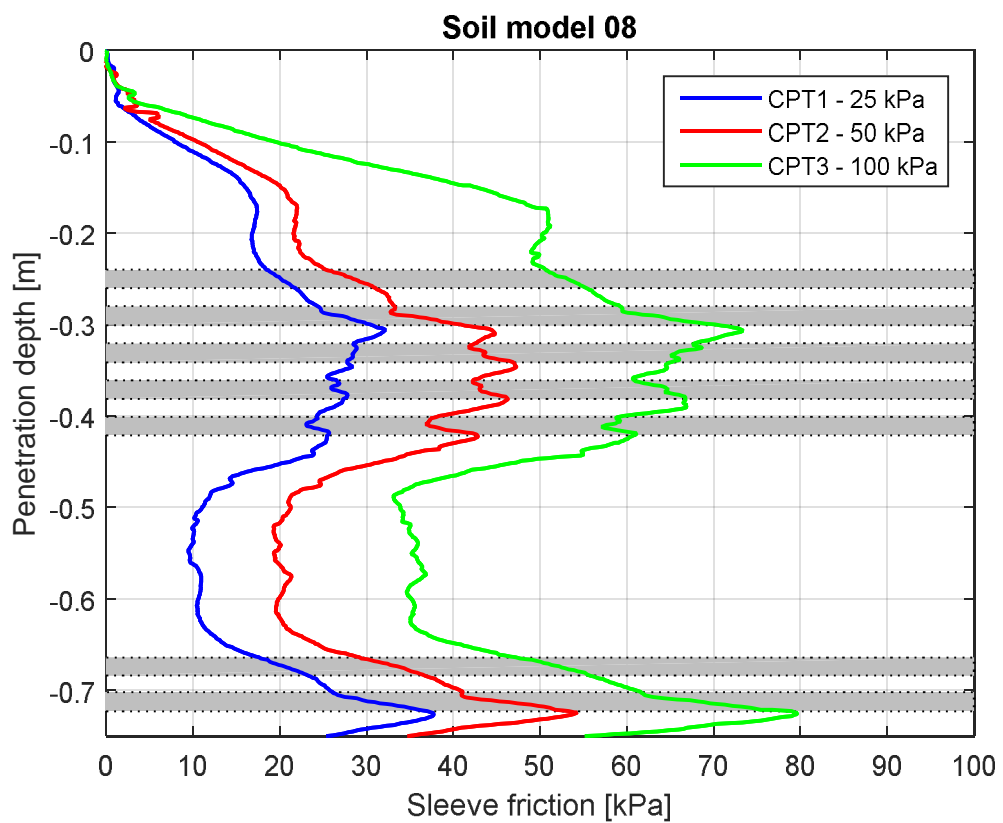
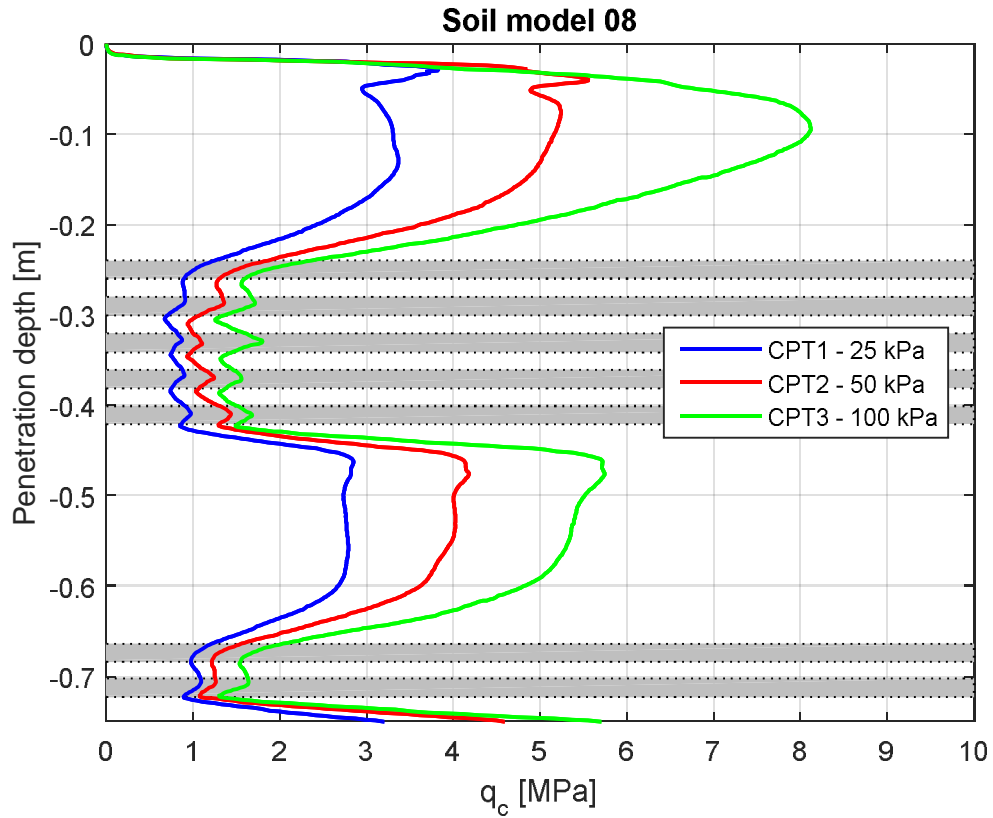


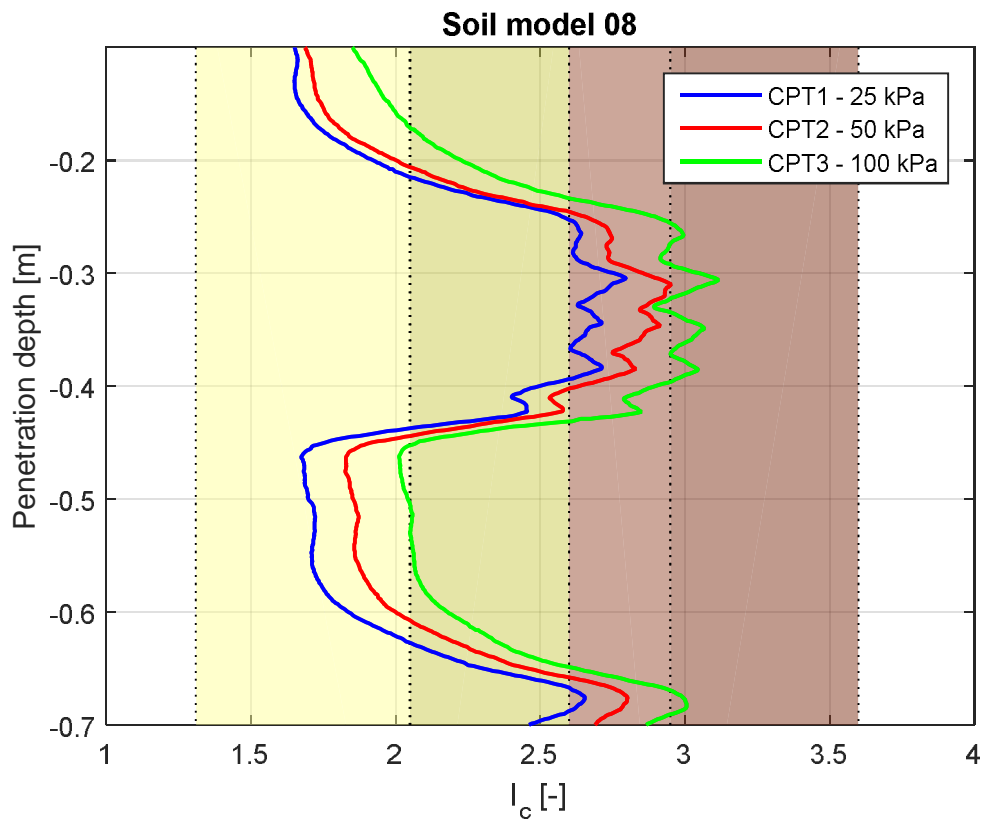
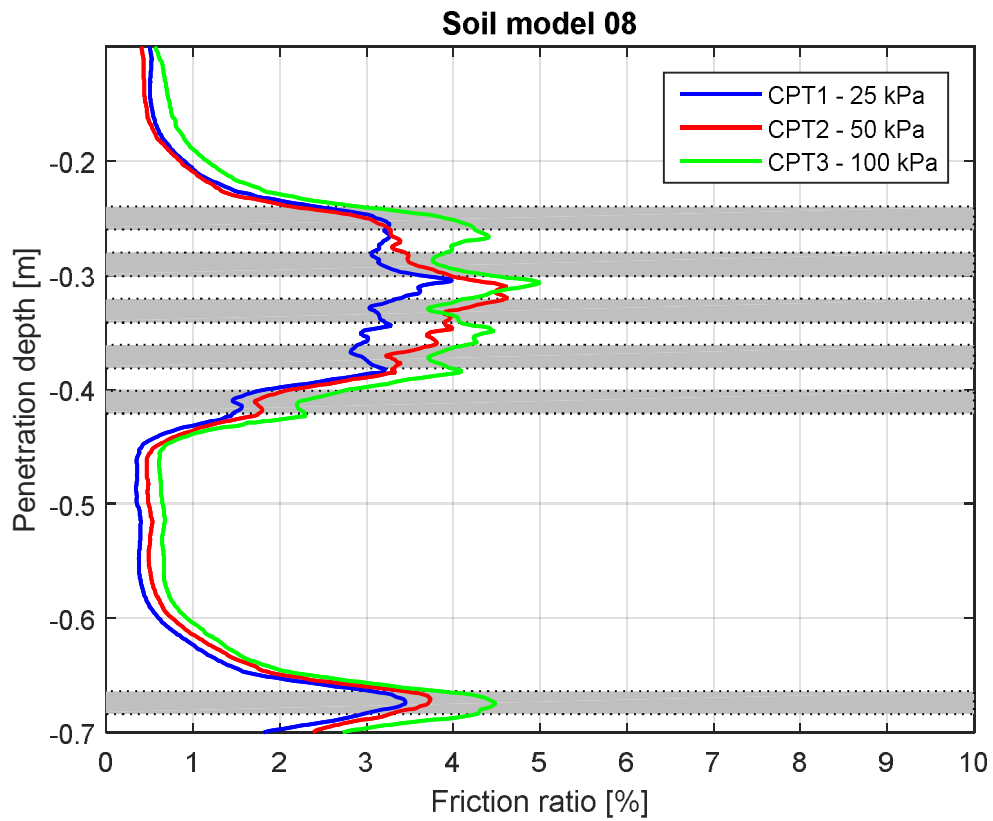
A.7 Soil model 7



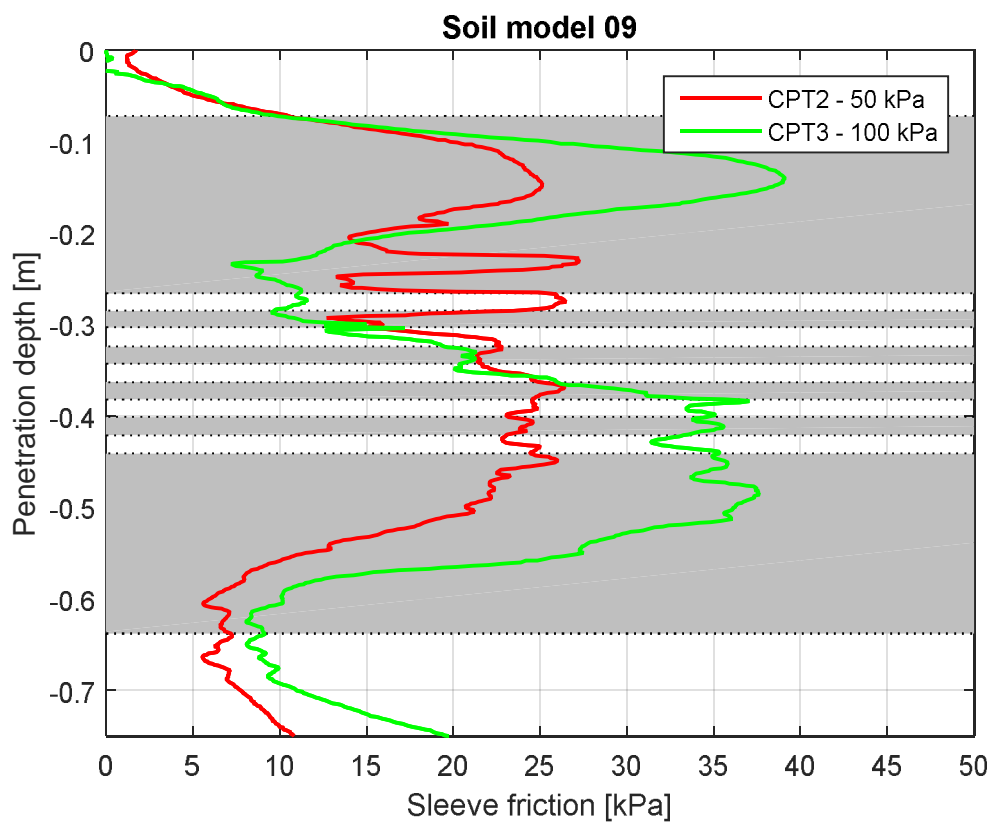
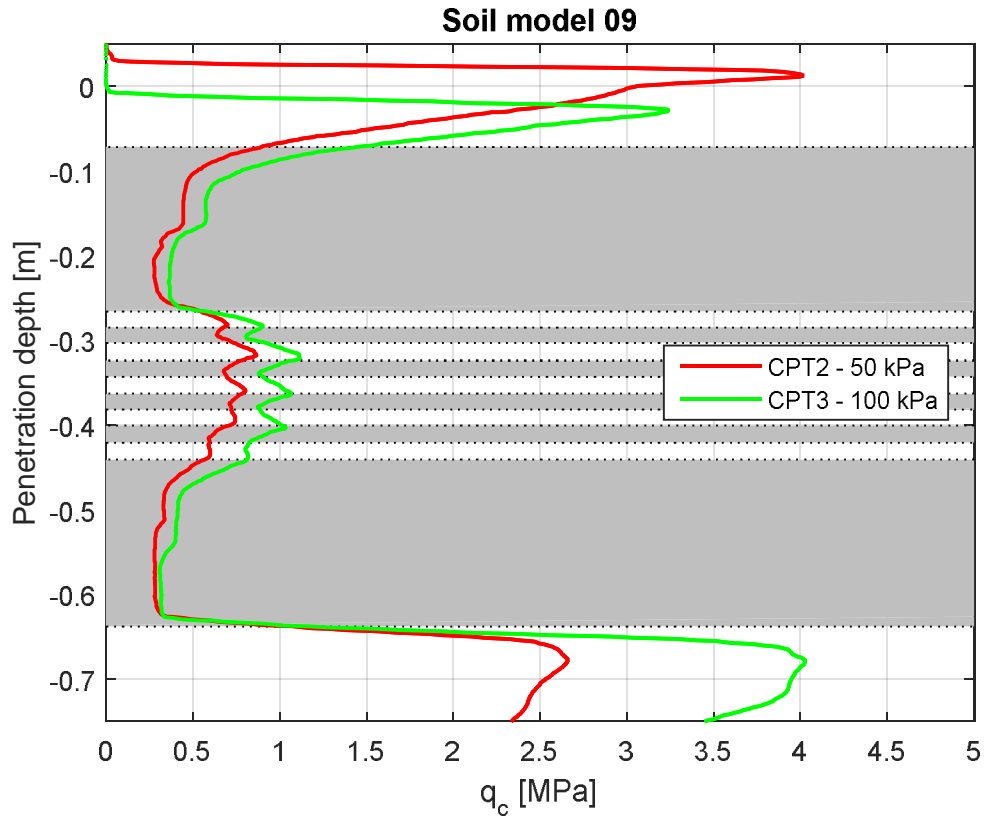


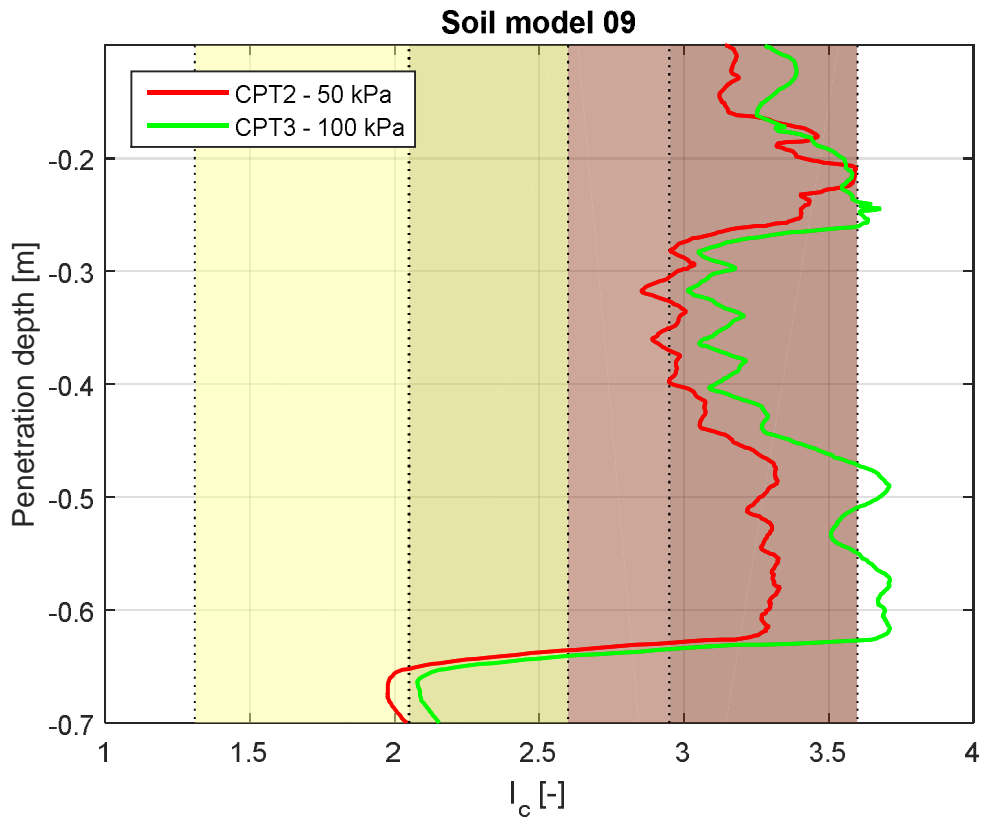
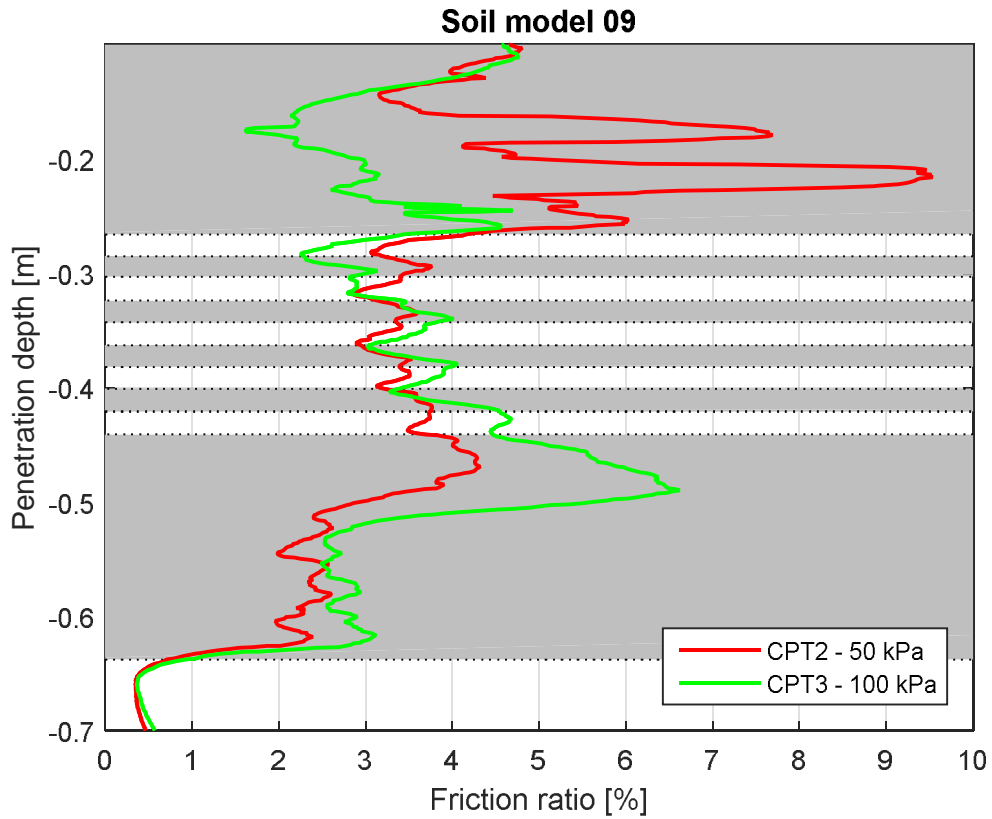
A.8 Soil model 8



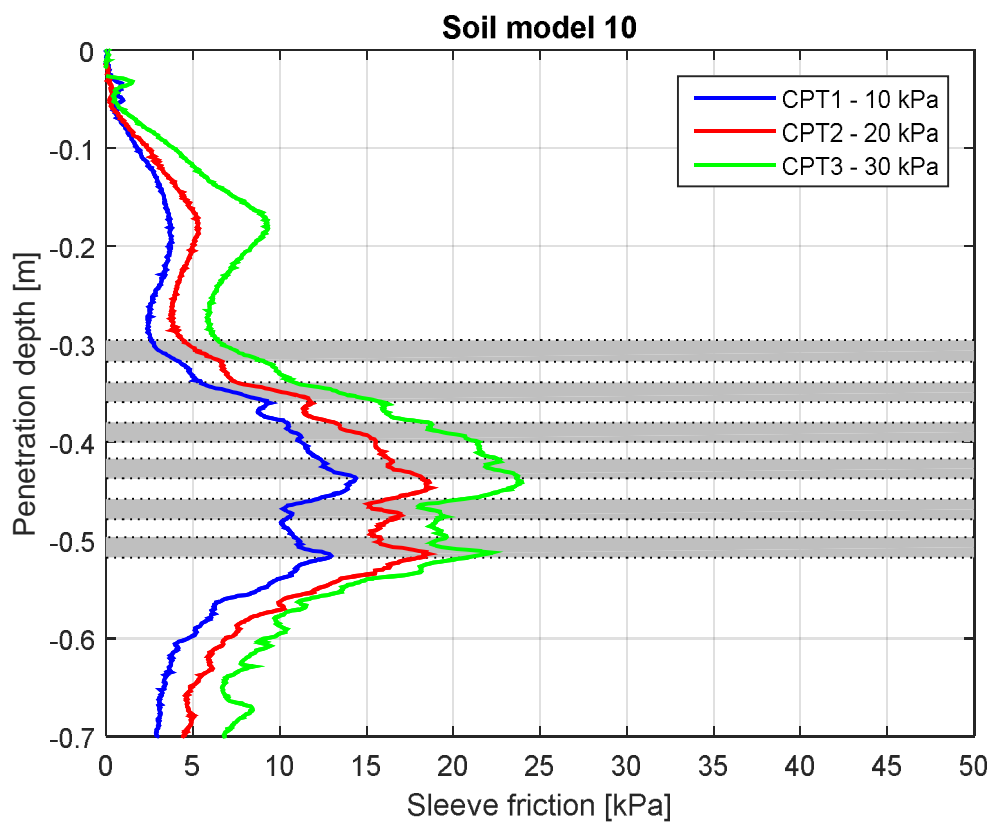
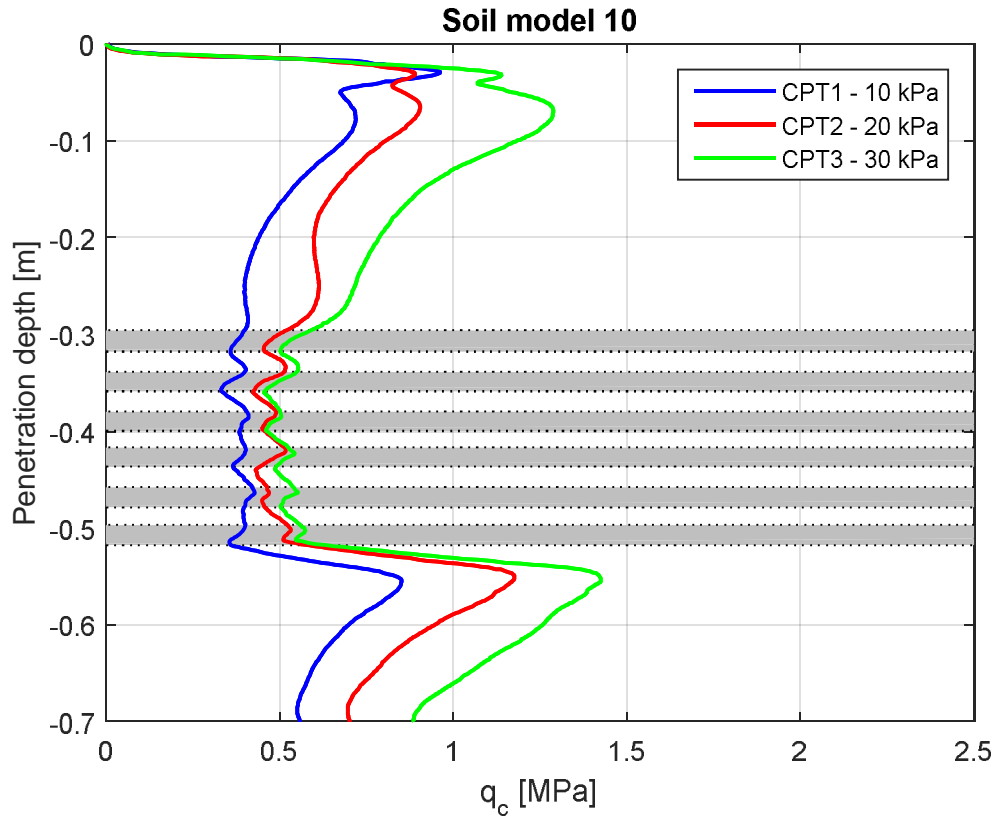


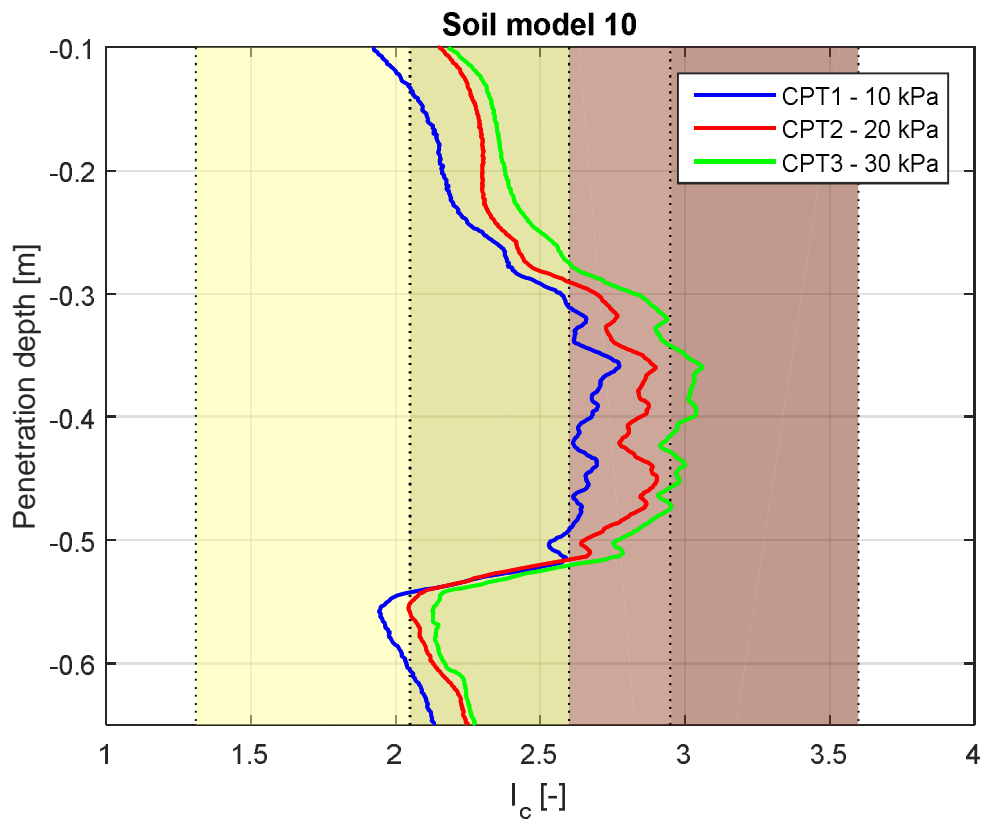
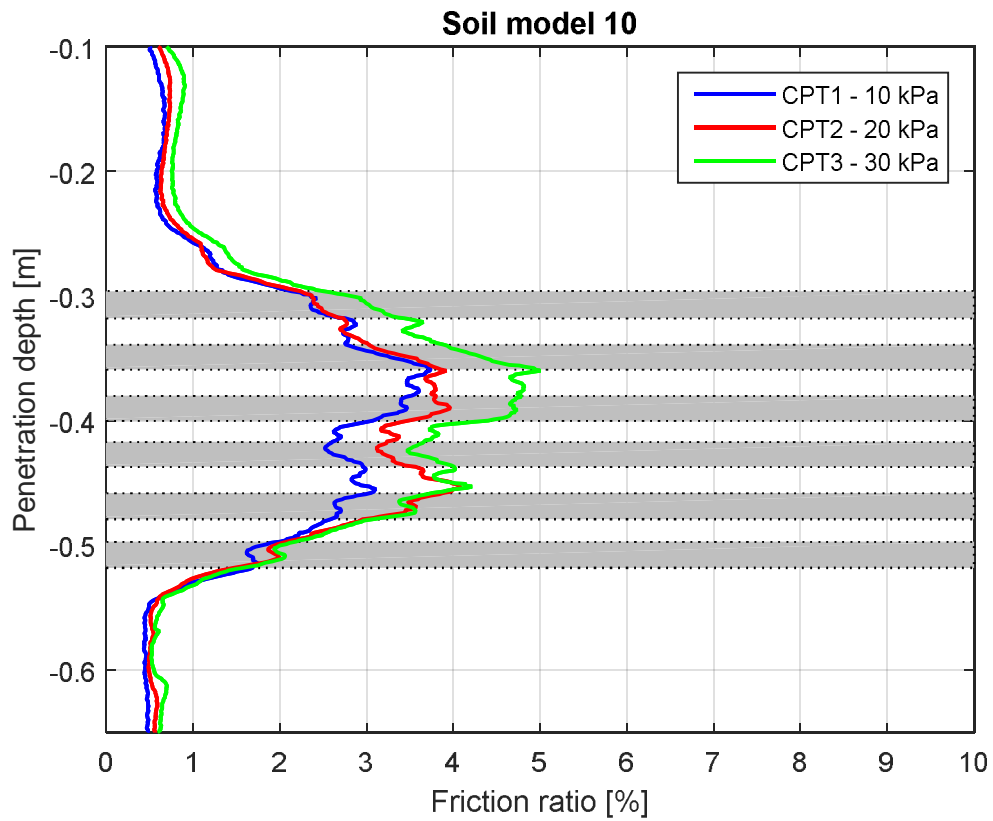
A.9 Soil model 9





A.10 Soil model 10





B Additional measurements

B.1 Post-test local density measurements

For each soil model the results of the samples taken after cone penetration testing to determine local density index are given.

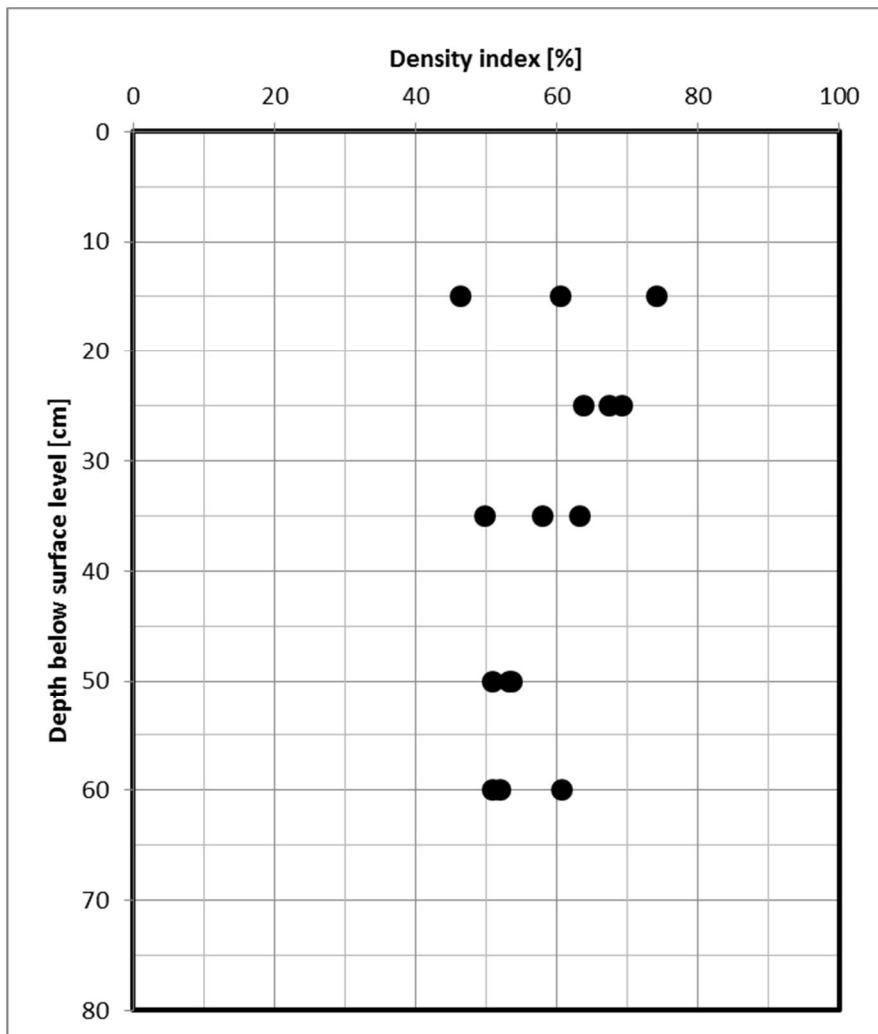


Figure B.1 Soil model 1

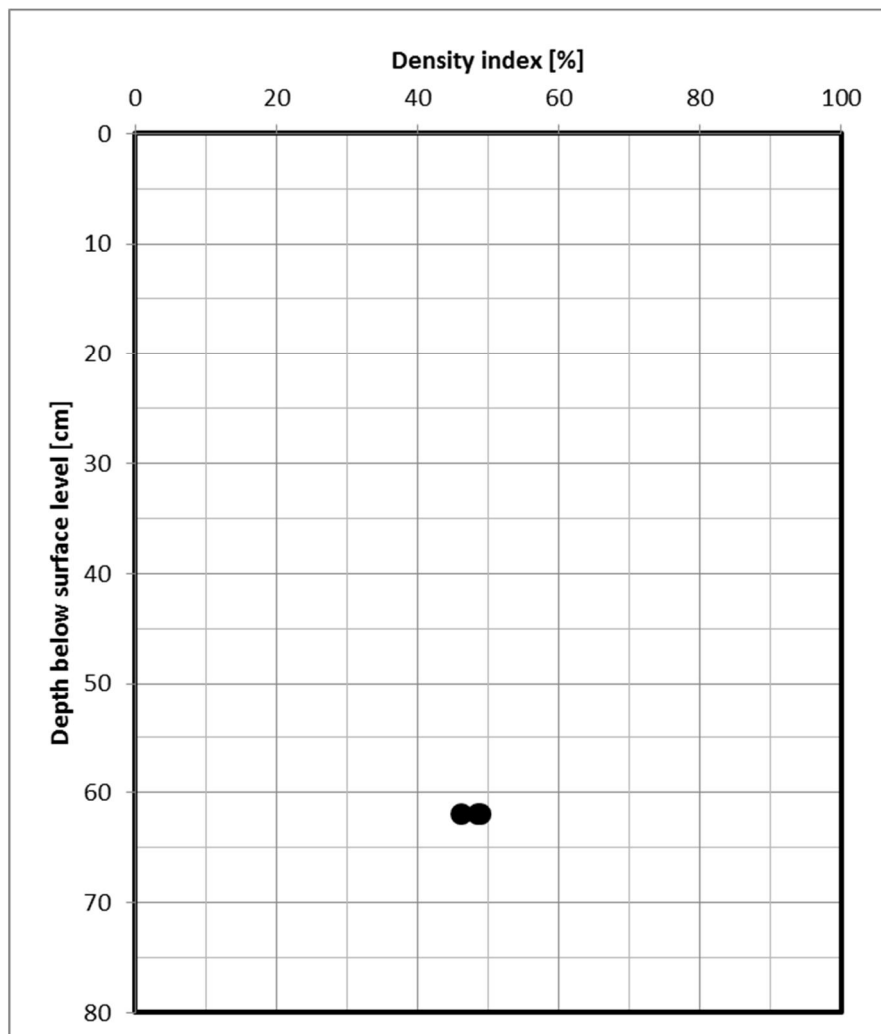


Figure B.2 Soil model 2

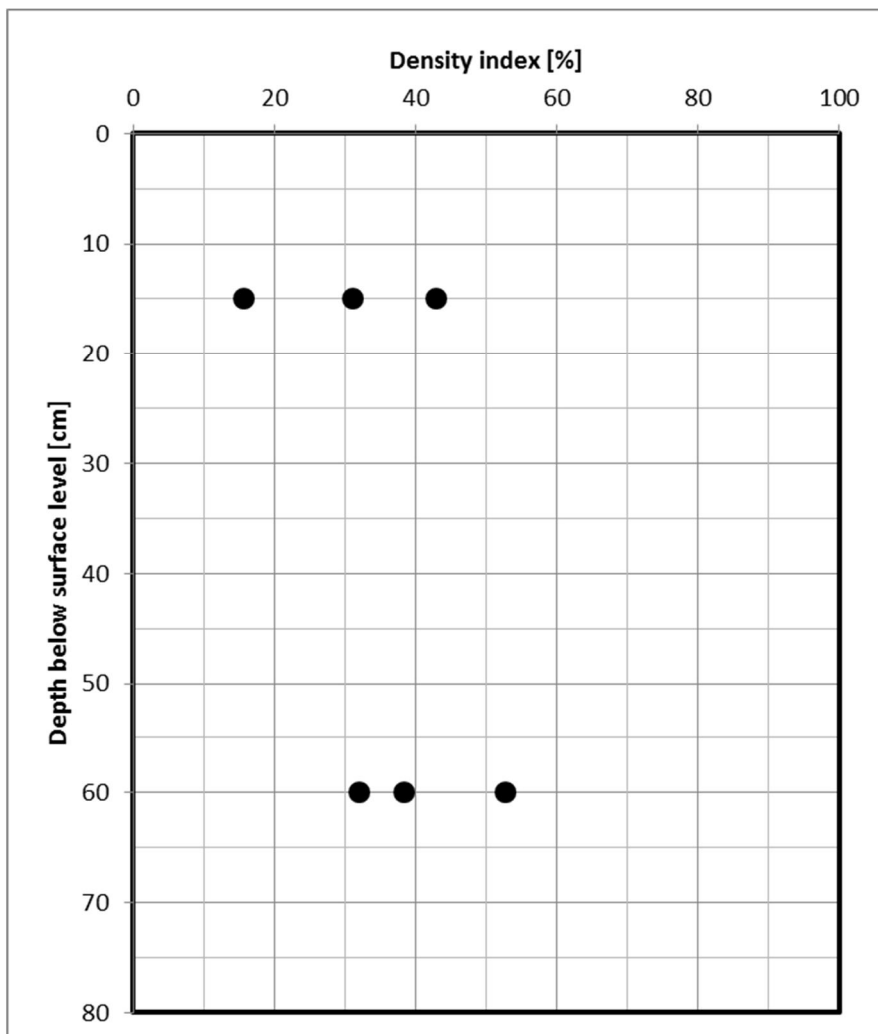


Figure B.3 Soil model 3

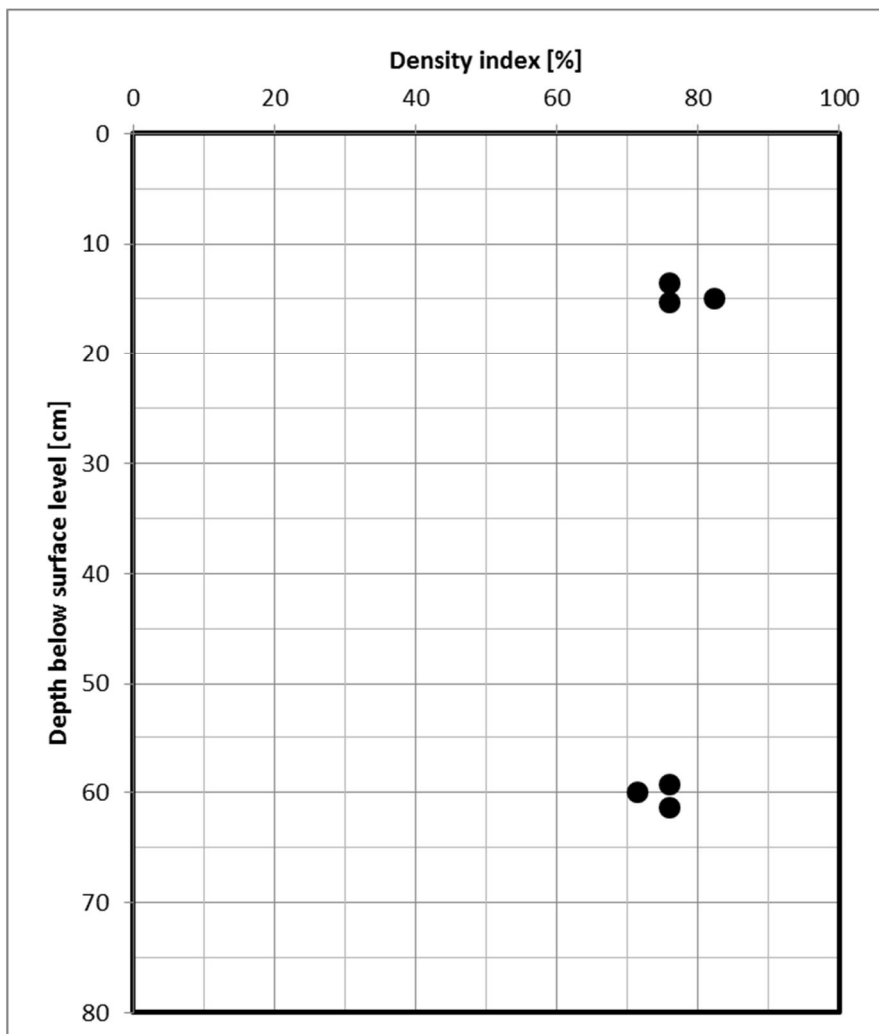


Figure B.4 Soil model 4

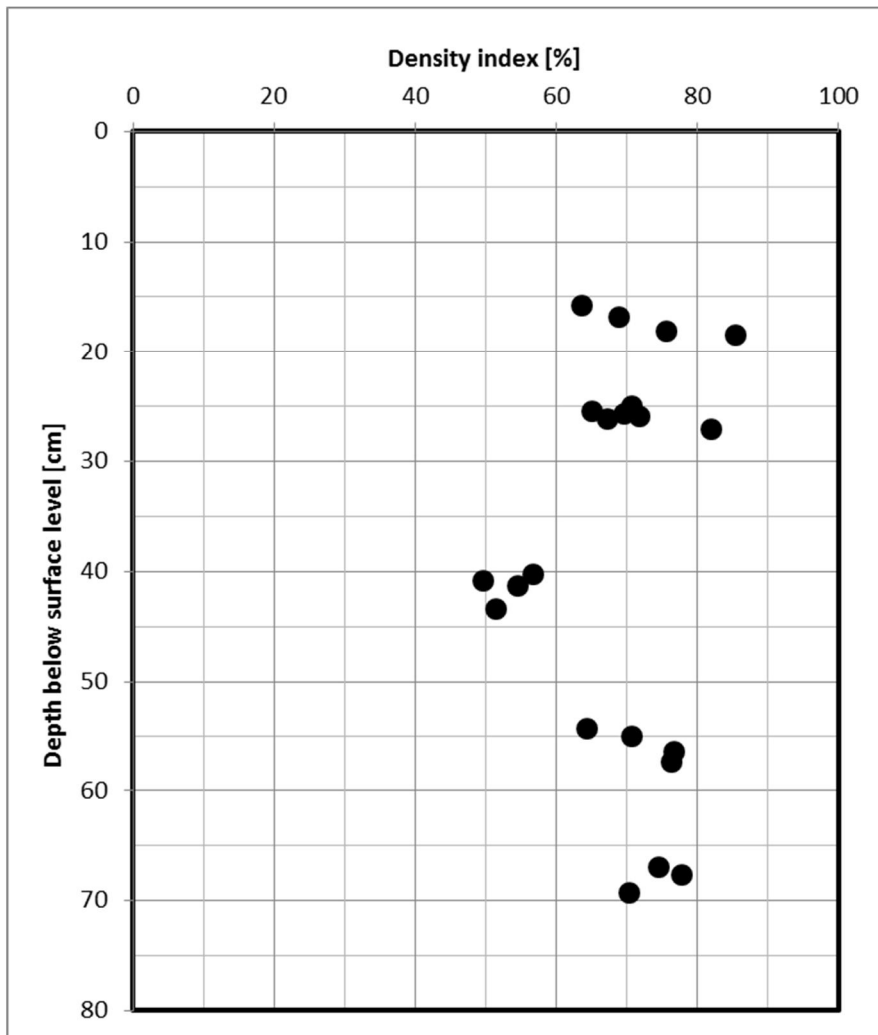


Figure B.5 Soil model 5

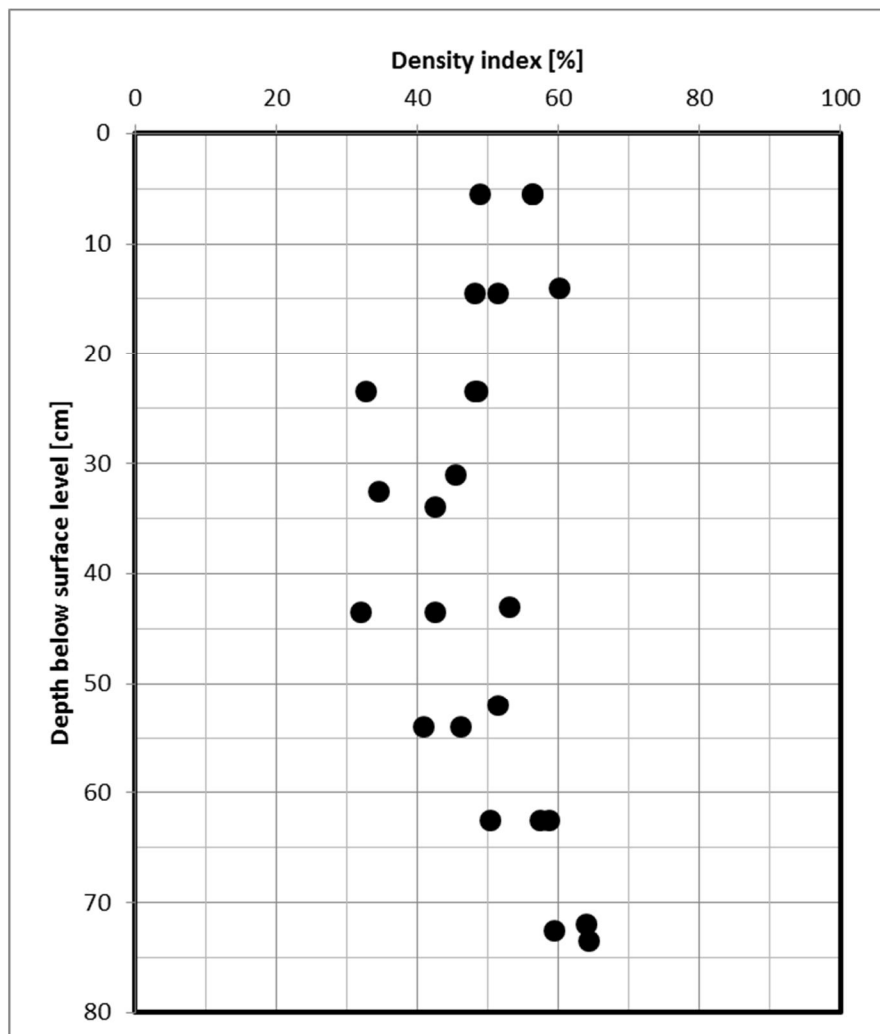


Figure B.6 Soil model 6

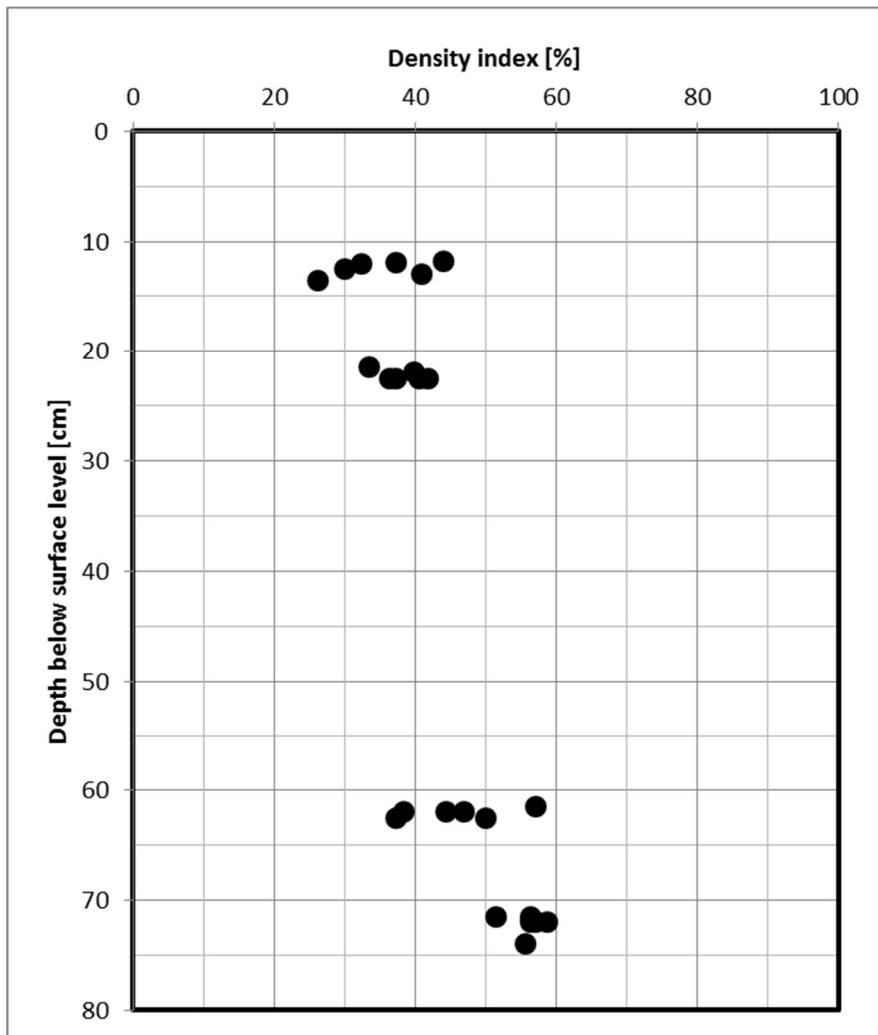


Figure B.7 Soil model 7

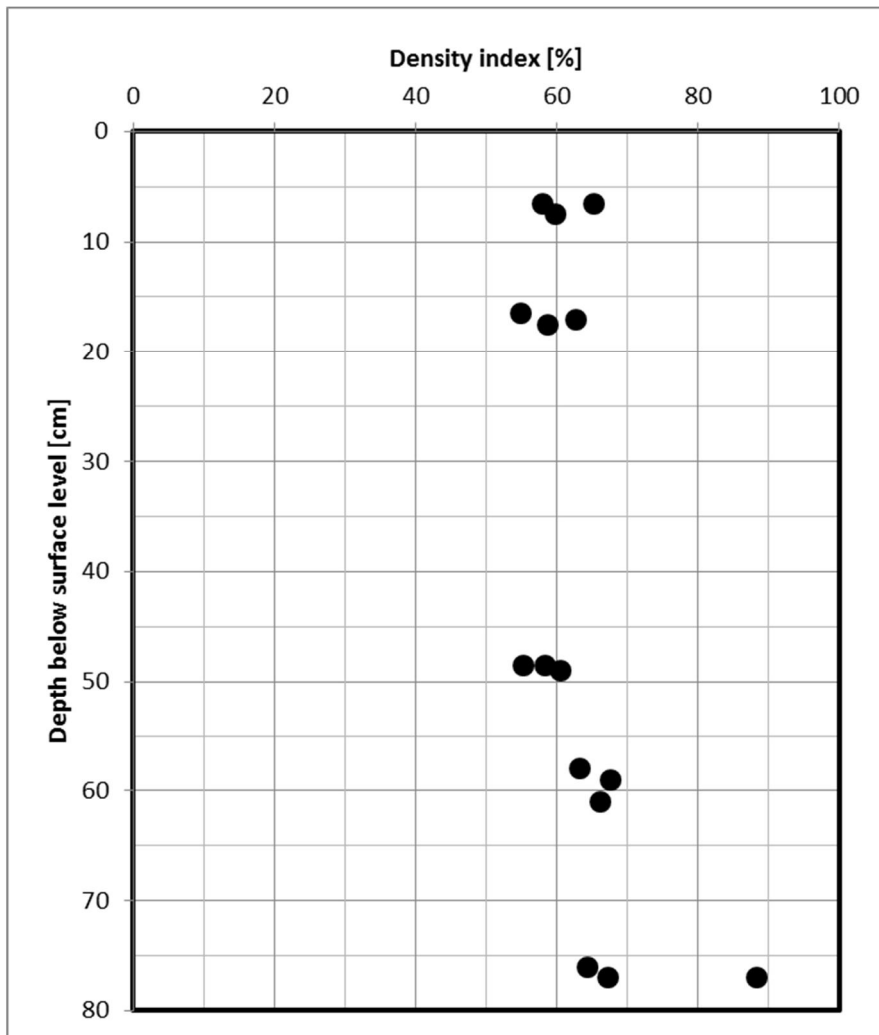


Figure B.8 Soil model 8

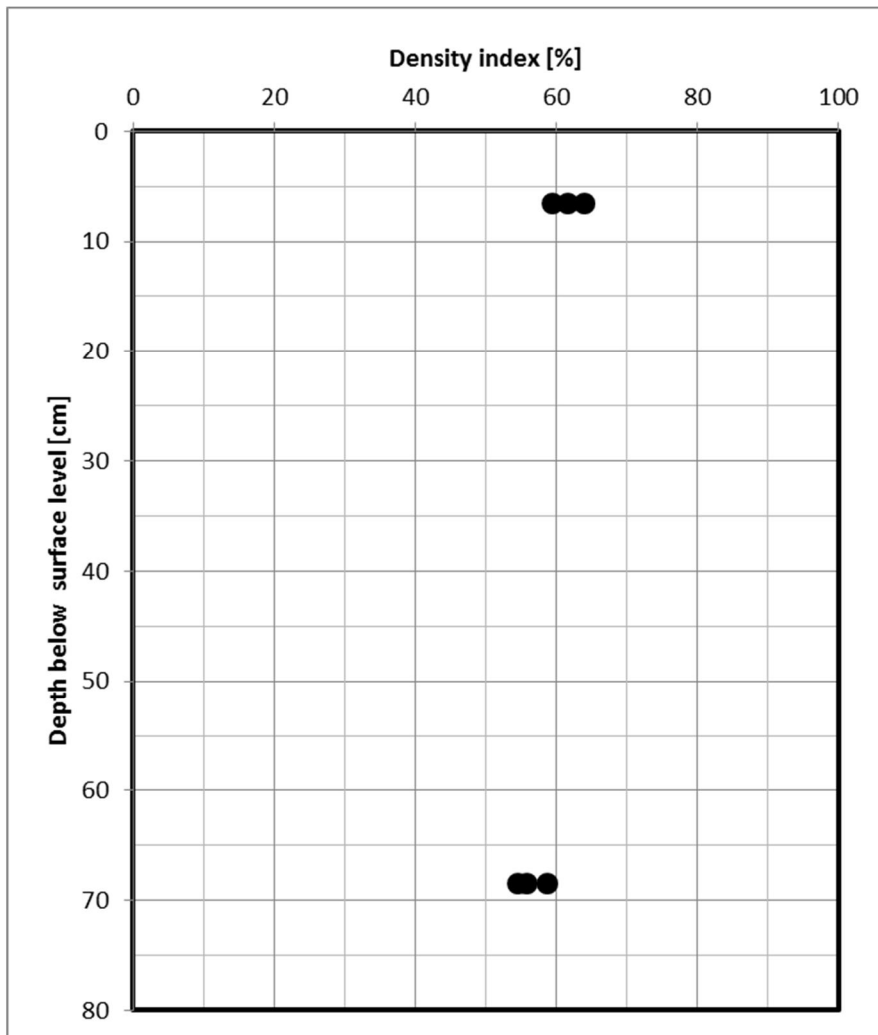


Figure B.9 Soil sample 9



Figure B.10 During excavation of soil model 9

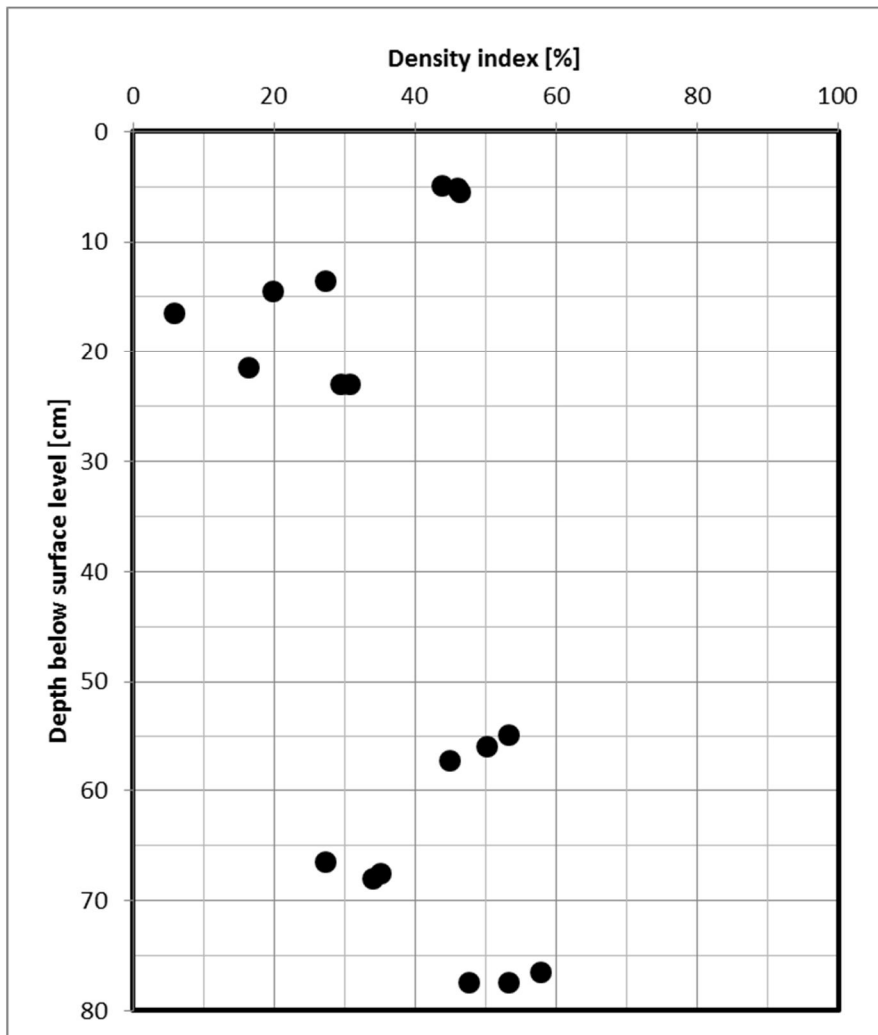


Figure B.11 Soil model 10



Figure B.12 During excavation of soil model 10

B.2 Stress and volume measurements

The applied lateral and vertical stress is measured using pressure transducers. Any change in volume of the soil model is monitored by measuring the volume change in the water supply of both the membrane and the cushion and any water dissipated through the bottom drain of the test setup. The total vertical soil stress is measured by a total stress transducer at a depth of 0.72 m. The following graphs gives the results for during cone penetration testing in soil model 1.

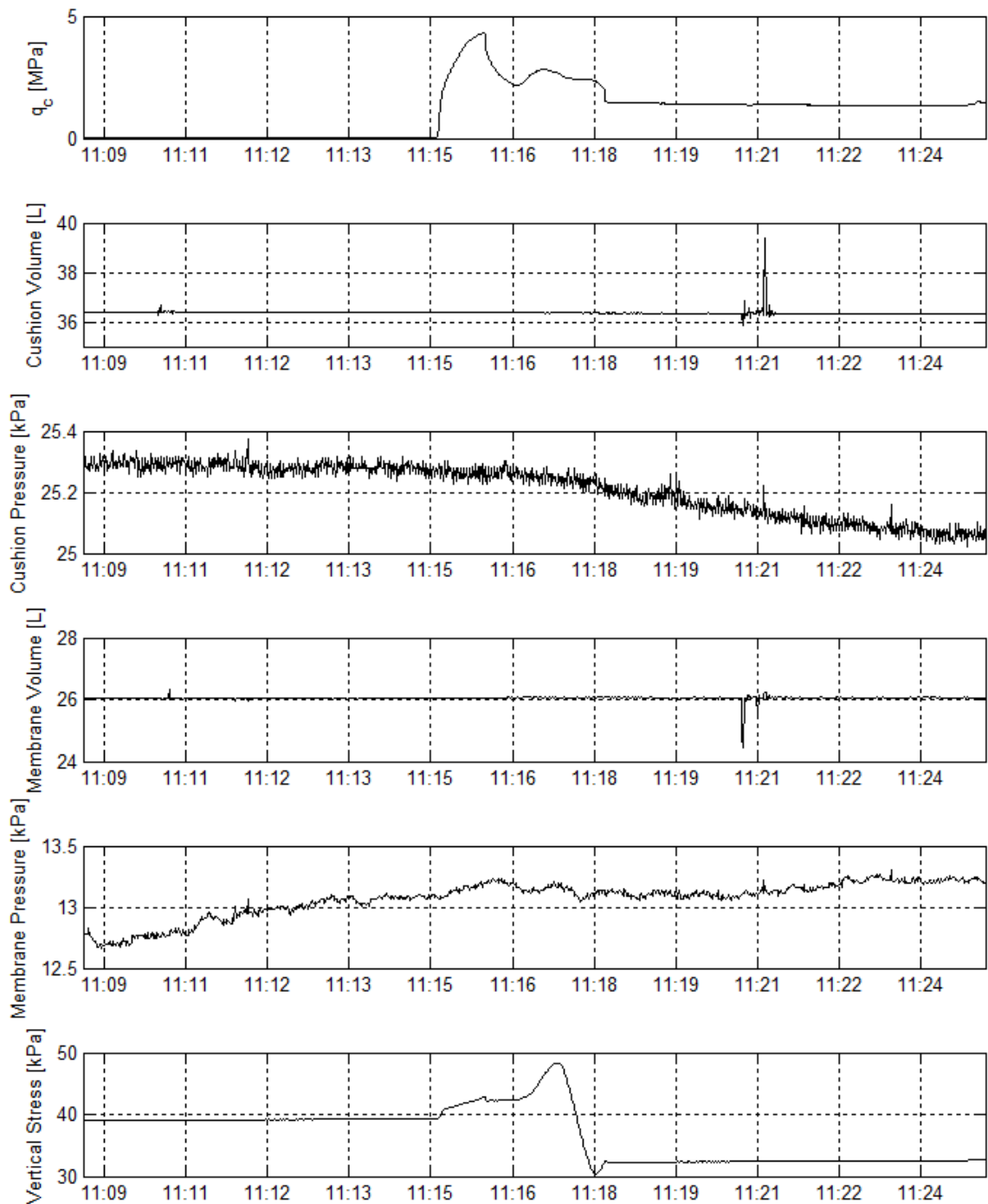


Figure B.13 Soil model 1 – CPT1

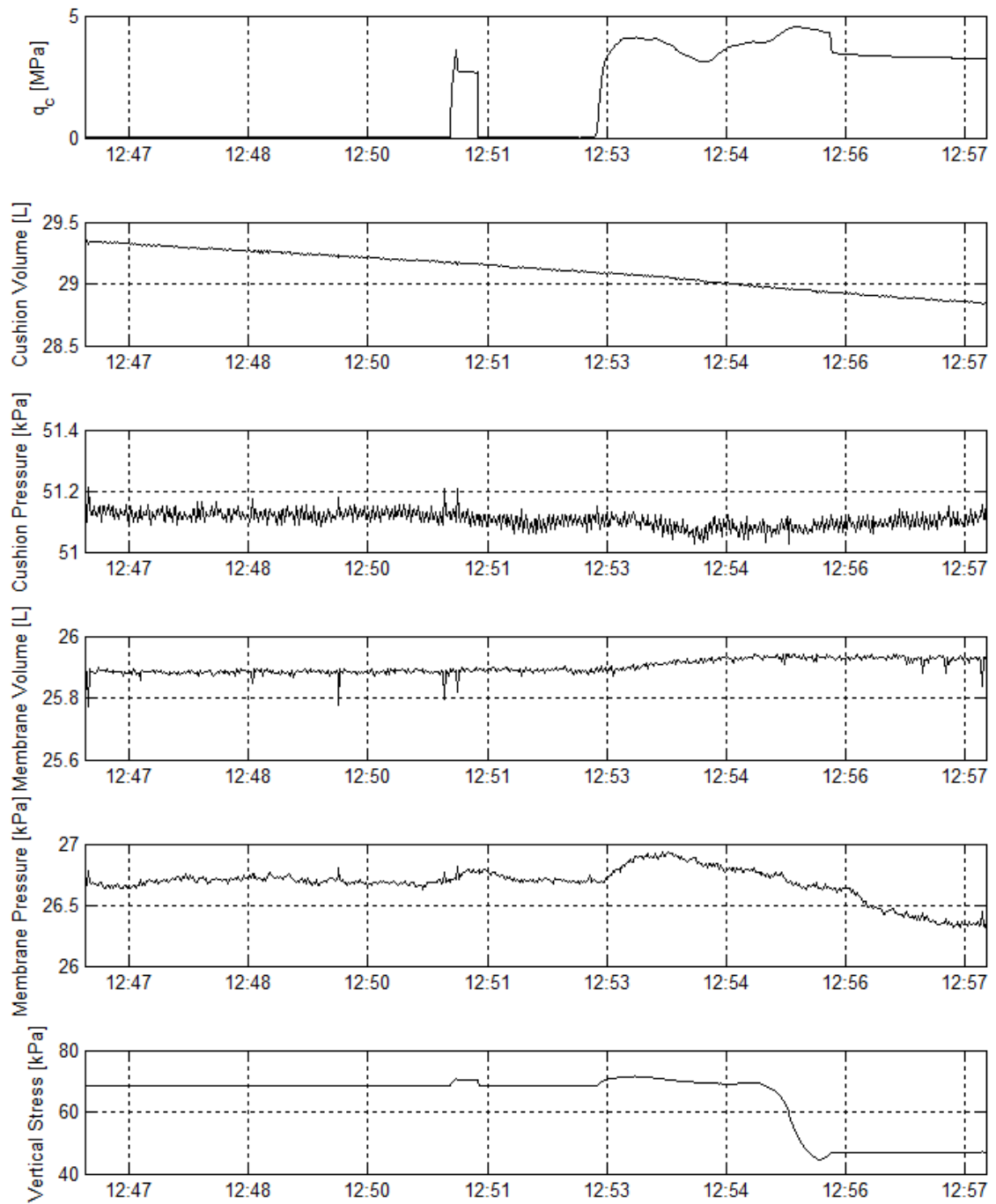


Figure B.14 Soil model 1 – CPT2

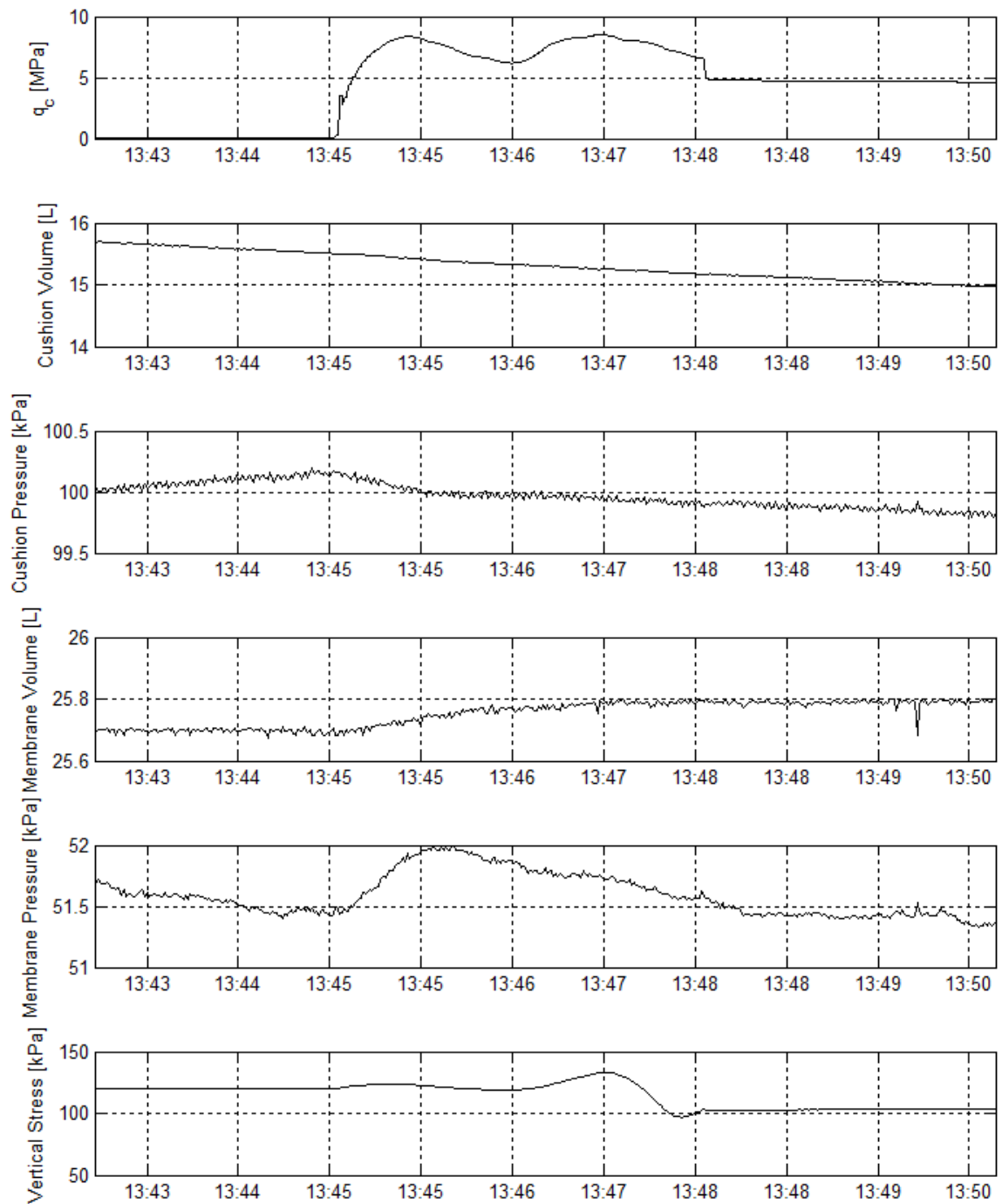


Figure B.15 Soil model 1 – CPT3

B.3 Volume change of soil model after cone penetration testing

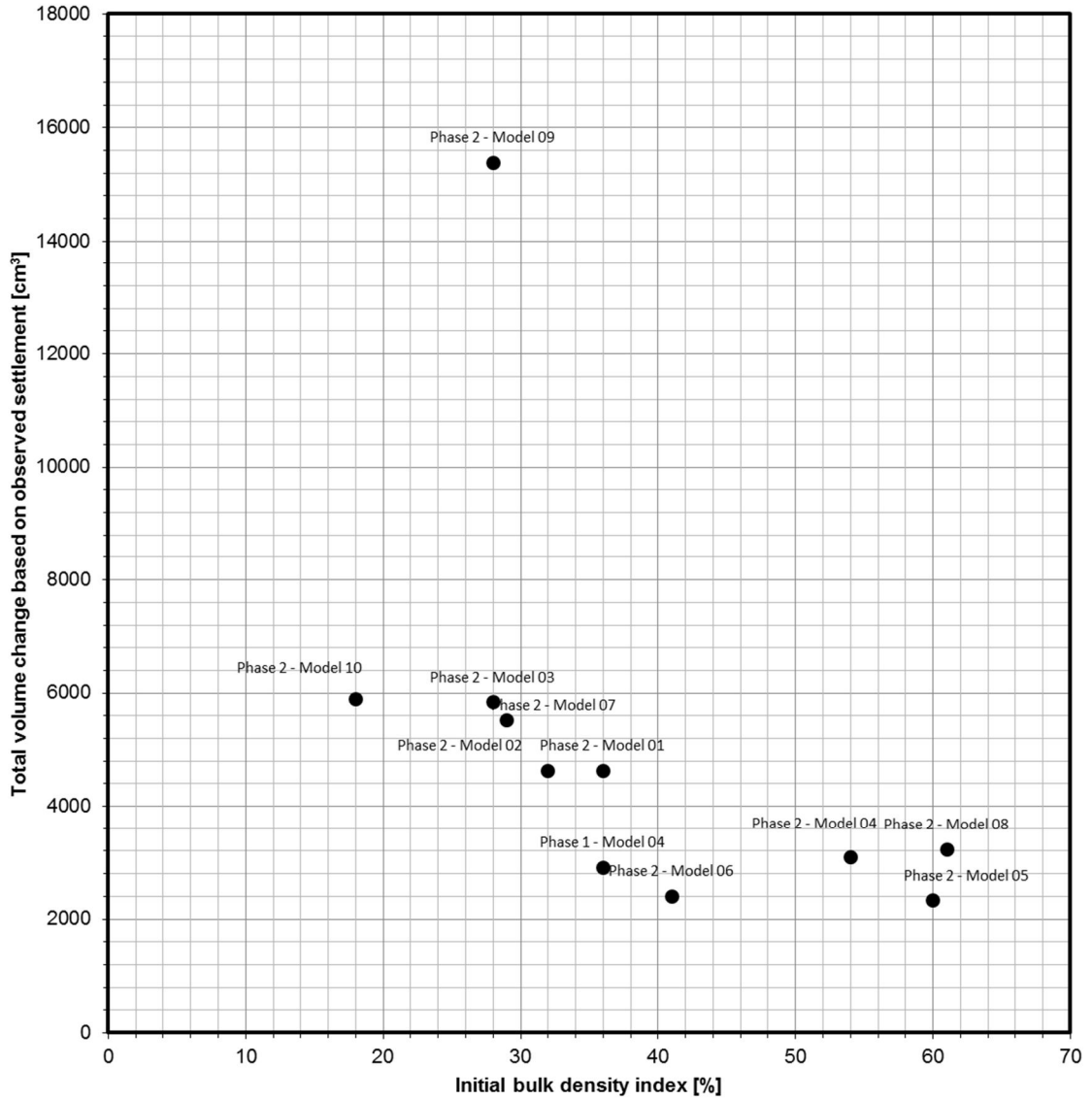


Figure B.16 Volume change due to testing based on observed surface level settlement and volume of the penetrated cones and rods

C Start-up phase

In the first phase, five exploratory tests have been performed in order to come up with a proper design of the test setup regarding to testing under increased stresses. First, the initial test setup and test procedure are briefly described. In the subsequent sections the tests and their results are described. At the end of this annex the results are summarized and discussed.

C.1 Test setup and procedure

C.1.1 Description setup

This section describes the test setup as used in the start-up phase of this project. The test setup consists of the following components:

- A bottom plate, acting as a foundation for the test setup, which is placed on a rubber mat in order to reduce vibrations transferred through the floor (samples having a low relative density are susceptible to disturbance due to vibrations), see Figure C.1, left-hand-side.
- Cylindrical stackable steel cells which contain the soil sample (rubber O-rings act as a seal between the cell interfaces).
- A hydraulic jacking unit in order to push the cone into the soil sample (not present in Figure C.1).
- A reaction frame (painted black, see Figure C.1, left-hand-side) for the hydraulic jacking unit.
- A circular steel plate on top of the soil sample with four gaps in order to be able to penetrate the soil sample with the cones, see Figure C.1 (right-hand-side, drawn in pink).
- Hydraulic jacks in order to create surcharge loading (Figure C.1 right-hand-side, drawn in red).
- A steel ring on top of the cells, which acts as reaction frame for the hydraulic jacks.
- A circular bottom plate, a circular filter plate and a circular geo-textile in between (in order to have drainage over the whole area).
- A drainage tap connected to the circular bottom plate in order to allow for a controlled variation of water-level.

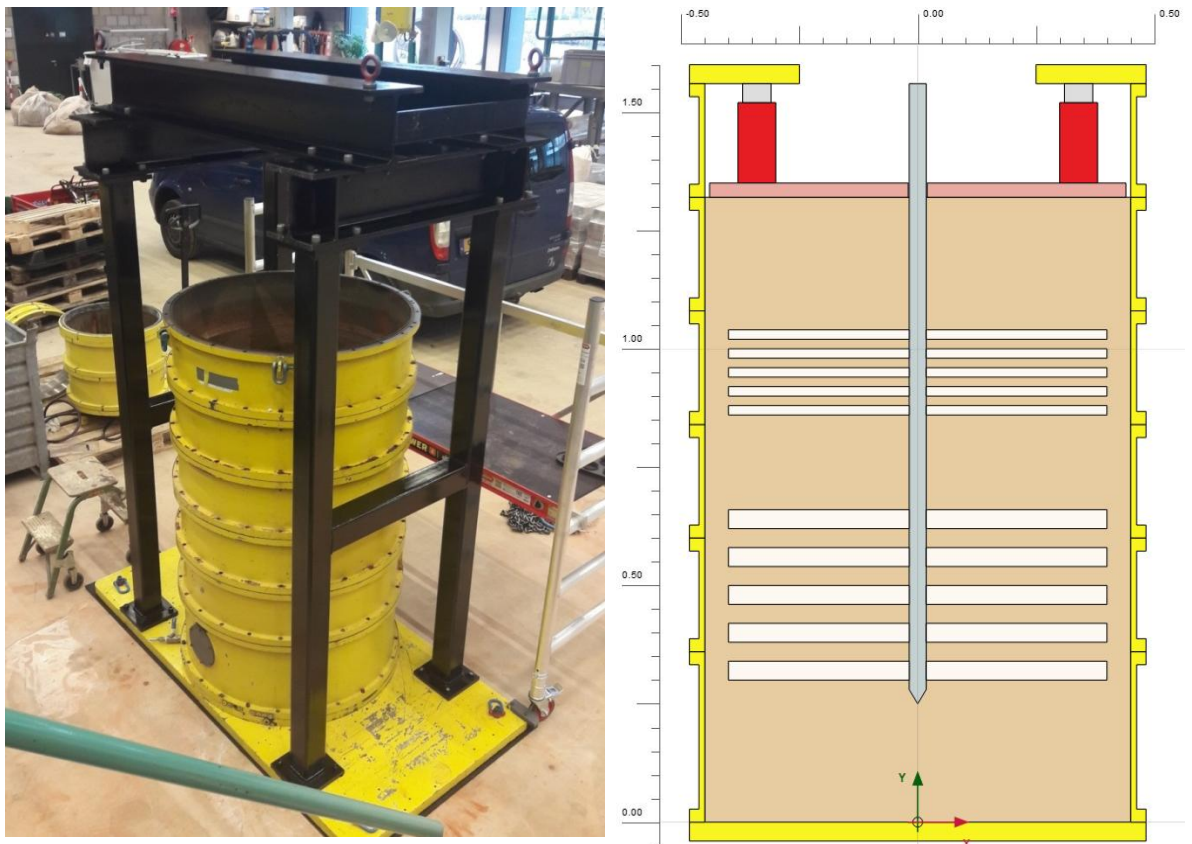


Figure C.1 Initial test setup

C.1.2 General Procedure

In general, the testing procedure for obtaining cone penetration test data for a soil model is as follows:

- Lower water-level to approximately 0.2 m below soil-level. This will result in a small under-pressure which provides additional soil strength due to capillary action while maintaining soil saturation and porosity.
- Position circular top steel plate on soil sample using an overhead crane.
- Assemble reaction frame and hydraulic jacking unit onto bottom plate.
- Mount hydraulic jacks and steel reaction ring.
- Increase vertical stress level by incrementally increasing hydraulic pressure to the jacks. Allow for consolidation in between increments.
- Connect cone penetrometer and install to desired penetration depth using hydraulic jacking unit.
- In case of three penetration tests (when employing the 25 mm cone penetrometer), increase the vertical stress to the next stress level and perform subsequent tests leaving the previous cone in place.
- After final cone penetration test, disconnect cone penetrometer, remove hydraulic jack, jacking unit and reaction equipment.
- Measure the local porosity using a density ring, while excavating the soil model, one steel cell ring at a time. Optionally, take photographs excavated soil model.

C.2 Soil models

C.2.1 Configurations

Three different soil model configurations were prepared in order to find the correction for a range of different layer thicknesses. These configurations are presented in Table C.1 (configuration 3 being the reference case: uniform sand). The total height of the soil model varies from 0.96 m to 1.32 m. The first three experiments (configurations 1 and 3) were performed with a model height of 1.32 m. For the two subsequent experiments (configuration 2 and 3) a lower model height was selected in order to reduce the amount of friction on the soil-cell sidewall interface to optimize the transfer of the applied vertical load to the bottom of the sample. The layered parts of configuration 1 and 2 consist of 5 clay layers with 4 sand layers of equal thickness in between. In between the layered parts of configuration 1, a sand layer with a thickness of 20 cm should offset the cone resistance after leaving the upper layered part (and before entering the next layered part). See Figure C.2.

Configuration	1	2	3
Top layer	28 cm sand	20 cm sand	Sand only
In between	18 cm layered soil: 5 clay and 4 sand layers layer thickness = 2 cm	40 cm layered soil: 3 clay and 2 sand layers layer thickness 8 cm	
	20 cm sand		(96 cm
	36 cm layered soil: 5 clay and 4 sand layers layer thickness = 4 cm		or
Bottom layer	30 cm sand	36 cm sand	132 cm)

Table C.1 Description of the soil model configurations

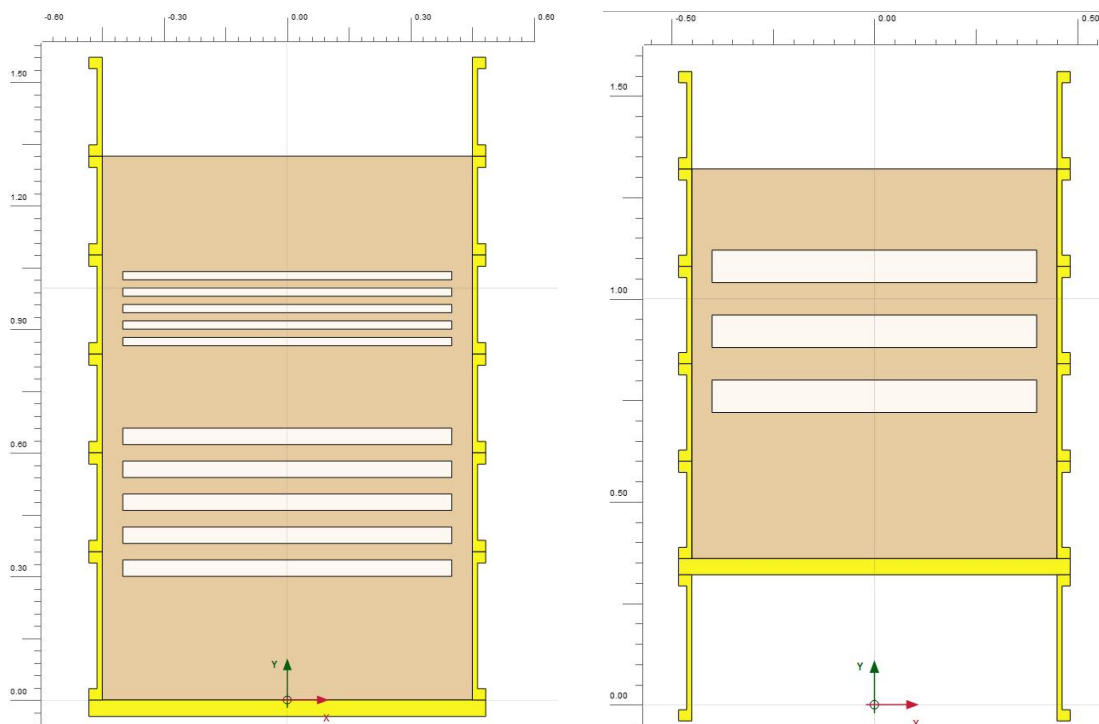


Figure C.2 Applied configurations 1 and 2

C.2.2 Model preparation

The principle method for sand preparation is free-falling dry sand from a limited height into a water-filled container (i.e. the raining procedure as described by Poel & Schenkeveld, 1998). This results in a sand model with a relative density of 0% to 5%. Further densification can be achieved by either dynamic fluidization-compaction (i.e. shock wave densification technique) or layered compaction (tamping technique). For the layered configurations however, the dynamic fluidization-compaction was considered to be not applicable, due to the presence of clay layers (less permeable than sand).

An alternative technique was used to obtain loose sand samples (30%), which consisted of gently pouring the sand into the water up to a layer thickness of 10 cm had been reached. By controlling and varying the free water height, different densities can be achieved. No tamping is needed for loosely packed samples. The achieved relative density was monitored by measuring the height of the layer in combination with the cell diameter and the known dry sand mass.

C.3 Test results

C.3.1 Soil model 1

Configuration 1 has been prepared first, because this configuration was considered to be the most challenging with the sand being loosely packed. The soil sample has been prepared in separate layers by layered wet raining with a water depth of 10 cm. The sand weight used for the sample was based on target density index of 30%. A bulk relative density of the sand layers of 36% has been achieved (average over total height of the model).

To estimate the degree of consolidation the plate settlement was measured during application of the surcharge load. Figure C.3 gives the settlement of the soil sample and the applied pressure at the soil sample as function of time. The cone penetration tests were performed after the settlement reached a constant value.

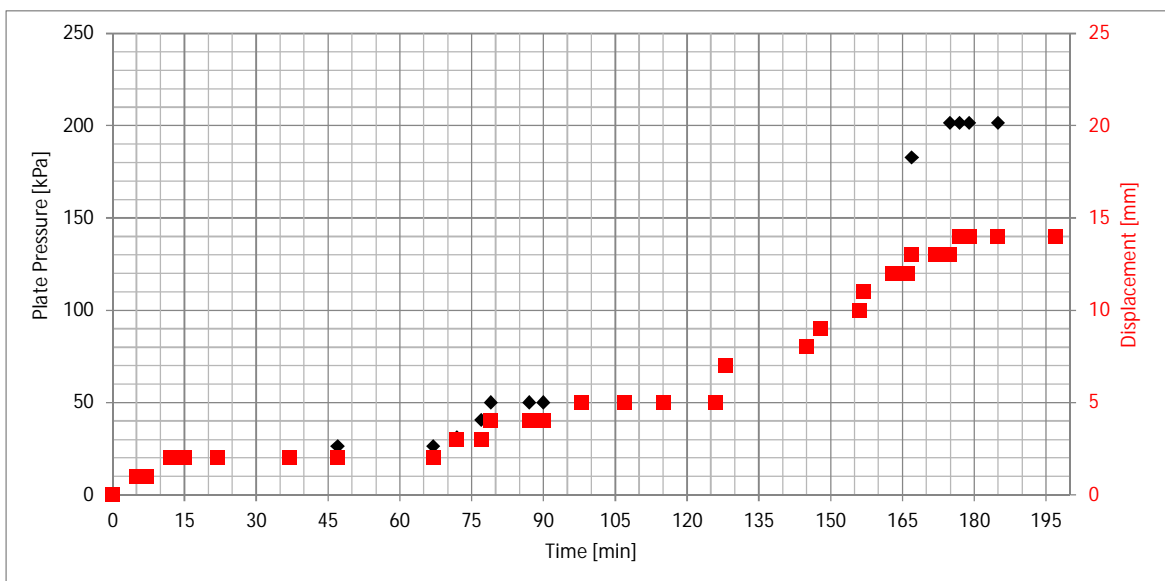


Figure C.3 Surcharge load and sample settlement as function of time

Figure C.4 depicts the measured cone resistances during the three tests performed. The layering and the effect of the vertical stress level are clearly visible. However, the decreasing resistance between ca. 0.5 m and 0.6 m penetration isn't fully understood at this moment. The results point to a decreasing stress level with depth, which could be a result of side friction and/or arching effects in the soil sample.

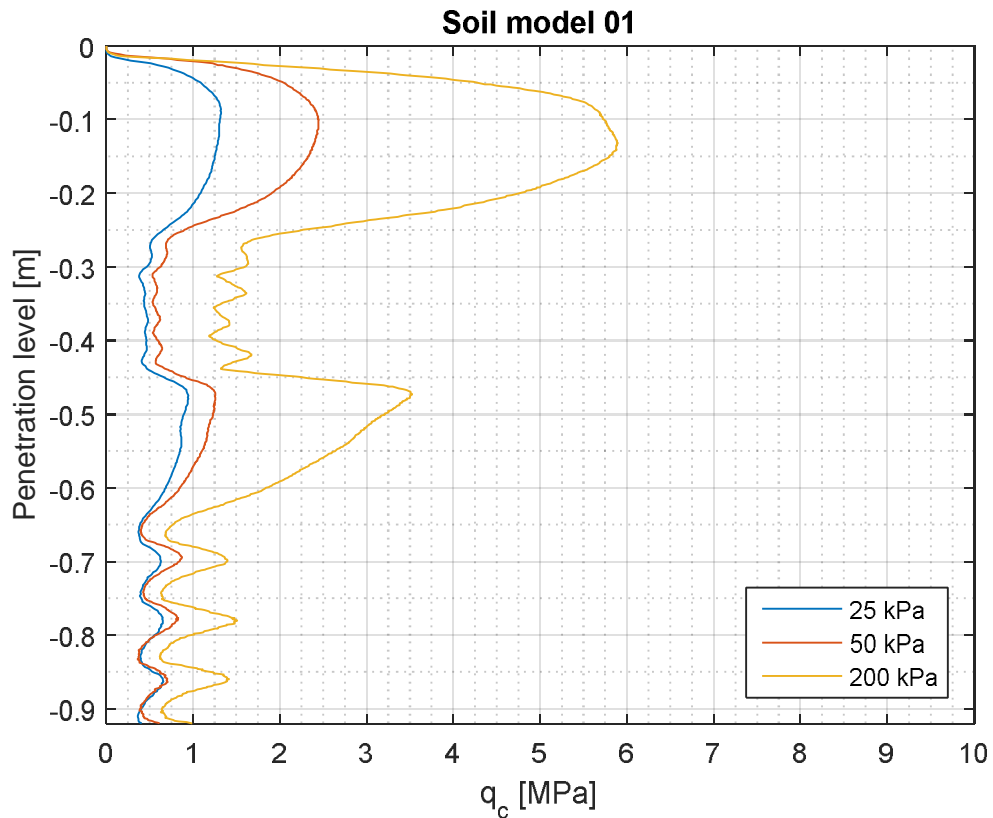


Figure C.4 Cone resistance as function of penetration level and surcharge load

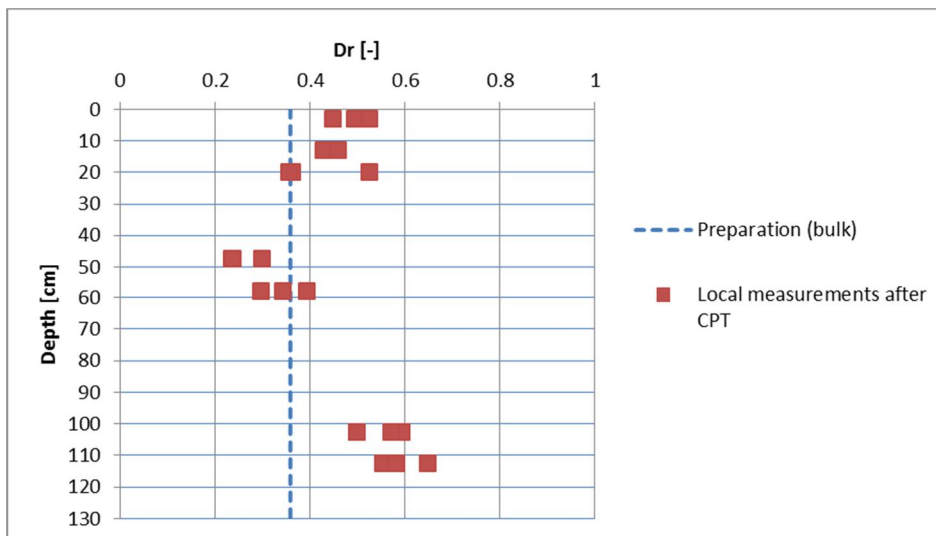


Figure C.5 Relative density after sample preparation (bulk) and after cone penetration testing (local samples)

After the CPTs were performed the soil sample was dismantled and excavated. Samples were taken in order to determine local porosities and photographs (of cross sections) were made. The results of the local porosity measurements are given in Figure C.5. Even though the samples were taken from “non-disturbed areas”, one has to keep in mind that the measurements may be affected by the penetration disturbances. The figure shows the relative density index as function of depth. The measurements below 1 m depth are considered non-reliable, since insufficient capillary forces could be created.

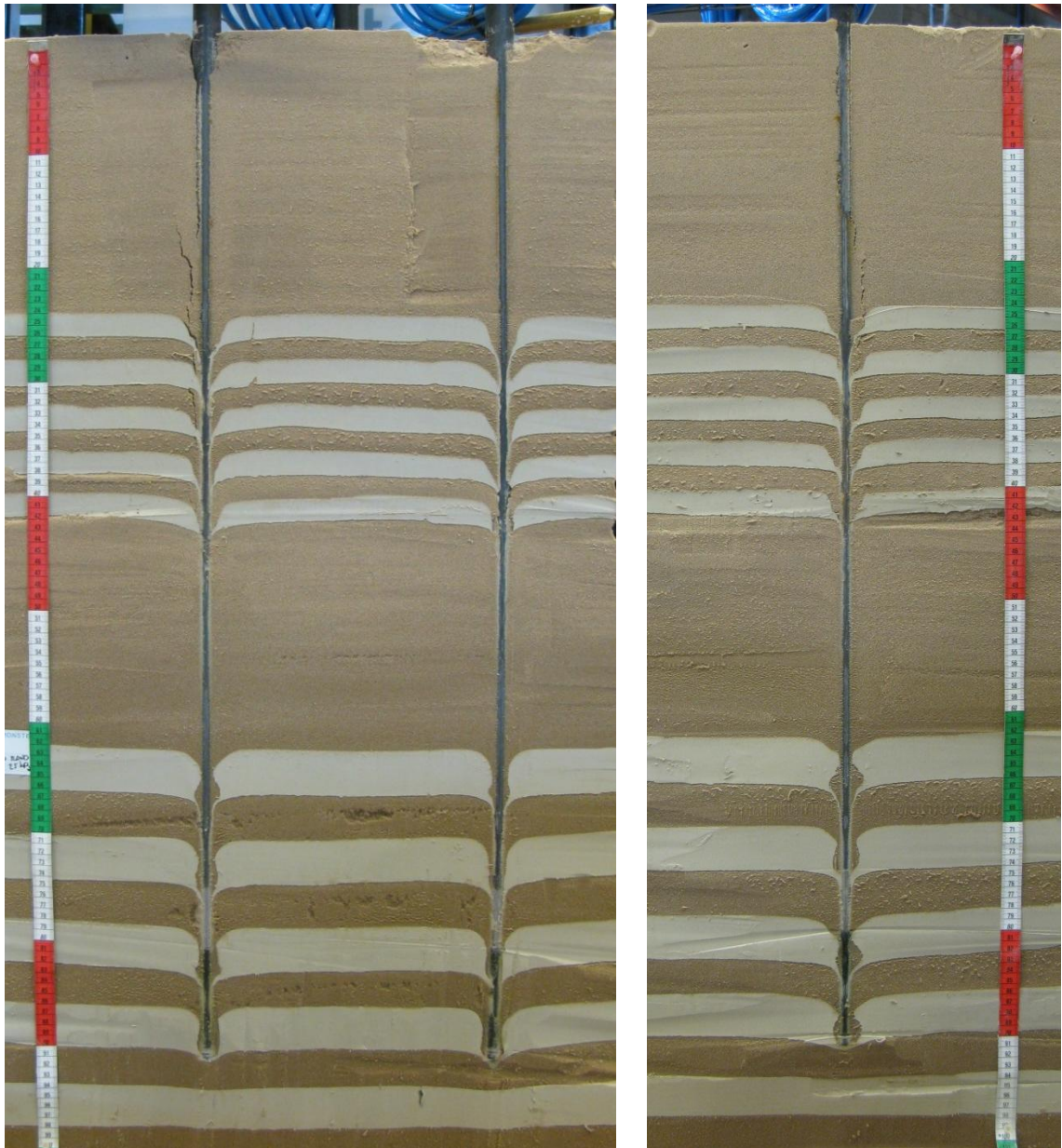


Figure C.6 Photographed cross sections of soil sample 1 after testing with on the left the cone penetrated with a surcharge load of 50 kPa, in the centre the cone penetrated with a surcharge load of 25 kPa and on the right the cone penetrated with a surcharge load of 200 kPa

Figure C.6 shows two photographs of the excavated cross-sections. As can be seen, the cones didn't penetrate through the deepest clay layer. Furthermore, it is concluded from the photographs that soil is pushed downward in front of the cone and the clay is taken into the intermediate sand layers. No significant differences are observed when comparing the patterns around the three different cones. However, the volume of the sand-bulb in the clay layers is larger for higher stress levels.

C.3.2 Soil model 2

The second soil model consisted only of sand (configuration 3, reference). The soil sample has been prepared in separate layers by layered wet raining with a water depth of 10 cm. A bulk relative density of 22% has been achieved (average over total height of the model).

Figure C.7 shows the settlement of the soil sample and the applied pressure at the soil sample as function of time. The cone penetration tests were performed after the settlement reached a constant value. Additional settlement (combined with a drop in pressure) is observed during the cone penetration tests.

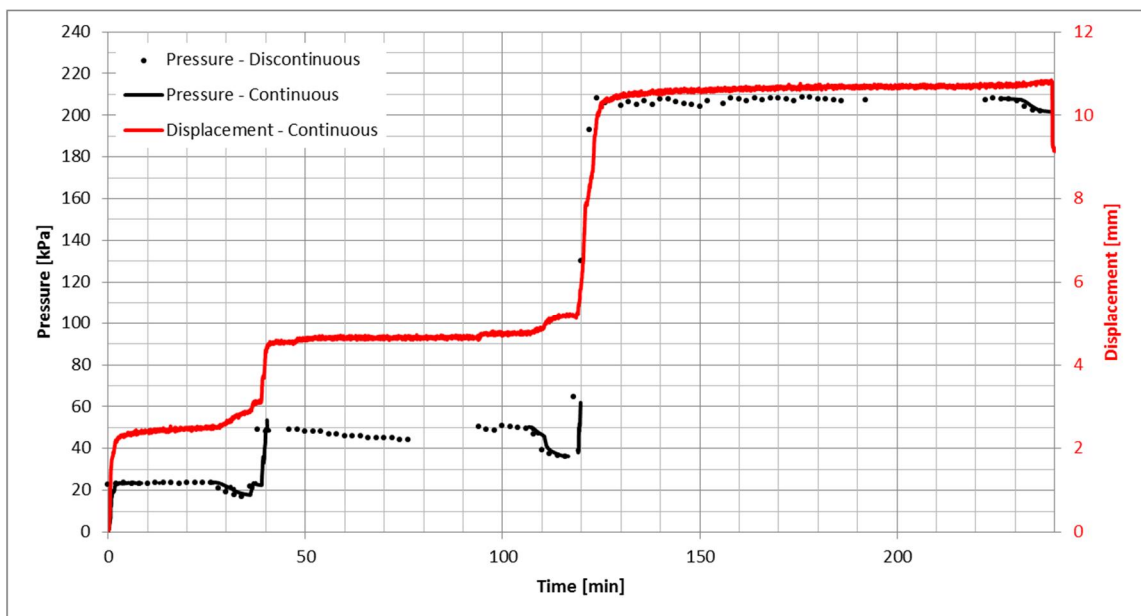


Figure C.7 Surcharge load and sample settlement as function of time

The cone resistances measured during the performed tests are given in Figure C.8. The effect of the vertical stress level is clearly visible. The results point again to a decreasing stress level with depth, which could be a result of side friction and/or arching effects in the soil sample. Also layering is visible, which is thought to be related to the soil preparation method. No uniform cone resistance has been developed over the depth interval. As can be seen, the penetration process of the 50 kPa and 200 kPa tests wasn't "smooth" at deeper levels. As result of the vibrating plunger additional soil compaction may have taken place.

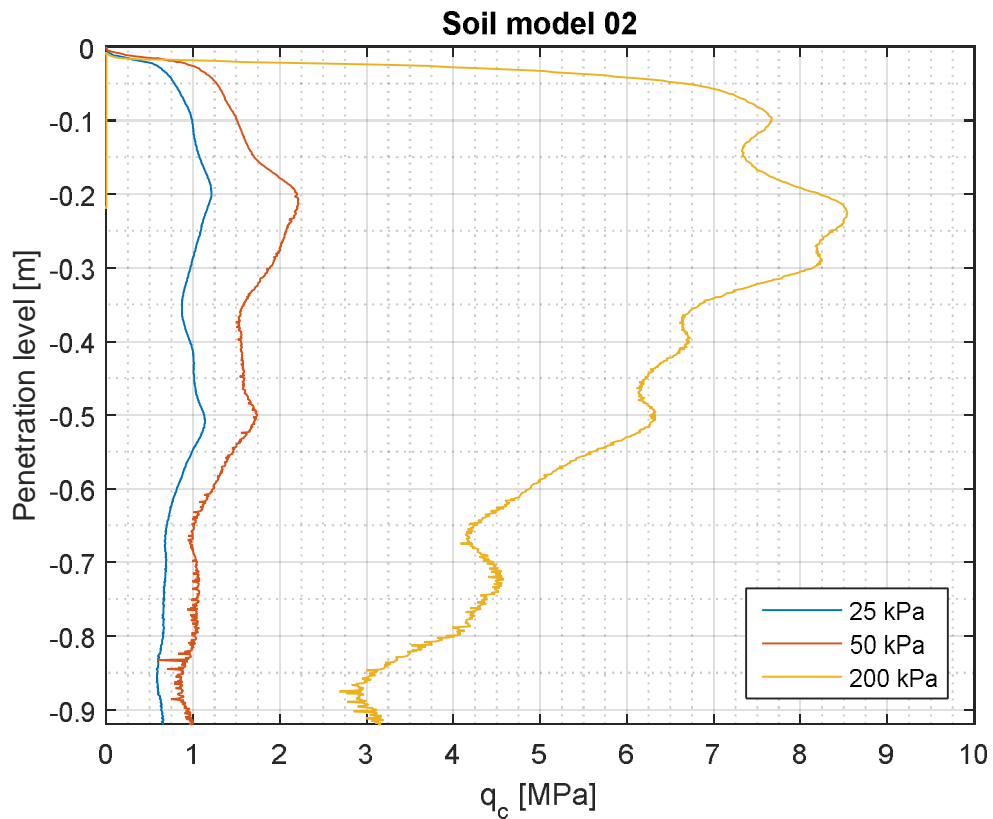


Figure C.8 Cone resistance as function of penetration level and surcharge load

The results of the local porosity measurements after cone penetration testing are given in Figure C.9. The measurements indicate higher relative densities in the upper 50 cm.

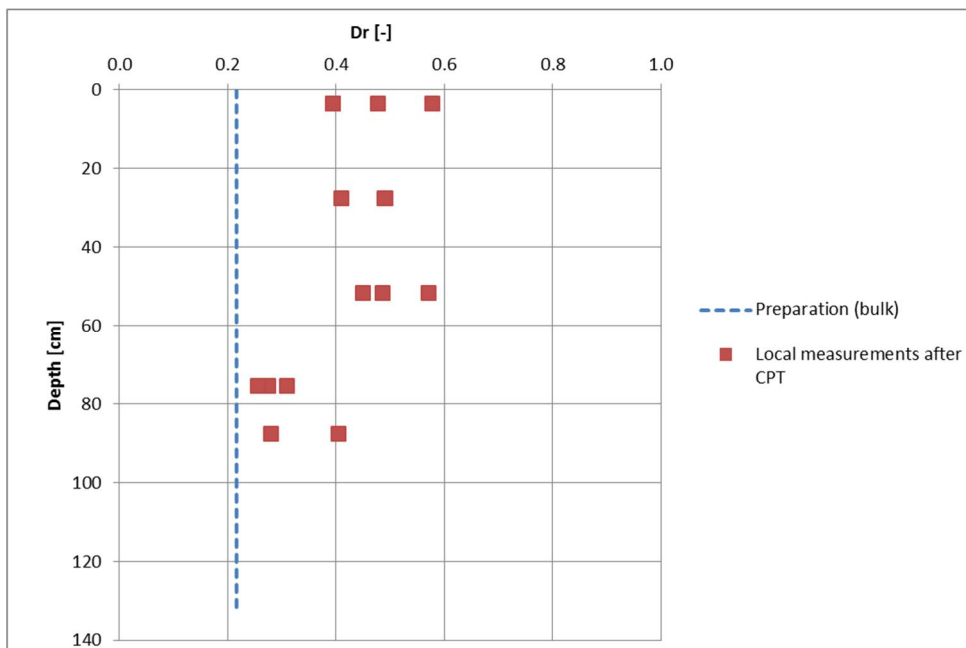


Figure C.9 Relative density after sample preparation (bulk) and after cone penetration testing (local samples)

Figure C.10 depicts one of the photographs made during the excavation of the soil sample. Penetration disturbance patterns are visible next to the rod.



Figure C.10 Photographed cross section of soil sample 2 after testing with the cone penetrated with a surcharge load of 50 kPa

C.3.3 Soil model 3

The third soil model was also prepared to perform reference tests (to measure representative cone resistances for a loosely packed sand sample). Because no uniform cone resistance has been developed over the depth interval in soil model 2, two aspects were altered: the preparation method of the soil model and the roughness of the side walls of the cylindrical cells. The soil sample has been prepared by the dynamic compaction method and a (bulk) relative density of 28% has been achieved. In order to reduce the side friction, Teflon foil has been placed at the walls of the container.

Figure C.11 shows the settlement of the soil sample and the applied pressure at the soil sample as function of time. The cone penetration tests were performed after the settlement reached a constant value.

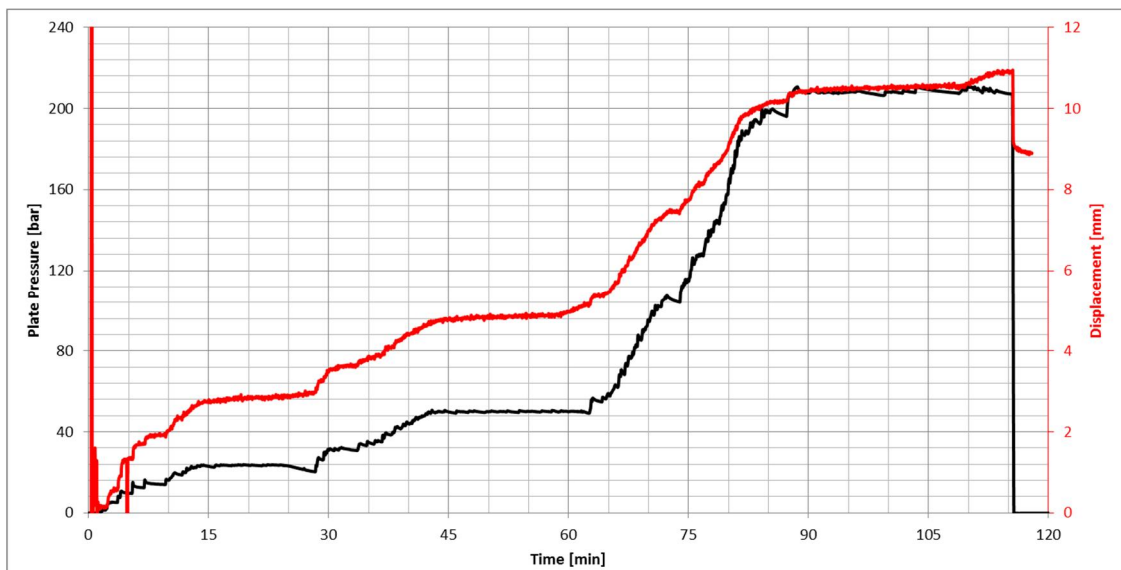


Figure C.11 Surcharge load and sample settlement as function of time

The cone resistances measured during the performed tests are given in Figure C.12. The effect of the vertical stress level is clearly visible. The results point again to a decreasing stress level with depth. The transition around 50 cm depth is striking.

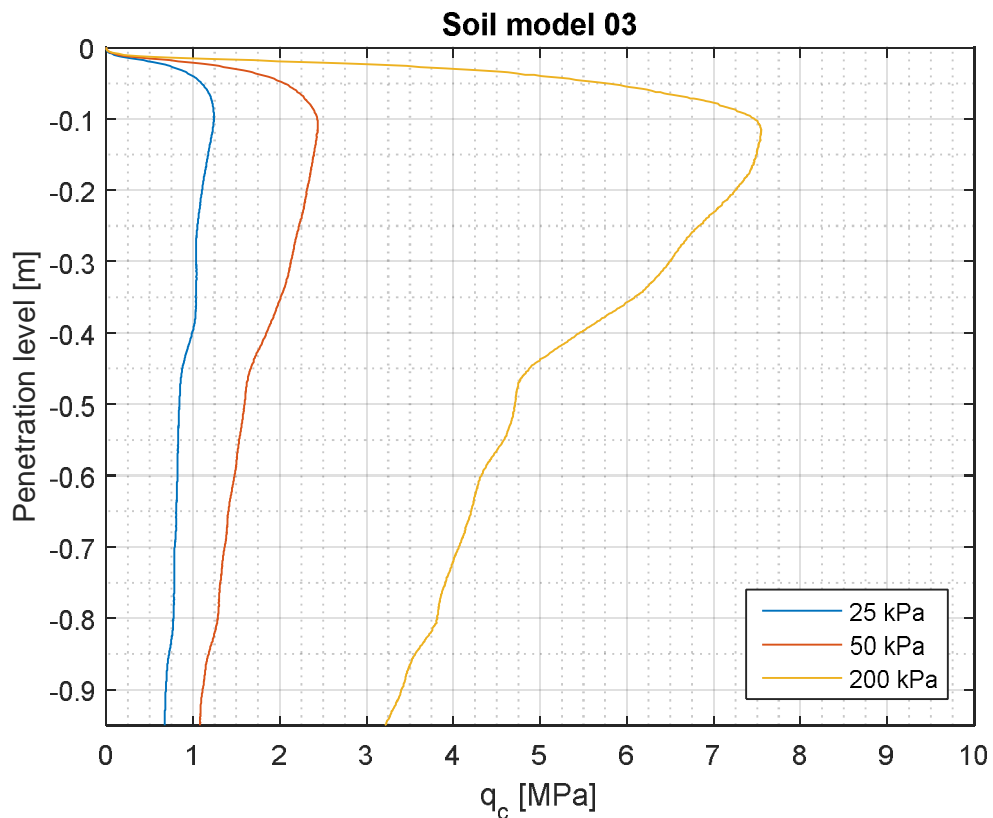


Figure C.12 Cone resistance as function of penetration level and surcharge load

After completion of the CPT testing the specimen is excavated and local density measurements are performed. Relatively high relative densities are measured close to the top plate, see Figure C.13. Compaction of the soil sample possibly took place mainly at the upper part of the sample due to arching and side friction effects (during sample preparation and surcharge loading).

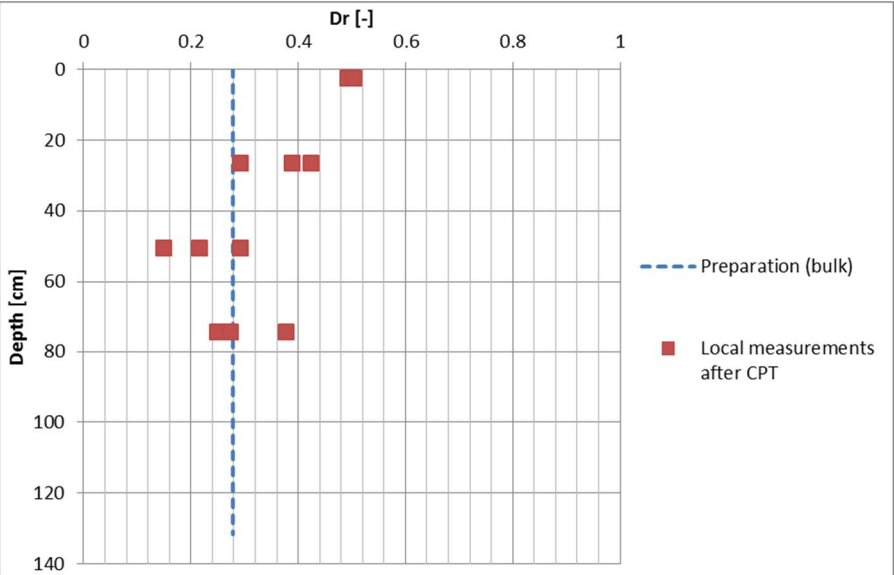


Figure C.13 Relative density after preparation (bulk) and after cone penetration testing (local samples)



Figure C.14 Photographed cross section of soil sample 3 after CPT testing

Figure C.14 depicts one of the photographs made during the excavation of the soil sample. It is thought that the visible patterns are mainly created during the preparation of the sample (dynamic compaction method).

C.3.4 Soil model 4

The fourth soil model contained three clay layers of 8 cm thickness. The height of the upper sand layer was reduced to 20 cm in order to create a sample with a reduced height to reduce the wall friction effect. The final penetration depth was 70 cm. By preparation of the sand layers by layered wet raining, a bulk relative density of 31% was achieved. The Teflon coating was still applied at the walls of the test container in order to reduce the side friction.

Figure C.15 shows the settlement of the soil sample and the applied pressure at the soil sample as function of time. The cone penetration tests were performed at moments in which the settlement didn't reach a constant value yet: the consolidation time was not sufficient to reach full consolidation of the 8 cm clay layers.

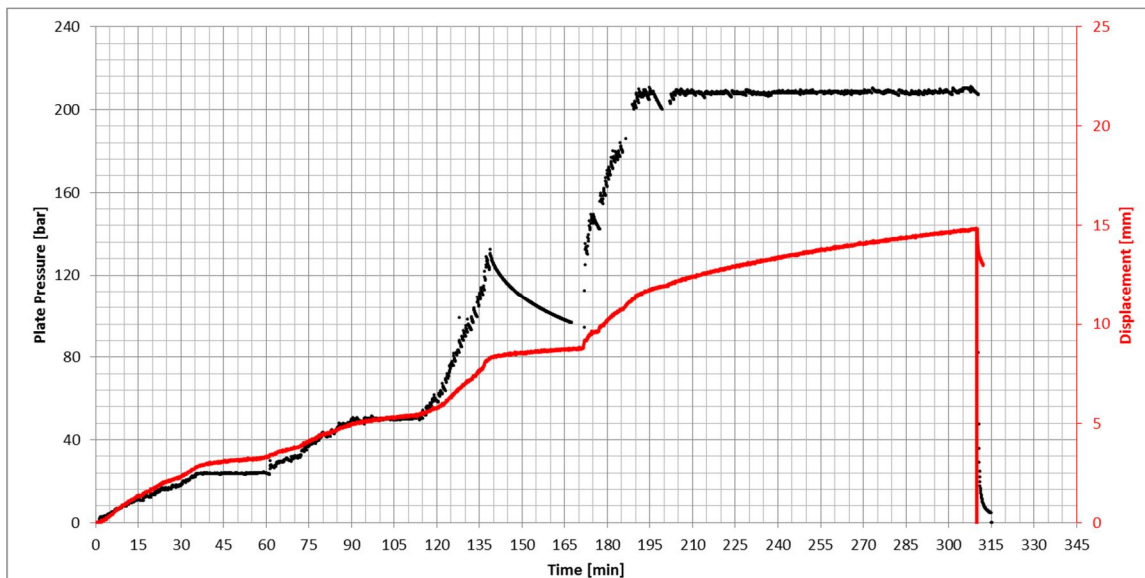


Figure C.15 Surcharge load and sample settlement as function of time

The cone resistances measured during the performed tests are given in Figure C.16. The soil layering and the effect of the applied surcharge load are both clearly visible. The measured resistances at a depth of ca. 60 cm are comparable with the resistances at a depth of ca. 10 cm. It is thought that due to the presence of the clay layers the arching effects are reduced.

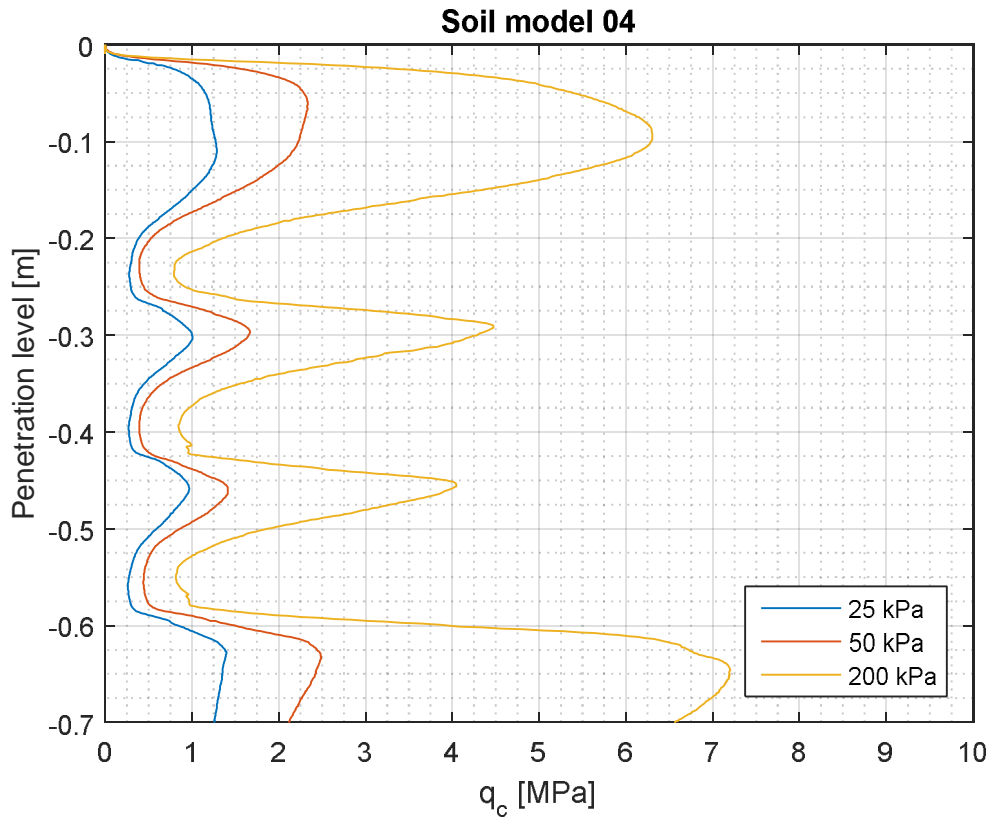


Figure C.16 Cone resistance as function of penetration level and surcharge load

After completion of the CPT testing the specimen is excavated and local density measurements are performed. Figure C.17 depicts the result of the local porosity measurements. It was hard to take samples because of the small layer height. Therefore, some measurements were considered to be unreliable (not presented in the graph).

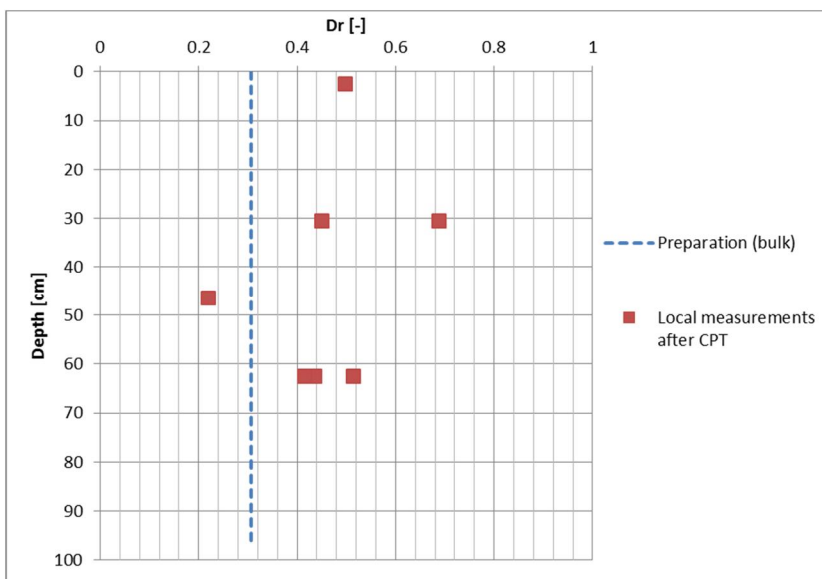


Figure C.17 Relative density after sample preparation (bulk) and after cone penetration testing (local samples)

Figure C.18 shows two photographs of the excavated cross-sections. These photographs confirm the conclusions made after the tests performed at the first soil sample: the soil is pushed downward in front of the cone and the clay is taken into the intermediate sand layers. The volume of the sand-bulb in the clay layers is larger for higher stress levels.

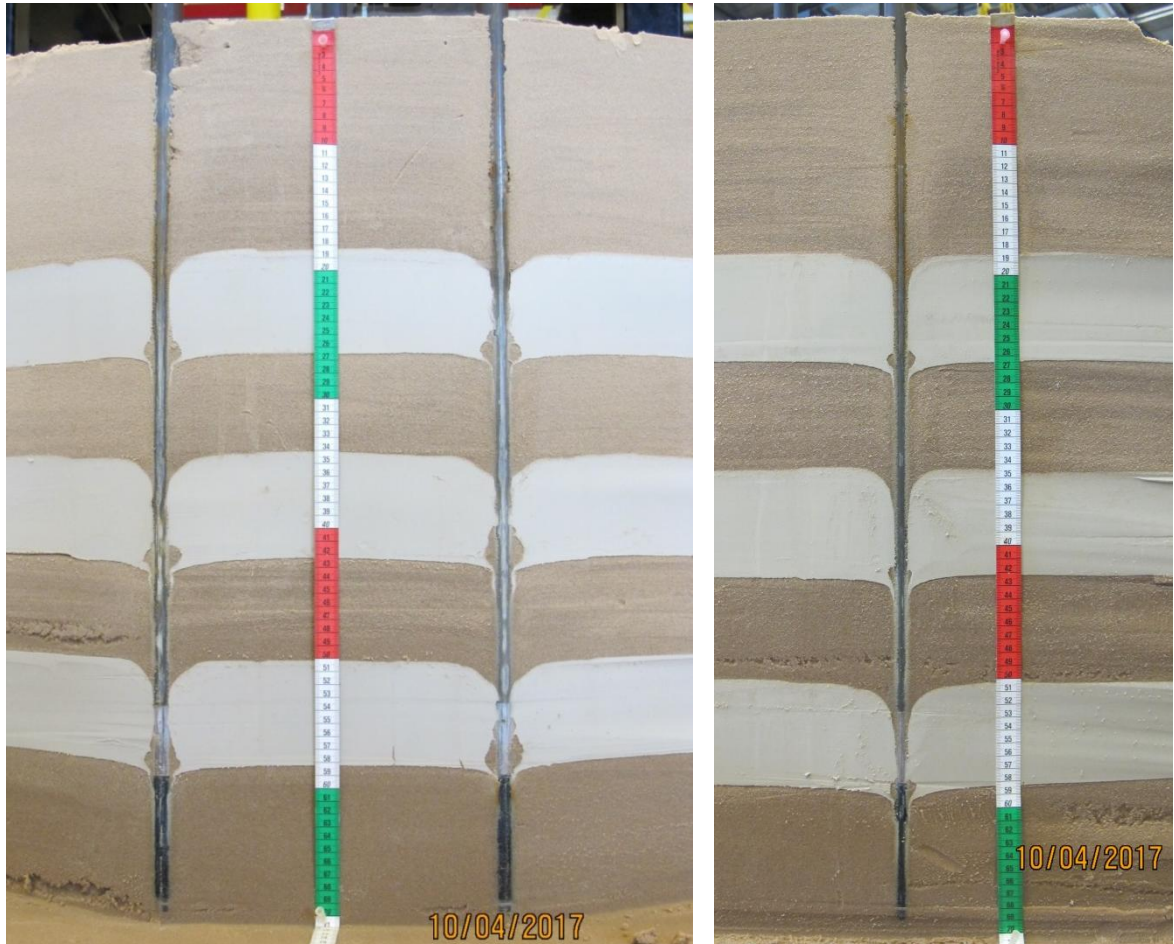


Figure C.18 Photographed cross sections of soil sample 4 after testing with left the cone penetrated with a surcharge load of 200 kPa, in the centre the cone penetrated with a surcharge load of 50 kPa and right the cone penetrated with a surcharge load of 25 kPa

C.3.5 Soil model 5

The fifth soil model was again prepared in order to perform reference tests at a sand specimen. Because no uniform cone resistance has been developed over the depth interval in soil models 2 and 3, another adaptation of the test setup was made. In order to reduce the side friction, plastic foil was placed at the Teflon coating at the walls of the container with Vaseline grease in between. The soil sample has been prepared by the dynamic compaction method and a (bulk) relative density of 30% has been achieved.

Figure C.19 shows the settlement of the soil sample and the applied pressure at the soil sample as function of time. The cone penetration tests were performed after the settlement reached a constant value. The surcharge load was kept constant during cone penetration as much as possible.

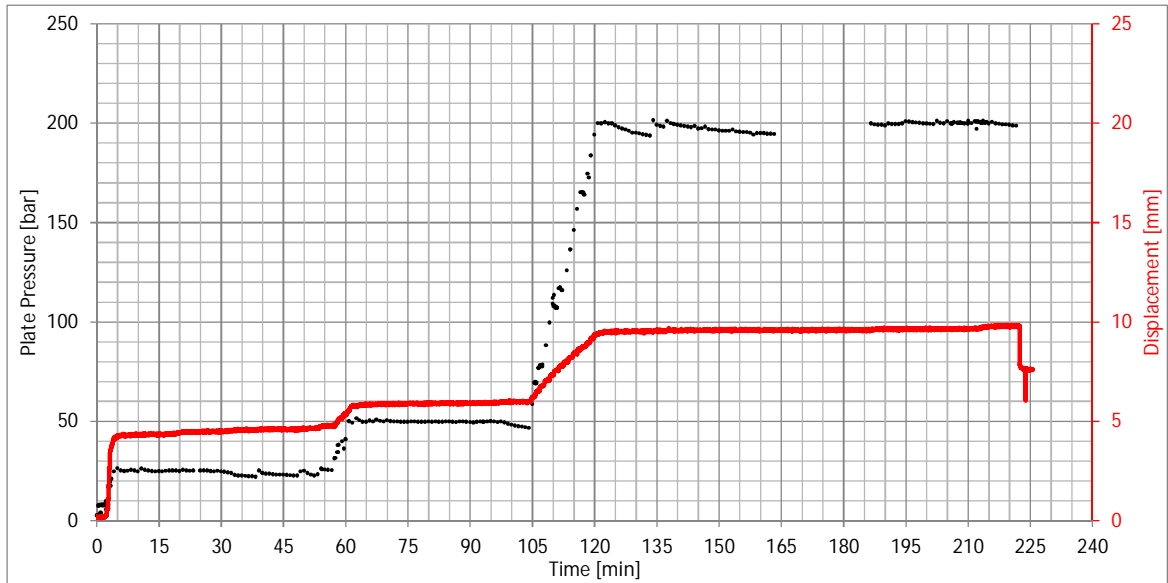


Figure C.19 Surcharge load and sample settlement as function of time

The cone resistances measured during the performed tests are given in Figure C.20. High cone resistances were met at depths around 10 cm relative to the other reference tests (performed at soil model 2 and 3). However, the resistance is still decreasing for deeper levels and again no uniform cone resistance has been developed over the depth interval.

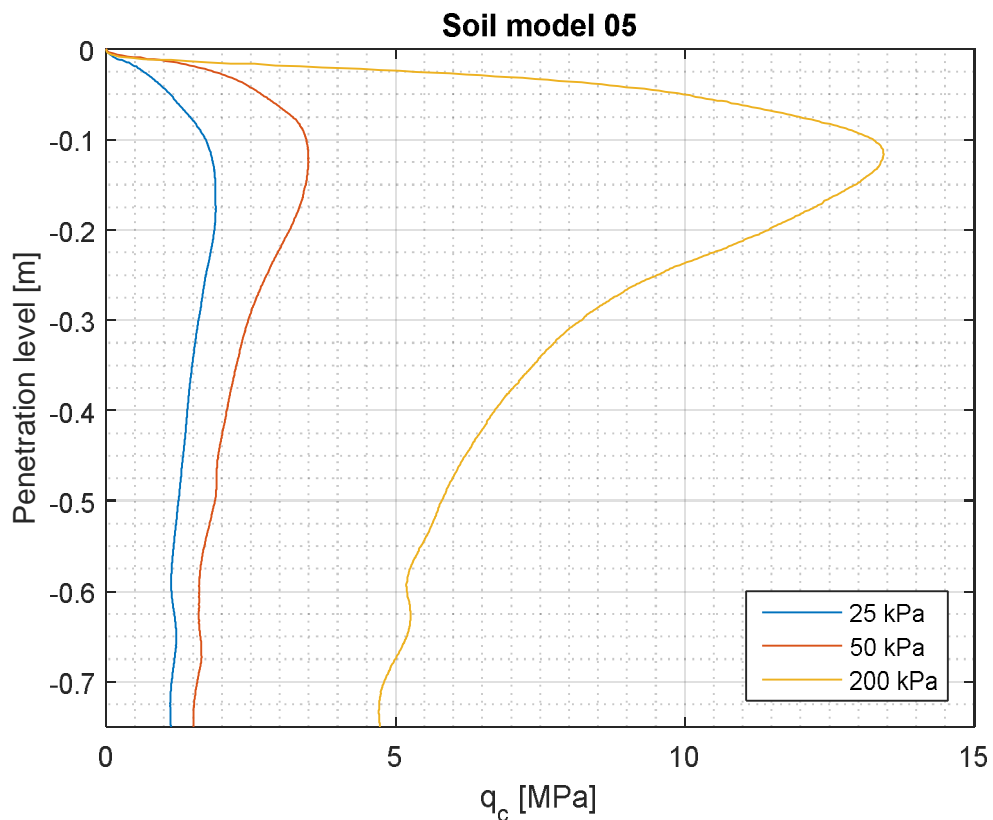


Figure C.20 Cone resistance as function of penetration level and surcharge load

After completion of the CPT testing the specimen is excavated and local density measurements are performed. No photographs were taken during excavation of the soil model. The measurements give an indication of reduction of relative density with depth. Relative high relative densities are measured close to the top plate, see Figure C.21. Densification of the soil sample took possibly mainly place at the upper part of the sample due to arching and side friction effects (during sample preparation and surcharge loading). The results of the CPTs confirm this indication.

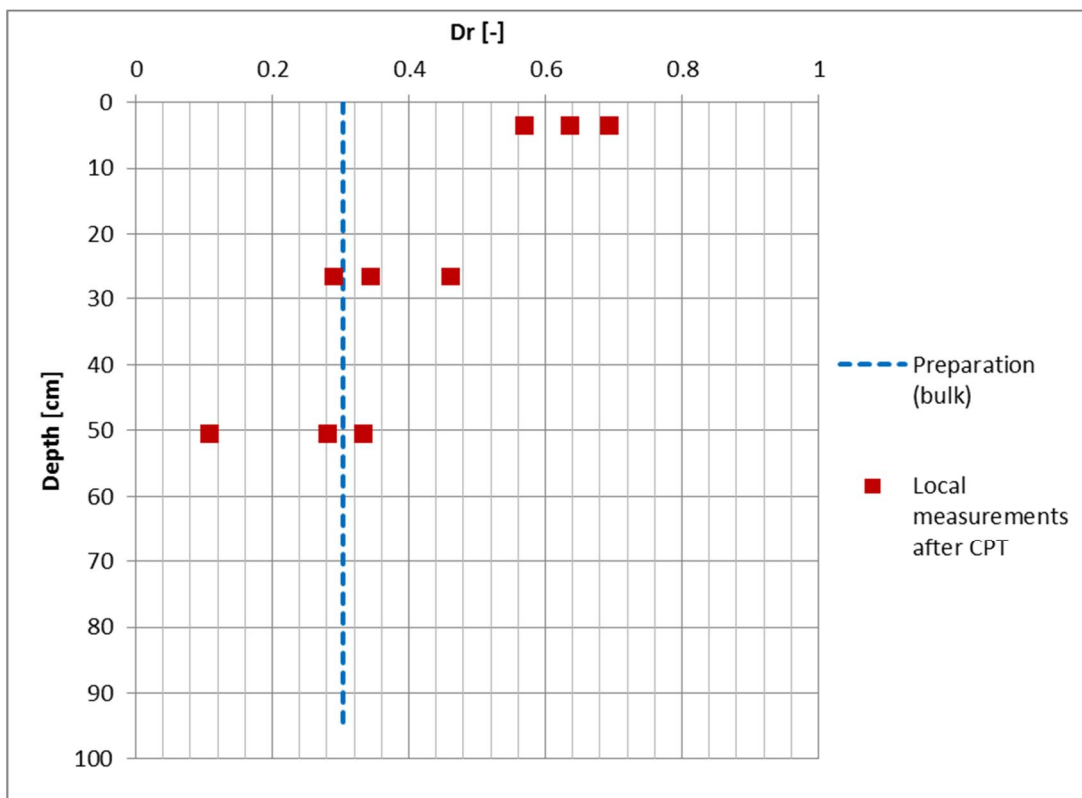


Figure C.21 Relative density after sample preparation (bulk) and after cone penetration testing (local samples)

The average values of the local porosity measurements are used to back-calculate the expected cone resistances according Lunne and Christoffersen (1983). The results are given in Figure C.22 as dashed lines. Also the test results are plotted in this graph (solid lines). The analysis indicates that the non-homogeneity of the soil sample together with the top boundary conditions have a major impact on the measured cone resistance. For the prior reference tests (model 2 and 3) also other factors must have played a role. Side friction and arching effects are thought to be these governing factors.

From the CPTs performed at the reference soil samples (sand only) it is concluded that no uniform cone resistance over depth is measured in these tests as a result of:

- Side wall friction / arching effects.
- Rigid top plate effects: the uniform displacement condition leads to a non-uniform stress distribution under the plate and counteracts the soil deformations at surface level as result of the penetration process.
- Non-homogeneous sand samples.

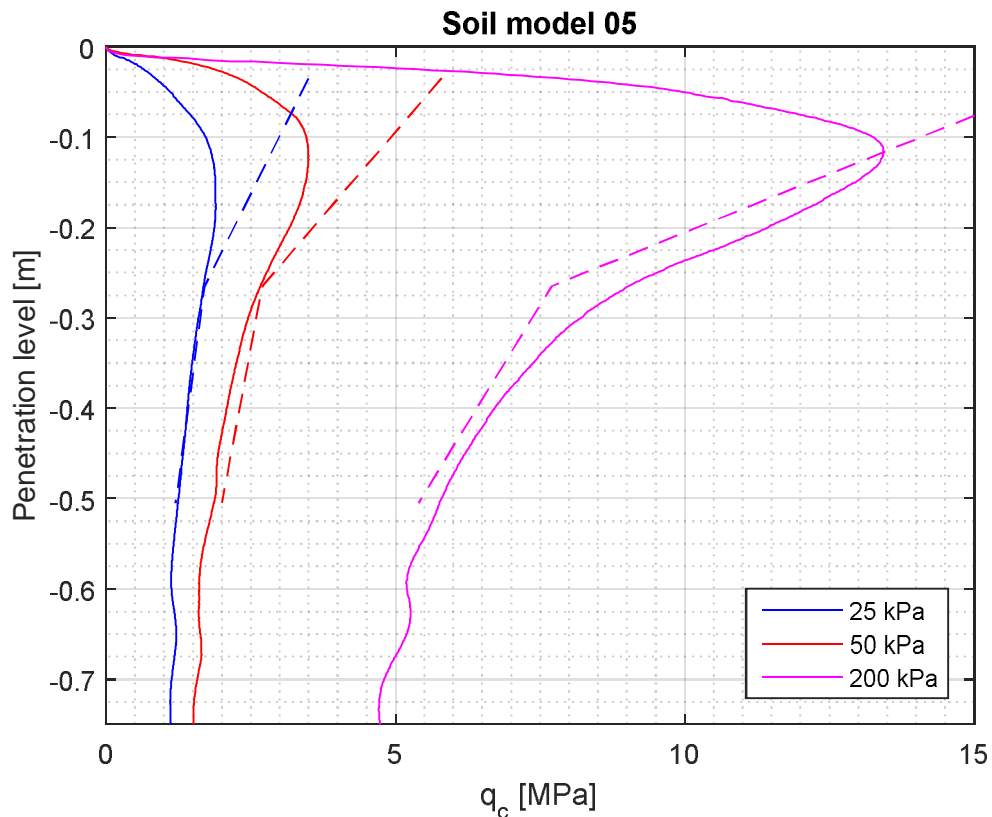


Figure C.22 The dashed lines present the expected cone resistance according Lunne based on the measured local relative density after cone penetration testing

C.4 Overview and discussion test results start-up phase

Table C.2 gives an overview of the tests performed during the first exploratory phase. Tests are performed at layered configurations and reference soil samples. Different sample preparation methods are applied. For soil samples 3 to 5, measures were taken in order to reduce the side friction. The latest applied measure seemed to work well. An overview of the test results is given in Figure C.23, Figure C.24 and Figure C.25. The soil layering, the effect of layer thickness and effect the applied vertical stress are clearly visible. However, the interpretation of the test result is hampered by the fact that no uniform cone resistance over depth is measured in the reference tests (configuration 3).

Soil model	Configuration	$D_{r,preparation,bulk}$ [%]	Preparation method	Measure reduction wall friction
1	1	36	Layered	No
2	3	22	Layered	No
3	3	28	Dynamic compaction	Teflon
4	2	31	Layered	Teflon
5	3	30	Dynamic compaction	Teflon, Vaseline grease and foil

Table C.2 Overview of performed tests during phase 1

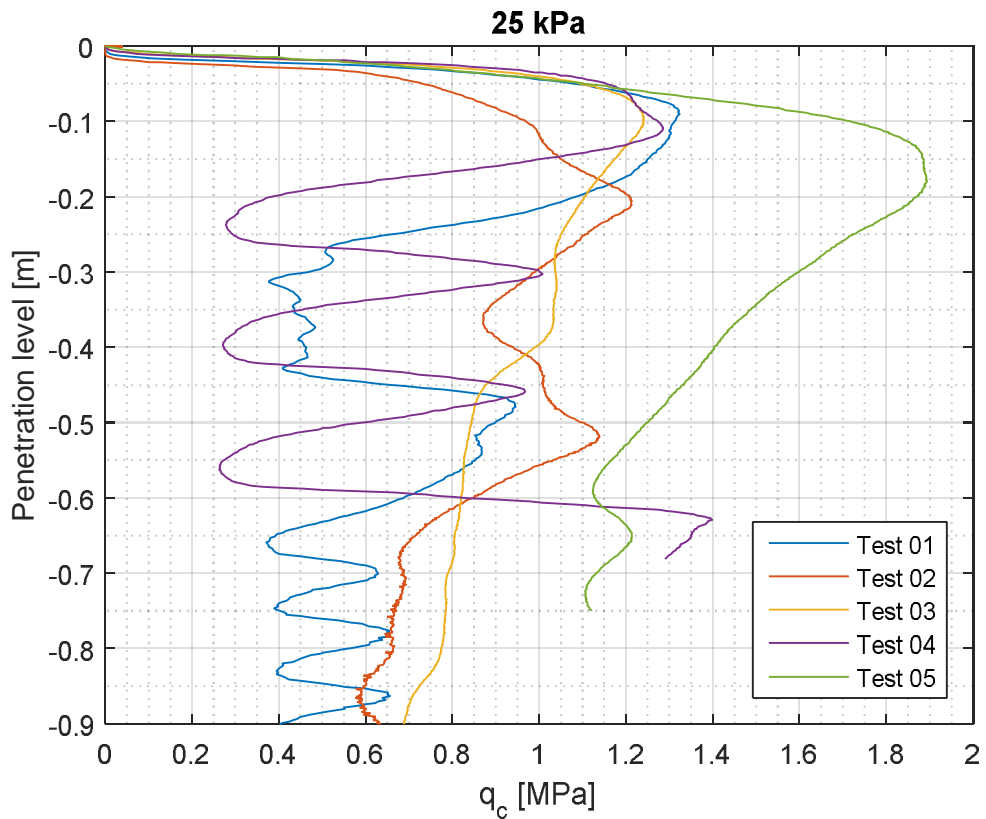


Figure C.23 Measured cone resistance in all prepared soil samples at a surcharge stress of 25 kPa

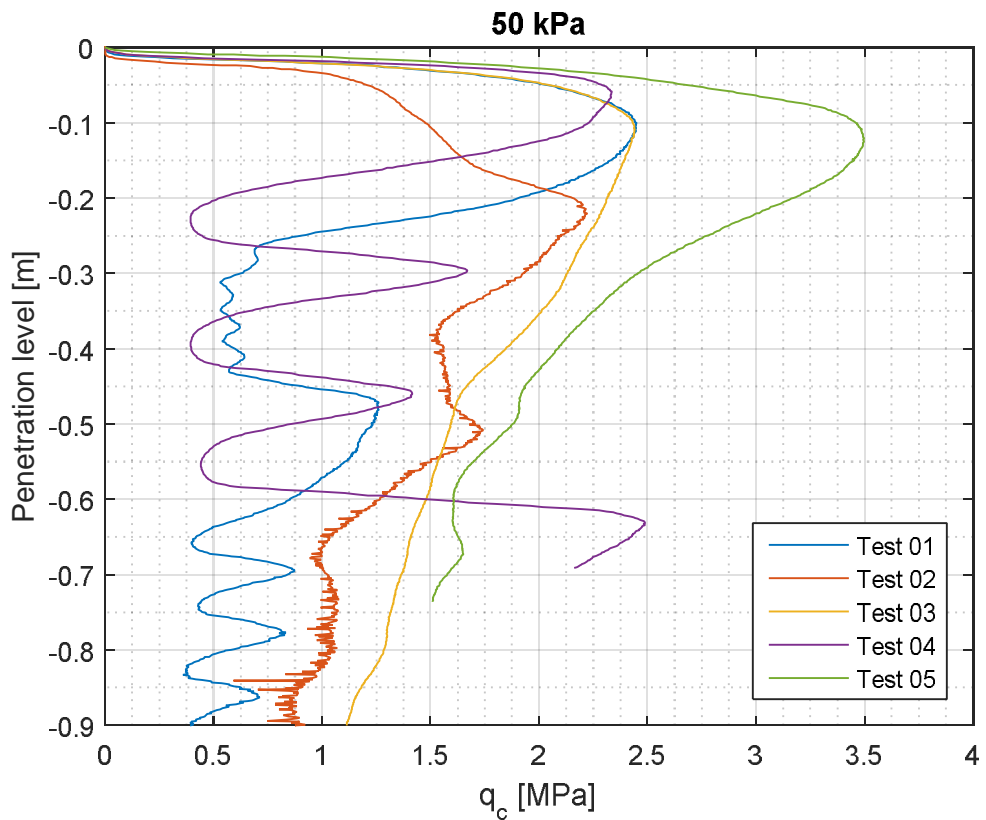


Figure C.24 Measured cone resistance in all prepared soil samples at a surcharge stress of 50 kPa

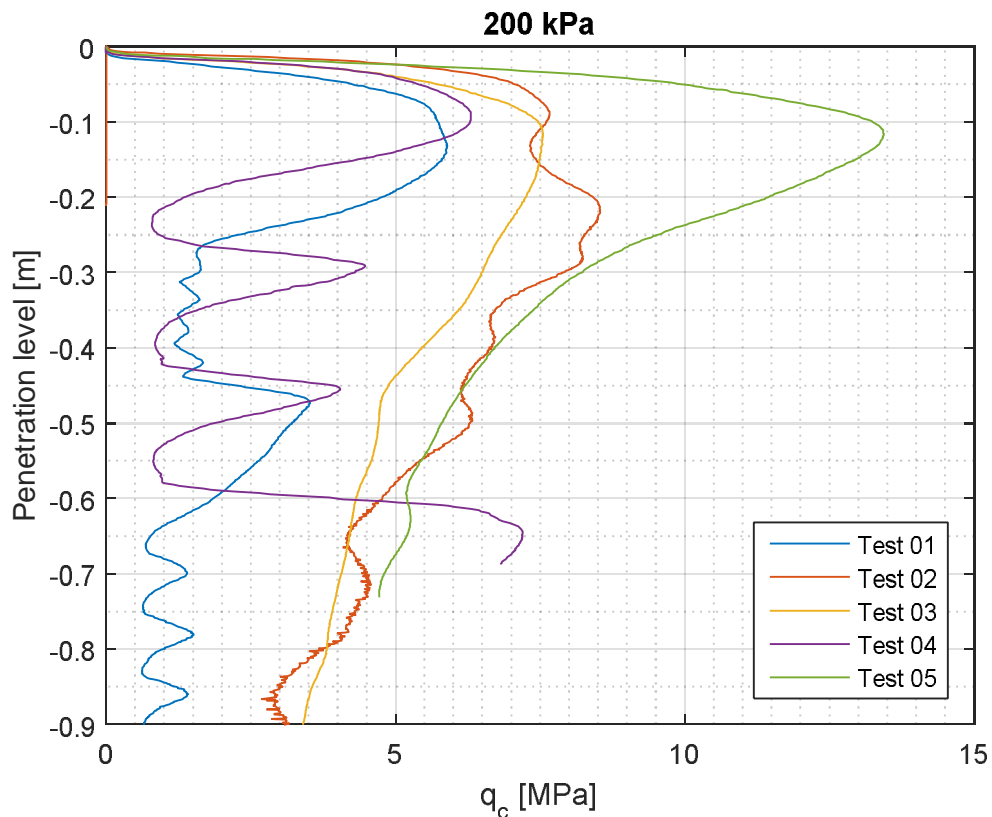


Figure C.25 Measured cone resistance in all prepared soil samples at a surcharge stress of 200 kPa

It is concluded that the test results (cone resistances) are affected by:

- Side wall friction / arching effects (no uniform stress distribution over depth of the soil sample).
- Rigid top plate effects: the uniform displacement condition leads to a non-uniform stress distribution under the plate and counteracts the soil deformations at surface level as result of the penetration process.
- Non-homogeneous distribution of the porosity of the sand samples (due to sample preparation method and/or the above mentioned arching and/or rigid top plate effects).